Integrating field data and a meta-ecosystem model to study the effects of multiple terrestrial disturbances on small stream ecosystem function

By

Hannah Adams

A thesis submitted to the school of Graduate Studies

in partial fulfillment of the requirements for the degree of

Master of Science

Department of Biology

Memorial University of Newfoundland and Labrador

September 2023

St. John's Newfoundland and Labrador

Abstract

Environmental stressors such as land development and climate change are key drivers of biodiversity loss. These stressors operate across a range of spatial and temporal scales and can propagate throughout the landscape. Meta-ecosystem theory can be used to develop models that represent these important cross-ecosystem interactions; however, these models are rarely applied to real ecosystems. We derived a meta-ecosystem model based on empirical data from the island of Newfoundland, Canada to predict how terrestrial disturbances (i.e., forestry, insect outbreaks, roads) will impact the functioning of small streams. Top statistical models for our empirical data showed that benthic invertebrate biomass increased with road density in the stream catchment as did erosion indicators (i.e., specific conductivity), while forest disturbance reduced the proportion of shredders in the benthic invertebrate community. We used disturbance simulations in the meta-ecosystem model to untangle mechanisms for how individual terrestrial disturbances were affecting these stream ecosystems: 1) apparent competition between benthic invertebrates and periphyton and 2) energy flux to higher trophic levels. Along with improving our mechanistic understanding of riparian-stream ecosystems, our integration of empirical data and mathematical modelling creates a framework for using meta-ecosystem models to make informed decisions about natural resource management and conservation.

Dedication

This thesis is dedicated to my parents, for their encouragement and support throughout this journey; to my partner Ari who helped me maintain (most of) my sanity; and to the many friends I've made over the last two years who made Newfoundland feel like home.

Acknowledgments

First, I would like to acknowledge that the lands upon which I lived, studied, and conducted research in this province are the ancestral homelands of the Mi'kmaq, Beothuk, Innu, and Inuit people. Indigenous peoples have lived on this land for thousands of years before it was colonized to become Newfoundland and Labrador. I acknowledge their relationship to the land as sacred, and I believe we can and must work towards true reconciliation and a future where we honour the land together.

I would like to thank my supervisor Shawn Leroux for consistent support and guidance over the last two years, and to my committee members Yolanda Wiersma and Kathryn Hargan for their valuable input.

Many thanks to the Ecosystem Ecology lab for the much-needed encouragement and reminders to be a human too! Thank you to Rachael Moran for being a wonderful friend to go through grad school with, and to Jeremy Hussy, Julia Ball, Jenna Scott, and Devon Bath for being a reliable and good-natured field crew.

Finally, I would like to thank my friends, family, and teachers who have helped me become who I am today- both as a researcher and as a person.

Table of Contents

List of figures

List of tables

Chapter 1: Introduction and thesis overview

1.1 Environmental change and landscape connectivity

It has been well-established that landscapes are highly connected from a microscopic to a global scale, and this connectivity is a crucial component to the function of the ecosystems that make up the Earth. To illustrate, mass drownings of wildebeests during the annual Serengeti wildebeest migration provide a large influx of nutrients into the Mara river that is gradually incorporated into the aquatic food web (Subalusky et al., 2017), and emergent aquatic insects can support a diverse guild of terrestrial predators during late summer in temperature forest watersheds (Nakano and Murakami, 2001). Current research on landscape connectivity is helping us understand some of the mechanisms behind the flow of matter on Earth. For example, seabirds act as global drivers of nitrogen and phosphorus cycles by moving nutrients between colonies on different continents and adding soluble (i.e., bioavailable) nutrients to coastal and continental waters (Otero et al., 2018).

However, landscape connectedness and animal movement are affected by anthropogenic activities like land use change, pollution, resource extraction, monoculture, and climate change exacerbated by burning fossil fuels (Bauer and Hoye, 2014; Tucker *et al.*, 2018; Schiesari *et al.*, 2019). The combined effect of these human activities has led to ongoing biodiversity reshuffling and loss and is causing undeveloped land to become an increasingly limited resource (Potapov *et al.*, 2017). It is therefore important to understand how environmental change impacts biodiversity and create practical ways for this mechanistic knowledge to inform environmental policy. Most ecological research and policy focuses on one ecosystem, but we must look at cross-ecosystem connections to predict how local ecosystems and landscapes will respond to global change (Harvey *et al.*, 2017; Gounand *et al.*, 2018).

1.2 Meta-ecology

Ecosystems (i.e., biological communities and their abiotic environment interacting together in a defined space) are impacted by the flux of material and energy across their (somewhat arbitrary) boundaries

across local, regional, and global extents (Richardson and Sato, 2015). For example, Lecerf and Richardson (2010) found that clear cut logging slowed the rate of decomposition of leaf litter in local streams due to changes in the structure of the benthic invertebrate community and the addition of fine sediment. More active flows of energy can have coupled feedback, such as the predator-prey relationship between a population of fish and fish-eating birds (Richardson and Sato, 2015). This yields a dynamic relationship between multiple connected ecosystems (i.e., a meta-ecosystem). Experiments by Dennert et al. (2023) found that nitrogen subsidies from salmon spawning events were being taken up by wildflowers in the terrestrial ecosystem. Similarly, Knight et al. (2005) found that fish were facilitating the pollination of nearby plants through a trophic cascade by preying on dragonfly larvae which prey on pollinators in their adult stage.

Meta-ecology theory provides a conceptual framework to help bridge the gap between this empirical knowledge about the spatial processes influencing ecosystem function and practical application in environmental management (Schiesari *et al.*, 2019). Meta-ecology theory includes meta-population ecology (local populations of a species that are linked by dispersal; Levins, 1969; Linke et al., 2019), meta-community ecology (local communities that are linked by dispersal of multiple interacting species; Leibold et al., 2004; Wilson, 1992), and meta-ecosystem ecology (local ecosystems that are linked by the flow of organisms, energy, and matter; Loreau et al., 2003). It can be more broadly defined as the study of interdependent mechanisms among ecological systems through the fluxes of organisms, energy, and matter across space (Schiesari *et al.*, 2019).

These concepts have greatly improved our understanding of population, community, and ecosystem dynamics. For example, the number of species on an island can be predicted by island size and isolation using island biogeography theory (MacArthur and Wilson, 1967), concepts at the core of meta-population dynamics. Using meta-population concepts, population persistence can be forecasted across a landscape as with caribou in western Canada (Apps and McLellan, 2006), and can be extended to studying how primary production or secondary production in one ecosystem is driven by fluxes in neighbouring

ecosystems (Gravel *et al.*, 2010; Leroux and Loreau, 2012). By continuing to build on these concepts, we develop the level of complexity to which we can understand and make predictions about the global environment.

1.2.1 Meta-ecosystem ecology

In this thesis, I use the framework of meta-ecosystem ecology to investigate interactions between multiple ecosystems. Meta-ecosystem ecology expands on the concepts of biotic movement of matter (e.g., meta-population ecology and island biogeography) and abiotic movement of matter to look at the mechanisms within and between ecosystems through a holistic lens; this cycling and movement of matter is a property of ecosystems that impacts species persistence, ecosystem productivity, and response to environmental change (Guichard and Marleau, 2021). The effects of material and organismal movement can propagate across landscapes, driving regional variation in ecosystem function (e.g., nutrients from litterfall and fish migration cycling throughout a watershed; Dennert et al., 2023). Materials and organisms move at different spatial and temporal scales, contribute to different ecosystem functions (i.e., primary or secondary production) at multiple spatial extents, and can dampen the paradox of enrichment (Gounand *et al.*, 2014). These flows have temporal variation as well, with changes in quantity and reciprocity throughout the year (Harvey *et al.*, 2011). For example, cross-ecosystem flux of aquatic and terrestrial invertebrate prey subsidized 25.6% of total annual energy budget for birds and 44.0% for fish in a temperate stream-riparian forest study system (Nakano and Murakami 2001).

According to Guichard and Marleau (2021)'s synthetic book on meta-ecosystem ecology, our understanding of the relationship between biodiversity and ecosystem function would benefit from 1) an improved mechanistic understanding of ecosystem dynamics, 2) developing ecosystem models that include the cycling of matter, and 3) developing theories that account for the strong variability present in ecosystems.

Current meta-ecosystem ecology is working to improve the application of our mechanistic understanding of ecosystem dynamics (Guichard and Marleau, 2021). However, meta-ecosystem ecology is rarely used

in applied ecology or the development of guidelines for managing environmental change (Harvey *et al.*, 2017; Gounand *et al.*, 2018). This is an important missing piece, as many facets of environmental change modify the spatial context, connectedness and dominant regulating processes of ecosystems (Schiesari *et al.*, 2019; McCann *et al.*, 2021). In principle, the meta-ecosystem perspective allows us to integrate community and landscape ecology to find insights into the dynamics and functioning of ecosystem from local to global scales, and predict the consequences of land-use changes on biodiversity and ecosystem services (Loreau, Mouquet and Holt, 2003). In this thesis, I will use a meta-ecosystem model to predict impacts of human activities and natural forest disturbances on coupled aquatic-terrestrial ecosystems.

1.2.2 Meta-ecosystem models

Meta-ecosystems models integrate spatial fluxes and cycling of inorganic and organic materials with the dynamics of biotic compartments such as primary producers and consumers. These flows interact with the mechanisms of population growth and species assembly that are key components of meta-population and meta-community theory. It is by building on these core population and community theories that meta-ecosystem models contribute to theoretical ecology (Guichard and Marleau, 2021).

A primary goal for meta-ecosystem modelling is to contribute to a more mechanistic understanding of ecosystem dynamics and their response to anthropogenic activity (Guichard and Marleau, 2021). In recent years, models have been used to understand species interactions and ecosystem stability (see Harvey et al., 2011; Tsakalakis et al., 2020) but are still lacking empirical validation and a strong empirical basis. Jacquet et al. (2022) incorporated a local and regional spatial scale into their meta-ecosystem model of a river network, which is a crucial step towards bridging the gap between empirical and theoretical ecology (Gounand *et al.*, 2018). Creating more empirically-motivated models can improve our predictions for and understanding of how global changes will impact biodiversity and ecosystem functions at the landscape scale (Harvey *et al.*, 2011; Schiesari *et al.*, 2019) and make them more useful for natural resource management application.

1.3 The island of Newfoundland

The empirical component of this thesis takes place on the island of Newfoundland, which is the traditional territory of the Beothuk and Mi'kmaq people.

1.3.1 Ecology of Newfoundland

The island of Newfoundland (51°38'–46°37'N, 59°24'–52°37'W; 111,390 km^2) is located within the boreal forest biome (Roberts, 1983). The island is primarily dominated by black spruce in the central region and by balsam fir along the western, northern, and eastern coasts (Bell, 2002). The mountainous terrain and steep coastline combined with cold ocean currents and prevailing westerly winds create the variable climates found throughout the province. Average annual precipitation is 1400 mm and average annual temperature is 5°C, with high variability across ecoregions (Arsenault *et al.*, 2016). Approximately 50% of the island is forested while the other 50% is composed of peatlands, barrens, and lakes, with a higher proportion of peatlands in the east (Roberts, 1983).

Geologically, Newfoundland can be divided into three zones: Western, Central, and Eastern (Colman-Sadd and Scott, 1994). The Long Range Mountains found in the western zone are the northernmost extension of the Appalachian Mountains, whereas the Central Zone is a plateau containing sedimentary and metamorphic rock along with volcanic and intrusive rocks from ancient volcanic island arcs (Colman-Sadd and Scott, 1994). The Eastern zone of Newfoundland changes to sedimentary and volcanic rock from the Precambrian era (Colman-Sadd and Scott, 1994).

Main ecoregions vary from the western coastal lowlands of the Northern Peninsula, the dense forest of Central Newfoundland, and the foggy Maritime Barrens of the South-eastern region of the island. Temperatures are moderated by the ocean, with mild summers (11-13°C) and winter temperatures ranging from -3.5 to -1°C. The "semi-coastal" climate of Newfoundland is cool and humid, which results in greater annual precipitation than evapotranspiration across the island. Large storms in fall and early winter produce the highest seasonal precipitation (Larson and Colbo, 1983). Newfoundland is known for dense fog, high winds, snowfall, and rainfall – especially along the eastern coast – and a short growing

season. The forests are dominated by balsam fir (*Abies balsamea*), white birch (*Betula papyrifera*), trembling aspen (*Populus tremuloides*), and tamarack (*Larix laricina*) in the lowlands, and black spruce (*Picea mariana*) at higher elevations. Kalmia heath and sphagnum moss are found in poorly drained areas, with dwarf black spruce and shrubs commonly found along exposed rocky outcrops (Bell, 2002).

Poor drainage due to a very thin soil layer results in many freshwater ponds, bogs, and rivers present across the island (Larson and Colbo, 1983). Watersheds are relatively small as no part of the island lies more than 130 km away from the coast. The many bogs and ponds along streams control water flow and erosion and moderate water temperature, and groundwater inputs from a high water table keep them cooler than ambient temperature in the summer and warmer in the winter. Flow is highest during snow melt in April and May, with low flow during late summer (Larson & Colbo, 1983).

The Labrador Current creates a seasonal lag in temperature and frequent cloud cover prevents insolation and daily warming, so most aquatic habitats are relatively cold, with a maximum temperature ranging between 13-23˚C (Kerekes, 1974). Lake shores are rocky, with sparse macrophyte growth. Brook trout (*Salvelinus fontinalis*) and American Eel (*Anguilla rostrata*) are found in the lakes, with populations of landlocked Arctic char (*Salvelinus alpinus*), Atlantic Salmon (*Salmo salar*), and smelt (*Osmerus mordax*). Lakes and rivers have low concentrations of major ions and productivity is primarily phosphorus limited as igneous and metamorphic rock are the main source (Kerekes, 1974, 1977). Waters are generally acidic with low levels of dissolved materials. Lakes are classified as oligotrophic or occasionally mesotrophic. High coloration is due to humic acids and complexed soluble iron from bogs (Larson and Colbo, 1983).

Primary production is low, limited by low nutrient availability, low solar irradiation, highly tannic waters (which reduce light penetration and thus photosynthesis), and nutrient depletion due to low water renewal rates. During high flow periods, rapid water renewal dilutes nutrient concentrations and displaces phytoplankton and periphyton (Kerekes, 1977).

The benthic invertebrate diversity is much lower in Newfoundland compared to adjacent mainland regions, consistent with island biogeography theory (MacArthur and Wilson, 1967). For example, there are 35 recorded species of Ephemeroptera in Newfoundland compared to 160 species in Maine (Larson and Colbo, 1983; Burian and Gibbs, 1991). The low diversity may result from a combination of poor environmental suitability and the barriers created by the coastal barrens and oceanic straits (Larson and Colbo, 1983).

1.3.2 History of disturbance

The island of Newfoundland is undergoing regular disturbances from logging, ATV trails and logging roads, insect outbreaks, wind, fire, and a hyper-abundant moose population (MacLean, 1980; Waight, 2014; Arsenault *et al.*, 2016; Leroux, Wiersma and Vander Wal, 2020). The combined effects of these disturbances have impacts across the island (Government of Newfoundland and Labrador and Nature Conservancy Canada, 2013).

1.3.2.1 Moose in Newfoundland

A pair of moose were first introduced to Newfoundland from New Brunswick in 1878 for sport hunting (Pimlott, 1953) and two males and two females were released in 1904 (Pimlott, 1959). Since then, the moose population has vastly increased due to a lack of natural predators (Bergerund and Manuel, 2016). Moose have functionally altered the Newfoundland landscape, where heavy moose browsing following an initial disturbance (i.e., wildfires or insect outbreaks) slows forest regeneration, creating moose-mediated meadows (McInnes *et al.*, 1992; Gosse *et al.*, 2011). Empirical studies of moose in Newfoundland and elsewhere demonstrate that this landscape change from forest to spruce meadow can have cascading impacts on the plant community (Charron and Hermanutz, 2016; Leroux *et al.*, 2021), aquatic systems (MacSween et al., 2019), habitat availability for terrestrial animals (Rae et al., 2014; Teichman, 2013), and nutrient cycles (Thompson *et al.*, 1992; Charron and Hermanutz, 2016; Ellis and Leroux, 2017).

In an effort to manage moose population density, the island of Newfoundland has been divided into moose management areas (MMA's) with different hunting quotas based on the current and target moose

population in that region (Department of Environment and Conservation, 2015). Moose population estimates are based on regular aerial surveys.

1.3.2.2 Spruce budworm and hemlock looper

Spruce budworm is a moth native to North America that feeds on the needles, flowers, and cones of balsam fir, white spruce (*Picea glauca)*, and to a lesser extent red spruce (*Picea rubens*) and black spruce (*Picea mariana*). Mature forests tend to be more severely impacted, and trees will typically die after 4-5 years of defoliation (MacLean, 1980). These outbreaks are part of the natural forest cycle, where defoliation and the death of mature trees open gaps in the tree canopy, allowing younger trees to grow (Dymond et al., 2010; MacLean, 1985). However, climate change is leading to earlier springs and warmer summers which may be exacerbating these effects. In addition, moose are feeding on balsam fir saplings, preventing forest regeneration and reducing the amount of adult fir trees for spruce budworm to consume (McInnes *et al.*, 1992). Along with the historical effects of defoliation and resulting moose-mediated grassland, high numbers of spruce budworm larvae may act as a large subsidy pulse for both terrestrial and aquatic predators (Yang *et al.*, 2008; Kawaguchi, Taniguchi and Nakano, 2018) and parasitoids (Eveleigh *et al.*, 2007).

Historically, Newfoundland has been impacted by spruce-budworm outbreaks in the 1970's, and again in 2006, with a new outbreak currently developing on the west coast of the Island (Gros Morne National Park, 2011). In 2021, the Government of Newfoundland and Labrador requested GMNP to be included in the Early Intervention Strategy for Spruce Budworm (EIS), which involves treating spruce budworm "hotspots" with bioinsecticides to slow the outbreak and minimize forest defoliation. The EIS has been successful in slowing down spruce budworm outbreaks in New Brunswick (MacLean *et al.*, 2019). These bioinsecticides affect all lepidoptera, which could have significant long-term impacts on these forest ecosystems (GMNP, 2021). After review and public consultation, both GMNP and TNNP have so far not allowed bioinsecticides within the park boundaries.

Hemlock looper (*Lambdina fiscellaria*) tends to affect less forested area but has a more significant impact on trees, with predictable outbreaks occurring every 15-20 years, moving in a semi-circle from south to north (Arsenault *et al.*, 2016). Both taxa have cycles that correlate with climatic conditions, and therefore may become more frequent and severe with climate change (Zhang *et al.*, 2023).

1.3.2.3 Logging industry

There is little information available on the history of logging in Newfoundland, but most of the wood harvest has occurred in the Central and Western Newfoundland Forest ecoregions, which represent 78% of the total historical harvest area of the island (Arsenault *et al.*, 2016). Logging began as a source for building materials in small, coastal towns, but over time many sawmills and a pulp and paper mill were built, and Newfoundland began exporting lumber in 1980 (Arsenault *et al.*, 2016).

Until Confederation in 1949 the government did very little to manage timber harvest, and the pulp and paper industry was a large component of the Newfoundland economy. There has recently been a push towards reforestation and environmental management as many concessions have been given to forestry companies in the past to retain jobs within the province. Currently, there is a combination of commercial and local timber harvesting, with clearcutting as the main method of harvest (Higgins, 2011).

1.3.2.4 ATV trails and logging roads

Trail density has been increasing in Newfoundland along with ATV use; while an official ATV T'railway began operation in 2010, many networks of unofficial trails have been created across the island (Perry, 2016). These trail networks cause habitat fragmentation, acting as a corridor for invasive species and diseases and changing the hydrology of the region (Arp and Simmons 2012; Kidd et al., 2014; Trip and Wiersma, 2015). These trails increase erosion and sediment loading into local streams and reduce stream quality within the watershed (Chin *et al.*, 2004). Increased sediment levels have been associated with decreased primary productivity and abundance of macroinvertebrates and fish, all of which are an area of concern for Newfoundland as Atlantic salmon populations are in decline (Cheong *et al.*, 1995).

1.3.2.5 Wind and wildfire

The Maritime Barrens and the Long Range Mountains have high winds throughout the year, often leading to windthrow after insect defoliation, made possible by the shallow roots of most boreal tree species and shallow soil across the island (Arsenault *et al.*, 2016). There is more windthrow along clear cut edges, such as riparian retention corridors. Severe insect defoliation leads to greater windthrow which increases the severity of the insect disturbance (Taylor and MacLean, 2009).

Wildfires occur the most frequently in the Central Newfoundland Forest and the Maritime Barrens, as they are located in the interior of the island and have a drier, more continental climate. Prescribed burning is conducted by Parks Canada in Terra Nova and by the Newfoundland Forest Service (Arsenault *et al.*, 2016).

1.4 Thesis overview

The objective of this thesis is to create an empirically based meta-ecosystem model of a riparian-stream system to untangle the mechanisms behind the effects of terrestrial disturbances on streams, using Newfoundland as a case study. We then simulate terrestrial disturbances in the model to see how the meta-ecosystem responds to these changes across a range of disturbance intensities. Documenting this process provides a framework for developing meta-ecosystem models that can be applied as a tool for environmental conservation and management in any landscape.

In Chapter 1 we give an overview of meta-ecology theory and the history of terrestrial disturbances in Newfoundland, providing context for the philosophical and practical aspects of the project. In Chapter 2 we provide methods, results, and discussion of our analysis of empirical data, meta-ecosystem model development, and disturbance simulations. By simulating disturbance from insect outbreaks, logging, and ATV trail and logging road development in our meta-ecosystem model, we test the following predictions: 1) increasing the intensity of both logging and insect outbreaks will increase periphyton and benthic invertebrate biomass, with logging having a greater effect, and 2) increasing ATV trail and logging road density (hereby referred to as “unpaved road density”) will decrease periphyton and benthic invertebrate

biomass. In Chapter 3 we discuss the nuances of our results in more detail and provide a review of literature and our own suggestions for applying meta-ecosystem models as a landscape management tool.

1.5 Co-authorship statement

Chapters 1 and 3 were written by Hannah Adams, while chapter 2 was co-authored with Shawn J. Leroux where we use "we" to refer to the authors. H. Adams developed the project idea and methods, conducted the field sampling and model development, analyzed the field data, generated disturbance simulations in the model, interpreted the results, and wrote the thesis and associated appendices. S. J. Leroux was awarded funding for the project and provided guidance on the project design and implementation, model development, analysis, interpretation of results, and writing. Chapter 2 will be reformatted and submitted to the *Journal of Applied Ecology*.

References

Apps, C.D. and McLellan, B.N. (2006) 'Factors influencing the dispersion and fragmentation of endangered mountain caribou populations', *Biological Conservation*, 130(1), pp. 84–97. Available at: https://doi.org/10.1016/j.biocon.2005.12.004.

Arp, C.D. and Simmons, T. (2012) 'Analyzing the impacts of off-road vehicle (ORV) trails on watershed processes in wrangell-st. elias National Park and preserve, Alaska', *Environmental Management*, 49(3), pp. 751–766. Available at: https://doi.org/10.1007/s00267-012-9811-z.

Arsenault, A. *et al.* (2016) 'Unravelling the past to manage Newfoundland's forests for the future', *Forestry Chronicle*, 92(4), pp. 487–502. Available at: https://doi.org/10.5558/tfc2016-085.

Bauer, S. and Hoye, B.J. (2014) 'Migratory animals couple biodiversity and ecosystem functioning worldwide', *Science*, 344(6179). Available at: https://doi.org/10.1126/science.1242552.

Bell, T. (2002) 'Ecoregions of Newfoundland', *Heritage Newfoundland and Labrador* [Preprint]. Available at: https://www.heritage.nf.ca/articles/environment/ecoregions-newfoundland.php.

Bergerund, A. and Manuel, F. (2016) 'Moose Damage to Balsam Fir-White Birch Forests in Central Newfoundland', *The Journal of Wildlife Management*, 32(4), pp. 729–746.

Burian, S. and Gibbs, K. (1991) 'Mayflies of Maine: An annotated faunal list', *Maine agricultural experiment station technical bulletin*, (142), p. 115.

Charron, L. and Hermanutz, L. (2016) 'Prioritizing boreal forest restoration sites based on disturbance regime', *Forest Ecology and Management*, 361, pp. 90–98. Available at: https://doi.org/10.1016/j.foreco.2015.11.003.

Cheong, A.L. *et al.* (1995) 'A discussion of suspended sediment in the Takla Lake region: the influence of water discharge and spawning salmon', *Canadian technical report of fisheries and aquatic sciences* [Preprint].

Chin, A. *et al.* (2004) 'Effects of all-terrain vehicles on stream dynamics', *Ouachita and Ozark Mountains symposium: ecosystem management research.*, pp. 292–296. Available at: http://www.treesearch.fs.fed.us/pubs/viewpub.jsp?index=6475.

Colman-Sadd, S.P. and Scott, S.A. (1994) 'Newfoundland & Labrador, Traveller's Guide to the Geology', *Newfoundland Section Geological Association of Canada* [Preprint].

Dennert, A.M., Elle, E. and Reynolds, J.D. (2023) 'Experimental addition of marine-derived nutrients affects wildflower traits in a coastal meta-ecosystem'. Available at: https://doi.org/10.1098/rsos.221008.

Department of Environment and Conservation, N. and L.W.D. (2015) 'Newfoundland and Labrador Moose Management Plan'. Available at: www.gov.nl.ca (Accessed: 25 March 2022).

Dymond, C.C. *et al.* (2010) 'Future spruce budworm outbreak may create a carbon source in Eastern Canadian forests', *Ecosystems*, 13(6), pp. 917–931. Available at: https://doi.org/10.1007/S10021-010-9364-Z/FIGURES/7.

Ellis, N.M. and Leroux, S.J. (2017) 'Moose directly slow plant regeneration but have limited indirect effects on soil stoichiometry and litter decomposition rates in disturbed maritime boreal forests', *Functional Ecology*, 31(3), pp. 790–801. Available at: https://doi.org/10.1111/1365-2435.12785.

Eveleigh, E.S. *et al.* (2007) 'Fluctuations in density of an outbreak species drive diversity cascades in food webs', *Proceedings of the National Academy of Sciences of the United States of America*, 104(43), pp. 16976–16981. Available at: https://doi.org/10.1073/PNAS.0704301104.

Gosse, J. *et al.* (2011) 'Degradation of boreal forests by nonnative herbivores in Newfoundland's National Parks: Recommendations for ecosystem restoration', *Natural Areas Journal*, 31(4), pp. 331–339. Available at: https://doi.org/10.3375/043.031.0403.

Gounand, I. *et al.* (2014) 'The Paradox of Enrichment in Metaecosystems', 184(6). Available at: https://doi.org/10.1086/678406.

Gounand, I. *et al.* (2018) 'Meta-Ecosystems 2.0: Rooting the Theory into the Field', *Trends in Ecology and Evolution*, 33(1), pp. 36–46. Available at: https://doi.org/10.1016/j.tree.2017.10.006.

Government of Newfoundland and Labrador and Nature Conservancy Canada (2013) 'Newfoundland and Labrador Human Footprint: A Snapshot of Human Influence on the Landscape', *Parks and Natural Areas Division, Department of Environment and Conservation*, p. 25.

Gravel, D. *et al.* (2010) 'Source and sink dynamics in meta-ecosystems', *Ecology*, 91(7), pp. 2172–2184. Available at: https://doi.org/10.1890/09-0843.1.

Gros Morne National Park (2011) 'What We Heard: Consultation on the request for inclusion of Gros Morne National Park in an Early Intervention Strategy Spruce Budworm Control Program'.

Guichard, F. and Marleau, J. (2021) *Meta-Ecosystem Dynamics: Understanding Ecosystems Through the Transformation and Movement of Matter*. Available at: http://www.springer.com/series/10049.

Harvey, E. *et al.* (2011) 'A general meta-ecosystem model to predict ecosystem function at landscape extents', *Ecology Letters*, 14, pp. 313–323.

Harvey, E. *et al.* (2017) 'Bridging ecology and conservation: from ecological networks to ecosystem function', *Journal of Applied Ecology*, 54(2), pp. 371–379. Available at: https://doi.org/10.1111/1365-2664.12769.

Higgins, J. (2011) 'Forest industries and the environment', *Heritage Newfoundland and Labrador* [Preprint].

Jacquet, Claire *et al.* (2022) 'Meta-ecosystem dynamics drive the spatial distribution of functional groups in river networks', *Oikos* [Preprint]. Available at: https://doi.org/10.1111/oik.09372.

Kawaguchi, Y., Taniguchi, Y. and Nakano, S. (2018) 'Terrestrial Invertebrate Inputs Determine the Local Abundance of Stream Fishes in a Forested Stream', *Ecological Society of America*, 84(3), pp. 701–708.

Kerekes, J.J. (1974) 'Limnological Conditions in Five Small Oligotrophic Lakes in Terra Nova National Park, Newfoundland', (August).

Kerekes, J.J. (1977) 'Factors Relating to Annual Planktonic Primary Production'.

Kidd, K.R., Aust, W.M. and Copenheaver, C.A. (2014) 'Recreational stream crossing effects on sediment delivery and macroinvertebrates in southwestern Virginia, USA', *Environmental Management*, 54(3), pp. 505–516. Available at: https://doi.org/10.1007/s00267-014-0328-5.

Knight, T.M. *et al.* (2005) 'Trophic cascades across ecosystems'. Available at: https://doi.org/10.1038/nature03962.

Larson, D.J. and Colbo, M.H. (1983) 'The aquatic insects: biogeographic considerations.', *Biogeography and ecology of the island of Newfoundland*, pp. 593–677.

Lecerf, A. and Richardson, J.S. (2010) 'Litter decomposition can detect effects of high and moderate levels of forest disturbance on stream condition', *Forest Ecology and Management*, 259(12), pp. 2433–2443. Available at: https://doi.org/10.1016/j.foreco.2010.03.022.

Leibold, M.A. *et al.* (2004) 'The metacommunity concept: a framework for multi-scale community ecology', *Ecology Letters* [Preprint]. Available at: https://doi.org/10.1111/j.1461-0248.2004.00608.x.

Leroux, S.J. *et al.* (2021) 'Cumulative effects of spruce budworm and moose herbivory on boreal forest ecosystems', *Functional Ecology*, 35, pp. 1448–1459. Available at: https://doi.org/10.1111/1365-2435.13805.

Leroux, S.J. and Loreau, M. (2012) 'Dynamics of Reciprocal Pulsed Subsidies in Local and Meta-Ecosystems', *Ecosystems*, 15(1), pp. 48–59. Available at: https://doi.org/10.1007/s10021-011-9492-0.

Leroux, S.J., Wiersma, Y.F. and Vander Wal, E. (2020) 'Herbivore Impacts on Carbon Cycling in Boreal Forests', *Trends in Ecology and Evolution*, 35(11), pp. 1001–1010. Available at: https://doi.org/10.1016/j.tree.2020.07.009.

Levins, R. (1969) 'The effect of random variations of different types on population growth', *Proceedings of the National Academy of Sciences*, 62(4), pp. 1061–1065. Available at: https://doi.org/10.1073/PNAS.62.4.1061.

Linke, S. *et al.* (2019) 'Global hydro-environmental sub-basin and river reach characteristics at high spatial resolution', *Scientific Data*, 6(1), pp. 1–15. Available at: https://doi.org/10.1038/s41597-019-0300-6.

Loreau, M., Mouquet, N. and Holt, R.D. (2003) 'Meta-ecosystems: A theoretical framework for a spatial ecosystem ecology', *Ecology Letters*, 6(8), pp. 673–679. Available at: https://doi.org/10.1046/j.1461-0248.2003.00483.x.

MacArthur, R.H. and Wilson, E.O. (1967) *The theory of island biogeography*. Princeton University Press.

MacLean, D.A. (1980) 'Vulnerability of Fir-Spruce Stands During Uncontrolled Spruce Budworm Outbreaks: A Review and Discussion', *The Forestry Chronicle*, 56(5), pp. 213–221. Available at: https://doi.org/10.5558/tfc56213-5.

MacLean, D.A. (1985) 'Effects of spruce budworm outbreaks on forest growth and yield', *Recent advances in spruce budworms research: proceedings of the CANUSA Spruce Budworms Research Symposium* [Preprint]. Available at: https://agris.fao.org/agris-search/search.do?recordID=US201302027941 (Accessed: 26 March 2022).

MacLean, D.A. *et al.* (2019) 'Positive results of an early intervention strategy to suppress a spruce budworm outbreak after five years of trials', *Forests*, 10(5). Available at: https://doi.org/10.3390/f10050448.

MacSween, J., Leroux, S.J. and Oakes, K.D. (2019) 'Cross-ecosystem effects of a large terrestrial herbivore on stream ecosystem functioning', *Oikos*, 128(1), pp. 135–145. Available at: https://doi.org/10.1111/oik.05331.

McCann, K.S. *et al.* (2021) 'Landscape modification and nutrient-driven instability at a distance', *Ecology Letters*, 24(3), pp. 398–414. Available at: https://doi.org/10.1111/ele.13644.

McInnes, P.F. *et al.* (1992) 'Effects of Moose Browsing on Vegetation and Litter of the Boreal Forest, Isle Royale, Michigan, USA', *Ecology*, 73(6), pp. 2059–2075. Available at: https://doi.org/10.2307/1941455.

Nakano, S. and Murakami, M. (2001) 'Reciprocal subsidies: Dynamic interdependence between terrestrial and aquatic food webs', *Proceedings of the National Academy of Sciences of the United States of America*, 98(1), pp. 166–170. Available at: https://doi.org/10.1073/pnas.98.1.166.

Otero, X.L. *et al.* (2018) 'Seabird colonies as important global drivers in the nitrogen and phosphorus cycles', *Nature Communications* [Preprint]. Available at: https://doi.org/10.1038/s41467-017-02446-8.

Perry, K. (2016) 'The economic impacts of constructing an ATV bypass route in the Town of Conception Bay South', *Canadian Economic Development*, (2005), pp. 1–23.

Pimlott, D. (1959) 'Reproduction and productivity of Newfoundland moose', 23(4), pp. 381–401.

Pimlott, D.H. (1953) 'Newfoundland moose'.

Potapov, P. *et al.* (2017) 'The last frontiers of wilderness: Tracking loss of intact forest landscapes from

2000 to 2013', *Science Advances*, 3(1), pp. 1–14. Available at: https://doi.org/10.1126/sciadv.1600821.

Rae, L.F., Whitaker, D.M. and Warkentin, I.G. (2014) 'Multiscale impacts of forest degradation through browsing by hyperabundant moose (Alces alces) on songbird assemblages', *Diversity and Distributions*, 20(4), pp. 382–395. Available at: https://doi.org/10.1111/ddi.12133.

Richardson, J.S. and Sato, T. (2015) 'Resource subsidy flows across freshwater-terrestrial boundaries and influence on processes linking adjacent ecosystems', *Ecohydrology*, 8(3), pp. 406–415. Available at: https://doi.org/10.1002/eco.1488.

Roberts, B. (1983) 'Soils of Newfoundland, an introduction', *Monograph Biology*, (48), pp. 107–161.

Schiesari, L. *et al.* (2019) 'Towards an applied metaecology', *Perspectives in Ecology and Conservation*, 17(4), pp. 172–181. Available at: https://doi.org/10.1016/j.pecon.2019.11.001.

Subalusky, A.L. *et al.* (2017) 'Annual mass drownings of the Serengeti wildebeest migration influence nutrient cycling and storage in the Mara River', *Proceedings of the National Academy of Sciences of the United States of America*, 114(29), pp. 7647–7652. Available at: https://doi.org/10.1073/pnas.1614778114.

Taylor, S.L. and MacLean, D.A. (2009) 'Legacy of insect defoliators: Increased wind-related mortality two decades after a spruce budworm outbreak', *Forest Science*, 55(3), pp. 256–267.

Teichman, K.J. (2013) 'Trophic cascades : linking ungulates to shrub-dependent birds and butterflies.'

Thompson, I.D. *et al.* (1992) 'Influence of moose browsing on successional forest growth on black spruce sites in Newfoundland', *Forest Ecology and Management*, 47(1–4), pp. 29–37. Available at: https://doi.org/10.1016/0378-1127(92)90263-9.

Trip, N.V.V. and Wiersma, Y.F. (2015) 'A comparison of all-terrain vehicle (ATV) trail impacts on boreal habitats across scales', *Natural Areas Journal*, 35(2), pp. 266–278. Available at: https://doi.org/10.3375/043.035.0207.

Tsakalakis, I., Blasius, B. and Ryabov, A. (2020) 'Resource competition and species coexistence in a two-patch metaecosystem model', *Theoretical ecology* [Preprint]. Available at: https://doi.org/10.1007/s12080-019-00442-w.

Tucker, M.A. *et al.* (2018) 'Moving in the Antrhopocene: Global reductions in terrestrial mammalian movements', *Science*, 469(January), pp. 466–469.

Waight, C.F. (2014) ‘Understanding all-terrain vehicle users : The human dimensions of ATV use on the island portion of Newfoundland and Labrador’, *Memorial University Research Repository* [Preprint].

Wilson, D. (1992) ‘Complex Interactions in Metacommunities , with Implications for Biodiversity and Higher Levels of Selection Author (s): David Sloan Wilson Reviewed work (s): Published by : Ecological Society of America Stable URL : http://www.jstor.org/stable/1941449’, *Ecology*, 73(6), pp. 1984–2000.

Yang, L.H. *et al.* (2008) ‘What can we learn from resource pulses?’, *Ecology*, 89(3), pp. 621–634. Available at: https://doi.org/10.1890/07-0175.1.

Zhang, B. *et al.* (2023) ‘Species distribution model identifies influence of climatic constraints on severe defoliation at the leading edge of a native insect outbreak’, *Forest Ecology and Management*, 544, pp. 378–1127. Available at: https://doi.org/10.1016/j.foreco.2023.121166.

Chapter 2: Integrating field data and a meta-ecosystem model to study the effects of multiple terrestrial disturbances on small stream ecosystem function

2.1 Introduction

Anthropogenic changes to landscapes are continuing to impact ecosystem functions; overharvesting, agricultural expansion, urbanization, resource extraction, and pollution have led to rapid environmental changes at a global scale (Steffen et al., 2007). These ongoing environmental changes alter important habitat for many species, resulting in biodiversity loss and modified global nutrient cycles. Such changes are further intensified by the progression of climate change (Crutzen, 2002, 2006; Dalby, 2013). Since landscapes are assemblages of highly connected ecosystems, these stressors can propagate throughout the region with effects on local ecosystems that are challenging to predict. For example, a review by Campbell et al. (2009) shows that climate change is expected to have widespread effects on biogeochemical cycling through changes to plant physiology, forest productivity, soil processes, hydrology, and consequently species composition. Most ecological studies focus on one ecosystem, but we need studies that look at cross-ecosystem connections to predict how local ecosystems and landscapes will function under global change (Harvey *et al.*, 2017).

Meta-ecosystem theory has emerged as a framework to understand how ecosystems are connected throughout the landscape by flows of energy, matter, and organisms (Harvey et al., 2021; Loreau et al., 2003; Massol et al., 2011, Guichard and Marleau, 2021). Ecosystems are open systems, receiving subsidies of nutrients and other forms of matter across a range of spatial and temporal scales with effects dependent on the timing, quantity, and duration of these "subsidy pulses" (Polis et al., 1997; Yang, 2004; Leroux & Loreau, 2012, 2015). Meta-ecosystem models can be powerful tools to make predictions about properties of connected ecosystems, such as patterns in diversity, productivity, and ecosystem stability (Gravel *et al.*, 2010; Leroux and Loreau, 2012; Harvey *et al.*, 2021; Jacquet *et al.*, 2022; Pichon *et al.*, 2023). However, these models are challenging to apply (and rarely applied) to the finite spatial area and temporal scales relevant for real-world application (Gounand et al., 2018; Harvey et al., 2021; Marleau et

al., 2014). In addition, most meta-ecosystem models (see review in Guichard & Marleau, 2021 but see Leroux & Loreau, 2012 and Harvey et al., 2021) assume flows occur across ecosystems of the same type (e.g., terrestrial-terrestrial fluxes) whereas flows across the boundaries of different ecosystems (e.g., aquatic-terrestrial) are very common in nature (see review in Osakpolor et al., 2021). Consequently, there is a need for meta-ecosystem models that incorporate more empirically based interaction equations for cross-ecosystem flows of all types to predict how these coupled systems will respond to global changes and inform natural resource management (Gounand *et al.*, 2018).

The riparian forest-stream is a common meta-ecosystem in many biomes and is threatened at both a global and local scale. For example, forest harvesting has led to declines in stream biodiversity in tropical (Iwata, Nakano and Inoue, 2003), temperate (Lecerf and Richardson, 2010), and boreal (Tanentzap *et al.*, 2014) ecosystems. Common drivers of forest harvesting mediated declines in stream biodiversity include increasing nutrient deposition (Keenan and van Dijk, 2010), decreasing shading (Kiffney, Richardson and Bull, 2003), and increased temperature (Johnson and Jones, 2000) in streams with harvested compared to non-harvested catchments. Here, we integrate empirical data with mathematical modelling to create a meta-ecosystem model based on a real boreal riparian forest-stream ecosystem. We use a meta-ecosystem model that captures key food web structure in our empirical system to untangle specific mechanisms or explanations for the patterns in our empirical data.

We conduct our study in the boreal ecosystem of the island of Newfoundland, an area undergoing regular disturbances. A hyper-abundant moose population (introduced to the island in 1878 for sport hunting; Pimlott, 1953) has transformed the landscape by selectively browsing on canopy-forming balsam fir (*Abies balsamea*) and slowing forest succession (Leroux et al., 2020, 2021; Gosse 2011). Spruce budworm (*Choristoneura fumiferana)* and Hemlock looper (*Lambdina fiscellaria*) are moths native to North America, known for population spikes (i.e., “outbreaks”) that occur in 30-40 year and 15-20 year cycles respectively, and cause severe tree defoliation (MacLean, 1980; Arsenault *et al.*, 2016). These outbreaks are occurring with more frequency and intensity, resulting from environmental changes

associated with climate change (Régnière, St-Amant and Duval, 2012). Additionally, strong all-terrain vehicle (ATV) culture driven by sport hunting has resulted in many unregulated trail networks being developed across the island (Waight, 2014).

Logging and insect outbreaks reduce the density of canopy forming evergreen tree species such as balsam fir and black spruce (*Picea mariana*), converting mature forest to early successional forest (Nuttle *et al.*, 2013), which are prevented from regenerating by moose herbivory, instead forming "moose mediated meadows" (Leroux *et al.*, 2021). Unpaved trails increase erosion and sediment loading into local streams and reduce stream quality and productivity within the watershed (Ryan, 1991; Chin *et al.*, 2004). These impacts on the terrestrial ecosystem can have an indirect impact on aquatic systems (MacSween et al., 2019); reduced tree density is expected to increase stream temperature (Johnson and Jones, 2000), which can indirectly have a positive effect on primary productivity in the stream (Kiffney, Richardson and Bull, 2003). Watersheds with less tree cover have less forest canopy rainfall interception, which increases the transport of dissolved nutrients (Gundersen *et al.*, 2010; Keenan and van Dijk, 2010) and increases the total nitrogen and specific conductivity of the runoff entering the stream (Richardson and Béraud, 2014). Increased sediment levels have been associated with decreased primary productivity and abundance of macroinvertebrates and fish, all of which are an area of concern for Newfoundland as many Atlantic salmon populations across the island are in decline (Ryan, 1991; Cheong *et al.*, 1995). These disturbances do not occur independently, and their combined effects have impacts at the landscape extent. It is therefore important to understand mechanisms that connect riparian forest and streams in the boreal ecosystem as this biome is changing due to human activity, and consequently affecting stream functioning in boreal forests (Leroux, Wiersma and Vander Wal, 2020).

Here we integrate *in situ* data collection, geospatial analysis, and mathematical modelling, heeding recent calls (see Gounand et al., 2018) for creating a framework for connecting meta-ecosystem models to real landscapes (Figure 1). Specifically, we 1) empirically measure the impact of terrestrial disturbances on boreal stream function at multiple spatial extents; 2) use these field data to parameterize a two-patch,

terrestrial-aquatic meta-ecosystem model that considers the effects of terrestrial disturbances on small streams at multiple spatial extents; and 3) use the meta-ecosystem model to predict aquatic primary and secondary biomass stocks and productivity under different disturbance scenarios. While the observational study looks at net effects of multiple disturbances (since we cannot isolate individual disturbances), the meta-ecosystem model allows us to tease apart relative and cumulative effects of disturbances on stream functions and test a greater range of disturbance conditions.

2.2 Methods

2.2.1 Empirical study

2.2.1.1 Study area

We established our field study in Gros Morne National Park (GMNP) on the west coast of the island of Newfoundland, Canada, and Terra Nova National Park (TNNP) along the inlets of Bonavista Bay, Newfoundland. GMNP is best described by the Northern Peninsula Forest ecoregion, where forests are dominated by balsam fir (*Abies balsamea*) and black spruce (*Picea mariana*), with *Kalmia* heath covering poorly drained areas (Bell, 2002). TNNP is in the Central Newfoundland Forest ecoregion, which has forests dominated by black spruce, balsam fir, white birch, and trembling aspen (Bell, 2002). Newfoundland is made up of relatively small drainage basins, as no part of the island is more than 130 km from a coast. Many ponds and bogs are present along streams, and the movement of water through the dense layers of peat acts to regulate stream flow and gives the water a transparent brown colour. The Labrador Current creates a seasonal lag in temperature, so most aquatic habitats are relatively cold, with a maximum temperature ranging between 13-23°C depending on the location (Kerekes, 1974). Streams tend to be acidic with low levels of dissolved material (Larson and Colbo, 1983), and are limited in primary production by phosphorus (Kerekes, 1977). The low pH, low concentration of dissolved nutrients, and high colouration of the water contributes to low aquatic productivity and diversity of aquatic insects (Larson and Colbo, 1983).

2.2.1.2 Site selection

We sampled 14 streams in GMNP and 14 streams in TNNP for a total of 28 study sites (Table A1, Figure 2). We selected streams within a Strahler stream order range of 1-4 and with a low gradient (and more than 50 m from a cascade or waterfall) to represent a similar aquatic habitat across sites. Many streams had been previously sampled by the parks as part of regular monitoring programs. We selected sites in areas that ranged from undisturbed to high disturbance from insect outbreaks and logging (based on % disturbed area in the stream catchment) and unpaved roads (based on road density – see below). Within each stream, we selected a study reach that contained riffles for collecting benthic invertebrates and periphyton samples and a run for sampling water chemistry following the Canadian Aquatic Biomonitoring Network (CABIN) guidelines (*CABIN Field Manual*, 2009). The total length of the study reach was five times the estimated bank full width of the stream as per the CABIN guidelines. All streams were part of distinct catchments to ensure independence between sites by avoiding "nesting" sites. We ensured that all reaches were more than 50 m downstream of the closest pond or waterfall, more than 50 m away from the nearest road, and more than 1 km from the ocean (*CABIN Field Manual*, 2009).

2.2.1.3 Field data collection and processing

We sampled all sites in a short period, between July 5 and August 4, 2022, to minimize temporal variation in stream functioning (see Table A1 in appendix A for sampling dates for each site). We followed standard protocols from CABIN to complete a qualitative assessment of each site and randomly select locations to measure channel morphology, water chemistry, benthic invertebrates, and periphyton. These measurements were used to create the following metrics for stream quality: benthic invertebrate biomass (gcm^{-2}), EPT index, periphyton biomass (gcm^{-2}), specific conductivity (SC; μScm^{-}), total dissolved nitrogen (TDN; mgL^{-1}), and proportion of benthic invertebrate functional feeding groups (see full details on sample collection and processing in appendix A).

2.2.1.4 Quantifying disturbance with geospatial data

For each study site we calculated the catchment upstream of the sampling location using QGIS (ver. 3.26.3; QGIS Development Team, 2021). We then quantified the terrestrial disturbances occurring in the

catchment of each study stream by manually outlining clearings in the forest greater than 10 m at the 1:2500 scale and classified them into four categories: insect outbreak, logging, cleared (i.e., trees removed from the shoulder of the highway or from private property), and forest fire (present at one site), noting that many of these sites were influenced by moose herbivory. Similarly, we manually digitized trails and paved roads using the Google satellite base map (2021) at the 1:2500 scale, referencing shapefiles of highways, snowmobile paths, and hiking trails provided by the park ecologists. As an alternative measure of combined anthropogenic disturbance in the watershed, we also included a raster of global human impact index data collected by the Government of Newfoundland and Labrador and Nature Conservancy Canada (2013) to determine regions that were more heavily impacted by anthropogenic activity, as these broader scale "human influence maps" are commonly used for management in boreal ecosystems (Vernier *et al.*, 2022). We used three nested spatial extents to quantify terrestrial disturbances surrounding each stream site following Roth et al. (1996) and Scholl et al. (2022): the catchment extent (upstream of each stream sampling location), the riparian extent (100 m on either side of the stream and upstream tributaries within the catchment extent), and the local extent (the closest 10% of the catchment area upstream of the sampling location); see appendix B for full details.

We created three metrics for quantifying terrestrial disturbances at each spatial extent: 1) percent disturbed forest area (forest that had been cleared, logged, experienced severe defoliation from an insect outbreak or experienced a recent forest fire; many of these areas had been converted to moose mediated meadow); 2) unpaved road density (unpaved trails or roads, including ATV trails, hiking trails, and logging roads); and 3) percent high human impact index (area with a human impact intensity ranking of 7-10 on a scale from 0-10). We also calculated percent wetland, lake, soil barrens, and rock barrens within each spatial extent as covariates in the statistical analysis since these land classes are expected to influence stream quality (Kerekes, 1974).

2.2.1.5 Statistical analysis of empirical data

We fit a general linear model to seven key stream metrics (i.e., benthic invertebrate biomass, EPT index, periphyton biomass, substrate embeddedness, SC, TDN, and proportion of the shredder functional feeding group in the benthic invertebrate sample) with disturbances as predictors (i.e., percent forest disturbance, trail density, and percent high human impact index) using R programming software (ver. 4.2.2; R Core Team, 2020). We also included stream characteristics of depth, width, and flow as covariates in these models, and we rescaled all model parameters to range from 0-1 using max-min scaling so we could compare the magnitude of the resulting relationships among variables. For each stream metric (i.e., response), we compared seven variations of predictor variable combinations to a null model (see Table 6 and Tables A9-A11) and selected the top ranked model using Akaike Information Criterion corrected for small sample size (AICc; Akaike, 1998). The goal of this analysis was to determine the relationship between terrestrial disturbances and the stream ecosystem to inform how we structured the meta-ecosystem model (see appendix B for details on the statistical analysis). We combined data from both parks for these analyses after determining that the streams had similar characteristics (Table 1).

2.2.2 Meta-ecosystem model

2.2.2.1 Model description and development

We developed a two-patch, terrestrial-aquatic meta-ecosystem model representing key stocks and flows of limited nutrients in the riparian forest and stream ecosystems at our field sites in Newfoundland (Figure 3; Tables 2 and 3). The riparian forest patch had three trophic levels: primary producers (trees, P_t), leaf litter that falls into the stream (L_t), and inorganic nutrients in the soil (N_t). The aquatic system had three trophic levels: herbivores (benthic invertebrates, H_a), primary producers (periphyton, P_a), and dissolved inorganic nutrients (N_a). N_t is taken up by P_t and P_a with uptake rate α, and H_a feeds on P_a with uptake rate β and efficiency e. A portion of P_t moves to L_t at rate ϵ, and a portion of L_t is foraged on by H_a at rate δ and efficiency ρ. Remaining leaf litter is recycled into N_a at rate γ. P_a, P_t, and H_a have a death rate of θ_a, θ_t, and τ_a respectively, and their biomass leaves the ecosystem at proportions $(1-\mu_a)$, $(1-\mu_t)$, and $(1-\eta_a)$, while the remaining biomass is recycled back into N_a or N_t by μ_a, μ_t, and η_a respectively. N enters the system at rate λ and leaches out at rate l. N moves between the terrestrial at aquatic system at rate ψ. Following other

meta-ecosystem models (e.g., Leroux & Loreau 2012), we did not include the decomposer community in the model, but it was represented by the recycling of nutrients from higher trophic levels back into inorganic nutrients.

The meta-ecosystem model is represented by the following group of ordinary differential equations:

$$\frac{dP_t}{dt} = \alpha_t P_t\, N_t - \theta_t P_t - \epsilon P_t \quad (1)$$

$$\frac{dL_t}{dt} = \epsilon P_t - \delta L_t H_a - \gamma L_t \quad (2)$$

$$\frac{dN_t}{dt} = \lambda_t + \theta_t \mu_t P_t + \psi_a N_a - \alpha_t P_t\, N_t - \psi_t N_t - l_t N_t\, n \quad (3)$$

$$\frac{dP_a}{dt} = \alpha_a P_a N_a - \beta_a H_a P_a - \theta_a P_a \quad (4)$$

$$\frac{dH_a}{dt} = \beta_a e H_a P_a + \delta \rho L_t H_a - \tau_a H_a \quad (5)$$

$$\frac{dN_a}{dt} = \lambda_a + \tau_a \eta_a H_a + \theta_a \mu_a P_a + \gamma L_t + \psi_t N_t - \psi_a N_a - \alpha_a P_a N_a - l_a N_a \quad (6)$$

Following Loreau (2010), we define productivity in the model as:

$$P_t\ productivity = \alpha_t P_t N_t$$

$$H_a\ productivity = \beta_a e H_a P_a + \delta \rho L_t H_a$$

$$P_a\ productivity = \alpha_a P_a N_a$$

We used Mathematica (Wolfram Research, 2022) to solve for all possible equilibria, ten in total. Of these, two were feasible and we selected the equilibrium that more frequently resulted in stable and feasible equilibrium states (see appendix B for details). Using R (ver. 4.2.2; R Core Team, 2020), we then generated random parameter combinations within a range of 0-10 (or between 0-1 if a proportion) and determined the equilibrium densities of each trophic level in the meta-ecosystem for each parameter combination using analytical equilibrium equations generated in Mathematica. We then selected for

feasible equilibrium states (non-negative trophic level densities) for all state variables (see Jacquet et al., 2022) and further selected for locally stable equilibria. For local stability analysis, we used Mathematica to find the Jacobian matrix and the base "eigen" function in R to determine the leading eigenvalue of the Jacobian matrix evaluated for each parameter set. We then selected the first 1000 feasible and locally stable parameter combinations to use for each disturbance level simulated – see below. This process took us between 200,000-300,000 parameter combinations to achieve (see appendix B).

We performed a global sensitivity analysis (GSA) on each trophic level and productivity metric of the model to identify the parameters creating the most uncertainty in the model (i.e., the most important parameters), following Bellmore et al. (2014) and Harper et al. (2011) (see appendix B).

We assessed the model at levels 0 (concept) and 1 (state variables) in comparison to our empirical data according to the CSPS framework for model validation (Hipsey *et al.*, 2020). See Chapter 3 section 3.3 for a discussion on best practices in validating models.

2.2.2.2 Simulating disturbance to the terrestrial system

Using patterns found in our empirical data and assumptions from literature, we simulated terrestrial disturbances by changing key parameter values in each of the feasible and stable equilibria (see above) to represent death and or removal of trees and increased sediment loading of the stream.

Since logging removes tree biomass from terrestrial ecosystems (Poudel *et al.*, 2012), we simulated logging in the terrestrial ecosystem by increasing the death rate of trees (θ_t) in a range from 0-10 t^{-1} by increments of 0.5 while keeping recycling of the trees back into the soil (μ_t) at a low proportion (μ_t=0-0.5). Insect outbreaks also increase tree mortality (MacLean, 1980) but do not remove tree biomass from the ecosystem, so we simulated an insect outbreak by increasing θ_t in a range from 0-10 t^{-1}, but kept the recycling rate high (μ_t=0.5-1) since dying trees are recycled back into the soil rather than removed (as is done with logging). We simulated increased erosion and sediment loading from ATV trails and logging roads by decreasing the uptake rate of periphyton (α_a) and benthic invertebrates (β_a) in a range from 0-1 to represent poor water conditions leading to reduced ability for periphyton to access nutrients and sunlight,

and for benthic invertebrates to collect food and find appropriate habitat (Ryan, 1991). We simulated each increment of these disturbance simulations in each of the stable equilibria to represent changes to an originally undisturbed ecosystem.

We compared these outcomes (i.e., biomass stocks, productivity, flux) to the empirical data to validate the connection between the real and theoretical ecosystems. However, the meta-ecosystem model is used to make predictions within and across empirically observed patterns (i.e., what happens if we increase forest harvesting?) and therefore, the breadth of model predictions is beyond our empirical study. Following White et al. (2014), we do not conduct statistical analyses on model simulations.

2.3 Results

2.3.1 Empirical data

Disturbance from logging and insect outbreaks covered a similar percentage of the study area at each spatial extent (5.77-9.12% for insect outbreaks and 7.90-9.32% for logging), with logging covering a slightly larger area at all but the local extent (Table 4). Both unpaved road density and percent high human impact were greatest at the local extent (Table 4). Streams had a mean reach length of 21.79 ± 8.84 m and mean width of 3.67 ± 2.02 m (Table 5). Benthic invertebrates had a larger mean biomass than periphyton (2.10 ± 1.77 $mg \cdot cm^{-2}$ and 0.16 ± 0.14 $mg \cdot cm^{-2}$ respectively; Table 5).

We observed similar qualitative effects of terrestrial disturbance on stream quality at all extents with small differences in magnitude. Benthic invertebrate biomass per cm^2 had a positive relationship with road density ($\beta = 0.61 \pm 0.16$) and a negative relationship with human impact index ($\beta = -0.25 \pm 0.10$) in top models at the local extent. In addition, percent shredders (a proxy for allochthonous inputs; see appendix A) decreased with human impact index at the local extent ($\beta = -0.29 \pm 0.10$), forest disturbance at the riparian extent ($\beta = -0.21 \pm 0.17$), and unpaved road density at the catchment extent ($\beta = -0.12 \pm 0.15$). Specific conductivity had a positive relationship with road density in top models at the riparian and catchment extent ($\beta = 0.38 \pm 0.13$and $\beta = 0.30 \pm 0.14$ respectively). Specific conductivity also had a positive relationship with human impact at the riparian ($\beta = 0.23 \pm 0.13$) and catchment ($\beta = 0.32 \pm 0.14$)

extents. Periphyton biomass per cm^2, total dissolved nitrogen, embeddedness, and EPT index did not have a strong relationship with any disturbance metrics (Figure 4; Table 6, Figure A6, Tables A9-A11). See appendix A for further details and results from the statistical analysis.

2.3.2 Disturbance simulations

Model simulations of forest disturbance show a negative relationship between benthic invertebrate (H_a) biomass and disturbance (increasing tree death (θ_t) and removal ($1-\mu_t$) from the system), and H_a productivity shows a similar relationship (Figure 5A and 5B). Periphyton (P_a) biomass has a positive relationship with forest disturbance, while P_a productivity follows a similar pattern to H_a productivity (Figure 5C, 5D). Simulations of logging (high tree death and low recycling; Figure 5, top right quadrant) have lower productivity but similar H_a and P_a biomass compared to the undisturbed system (Table B10). Insect outbreak simulations (Figure 5, lower left quadrant) show greater productivity and H_a biomass, but lower P_a biomass compared to the undisturbed system (Table B10). Overall, H_a biomass and productivity was slower to decline under increasing tree death (θ_t) than periphyton (Figure 5A-C). These patterns relate to trends in the empirical data where periphyton biomass had a stronger negative relationship with tree disturbance (Tables A9-A11).

Simulations of unpaved road density show that benthic invertebrate (H_a) biomass and productivity do not change much as ATV trail density increases (assuming both uptake rates decrease proportionally) and is greatest at low H_a uptake and high P_a uptake (Figure 6A). Periphyton (P_a) biomass is greatest at a very low uptake rate by H_a but is not greatly changed with the region of low to moderate road density (Figure 6C). P_a productivity is similar to H_a, greatest at low H_a uptake rate and high P_a uptake (Figure 6D). Biomass and productivity for both H_a and P_a are comparable to the undisturbed system (Table B10). These trends are also similar to the fitted empirical models, where benthic invertebrate biomass increased with road density and periphyton biomass has a weakly positive relationship (Figure 4, Figure A6, Tables A9-A11).

Note that to simplify the model, we omitted the effect of changes to leaf litter quality at disturbed sites (increasing proportion of early successional, deciduous trees such as alder that are more easily foraged on by benthic invertebrates), and the influence of nitrogen fixation by a large density of alder at disturbed areas increasing stream nitrogen concentration (Wipfli and Musslewhite, 2004). Additionally, while moose are an invisible presence in the model as there is no forest succession after forest disturbance, we did not incorporate them as a trophic level that could change in magnitude to simulate the changes in moose density across the island.

2.4 Discussion

Statistical analysis of our empirical data showed that unpaved road density had a positive relationship with specific conductivity and (surprisingly) benthic invertebrate biomass; forest disturbance had a negative relationship with shredders; and human impact index had a negative relationship with benthic invertebrate biomass and percent shredders but a positive impact on specific conductivity (Figure 4, Table 6). While some results seem straightforward (e.g., road density and human impact index have a positive relationship with specific conductivity through increased erosion rates), we could not determine the mechanisms for most of these effects within our empirical study (see appendix A section 5 for a thorough discussion of the empirical results).

It is well understood that local stream habitat, diversity, and productivity are influenced by the surrounding landscape through many spatially nested mechanisms, where characteristics of the stream catchment (i.e., slope, soil and rock type, vegetation) influence local stream habitat and biota through highly connected and complex processes, and anthropogenic activity can directly influence stream quality by changing components of these mechanisms at the landscape scale (Allan, 2004). While it was not possible to simply determine the reason for these patterns through analysis of our empirical data, we were able to use the disturbance simulations in our meta-ecosystem model to help elucidate potential mechanisms behind these empirical trends and to look at a broader range or gradient in disturbance than

observed in our empirical sites. Our simulations suggest that trophic interactions and energy flux may be key mechanisms that impact outcomes of ecosystem connections.

2.4.1 Mechanisms behind the influence of terrestrial disturbance on stream productivity and biomass

Our model suggests two main mechanisms behind the effects of terrestrial disturbance on stream ecosystems: apparent competition and energy flux.

1) Apparent competition occurs when two resources share a common consumer, where an increase in one resource may lead to an increase in the consumer with subsequent negative effects on the other resource (Holt, 1977). This process may be occurring in our model and in natural systems when benthic invertebrates consume *in situ* allochthonous resources (e.g., leaf litter) along with periphyton. When leaf litter is an abundant resource (i.e., there are plenty of healthy trees), benthic invertebrate biomass can grow and increase foraging pressure on periphyton, decreasing periphyton biomass despite high periphyton productivity (Figure 5A-E). While apparent competition may be a common mechanism governing stream (Baxter, Fausch and Saunders, 2005), lake (Schoen *et al.*, 2015), forest (Cobb, Meentemeyer and Rizzo, 2010) and grassland (Orrock, Holt and Baskett, 2010) function, we show how different disturbances can modulate the strength of apparent competition and therefore the functioning of small streams. Specifically, disturbances such as logging can reduce litterfall and can reduce the strength of apparent competition in streams leading to higher levels of periphyton (and potentially eutrophication of the ecosystem) compared to streams in mature forests.

2) Energy availability may also play a role in the relationship between periphyton biomass and terrestrial disturbance. Based on the theory of exploitation ecosystems (Oksanen *et al.*, 1981), more energy at basal levels supports more (and larger) trophic levels. The removal of trees through logging or road development, which impacts terrestrial primary production and energy, may reduce energy available for persistence of higher trophic levels in forest and adjacent stream ecosystems (see Hernandez et al., 2005; Tanentzap et al., 2014). We saw signs of this in our empirical data where there was a lower proportion of

shredders in areas with greater unpaved road density, indicating fewer allochthonous inputs (Tables A7-A9).

While we used the mechanism of energy flux (i.e., reducing nutrient uptake rates) to simulate the presence of ATV trails and logging roads, experimental simulations of nutrient enrichment, sediment loading, and increasing water temperature (outcomes associated with forest degradation and increased erosion) by Piggott et al. (2012) found that these interactions are highly complex. In their experiments, sediment loading had a positive effect on benthic invertebrate and periphyton biomass up to intermediate levels before it began to notably reduce nutrient uptake and light availability, with benthic invertebrates being more tolerant of suspended sediment (similar to the outcomes from our empirical models; Tables A9-A11). However, the sediment type, associated nutrient subsidy, water temperature, and species present in the system strongly affected the nuance of these relationships (Piggott *et al.*, 2012).

Terrestrial disturbances can result in many changes to energy flux, such as increasing nutrient leaching from soil or increasing the particulate organic material in runoff (Stone and Wallace, 1998). While our model had energy flux between the terrestrial and aquatic systems through L_t and N_t, it was simplistic in how disturbance only removed tree biomass rather than providing a subsidy of resources by increasing the rate of N_t flowing into the stream. Future models could include more nuance in how terrestrial disturbances provide fluxes of energy into aquatic systems (see Jacquet et al., 2022).

2.4.2 Thresholds for stream community response to terrestrial disturbance

Modelling disturbance in the meta-ecosystem helped inform how different components of the stream ecosystem may respond at different disturbance intensities. Our model allowed us to explore a larger range of disturbance intensities than were present at our study sites, and therefore understand how levels of disturbance observed in our larger study landscape may impact streams. Spruce budworm outbreaks can lead to death of forest stands and a significant amount of deadwood (MacLean, 1985), but our model simulations of this forest disturbance showed that insect outbreaks may have a lower impact on stream productivity and invertebrate community biomass compared to the removal of trees through logging

(Figure 5). A similar distinction was found by Hernandez et al. (2005) when comparing the effects of clear cut timber harvest to other less-intensive timber harvest on Alaskan streams. While periphyton appears to be more sensitive to forest disturbance than benthic invertebrates, high tree recycling present under even severe insect outbreaks may allow for periphyton productivity to be maintained via a nutrient subsidy, while the lower tree recycling found in logging scenarios may result in a much more dramatic decrease in stream primary productivity (Figure 5). This also suggests that maintaining moderate recycling of tree biomass by following more conservative logging practices may help reduce the impact on local stream ecosystems (Mori and Kitagawa, 2014).

Our simulations of ATV trails and logging roads indicated distinct thresholds for both biomass and productivity in benthic invertebrates and periphyton (Figure 6). The main mechanism for this threshold is foraging pressure of benthic invertebrates on periphyton; periphyton biomass only decreases along the x axis where benthic invertebrate uptake is decreasing (Figure 6B). Piggott et al. (2012) found that other thresholds exist for the effect of sediment loading in their stream experiments: low to moderate sediment load increased both periphyton and benthic invertebrate biomass as it provided a heterogeneous environment for foraging and growth, while high sediment levels had a negative effect on both communities by reducing light availability for periphyton and clogging the breathing apparatus of the benthic invertebrates (Piggott et al., 2012). The proportions of sediment compared to organic material in the suspended material strongly influences stream productivity as well, where high sediment concentrations have been shown to negatively impact productivity, even in nutrient limited streams such as ours (Lloyd, Koenings and Laperriere, 1987).

In our empirical data, periphyton biomass did not have a strong relationship with the range of trail density found at the sites, suggesting that suspended solids may have not reached the threshold conditions required to meaningfully reduce nutrient uptake rate by benthic invertebrates and periphyton (see threshold ranges in Bilotta & Brazier, 2008).

2.4.3 Disturbance in nutrient limited ecosystems

Since freshwater ecosystems in Newfoundland tend to have low productivity due to nutrient limitation (Larson and Colbo, 1983), it is possible that terrestrial disturbance has a different relationship at our study sites than it would in a system with greater nutrient availability. The main reason behind the increase in periphyton and benthic invertebrate biomass in areas with greater disturbance may be the nutrients introduced to the aquatic system through increased leaching from soil after tree removal and ATV or logging road development. Hernandez et al. (2005) observed similar relationships between logging and stream productivity in nutrient-poor streams in southeastern Alaska. These disturbances may be adding limiting nutrients such as nitrogen and phosphorus that allow for greater primary productivity which can then sustain a larger benthic invertebrate community. Thus, when considering the subsidy-stress spectrum (Odum, Finn and Franz, 1979) there is perhaps a larger stress tolerance for these nutrient limited ecosystems when they provide an otherwise rare subsidy of resources.

It is also possible that food web dynamics within the benthic invertebrate community are at play (see MacSween et al., 2019); future work could include measuring isotopes to have a better knowledge of food sources in these systems and how they affect the mechanisms linking terrestrial and stream ecosystems (see review in Layman et al., 2012). For example, Rasmussen (2010) uses isotopes to investigate proportional resource contributions to benthic invertebrates in streams.

2.4.4 Value of fitting theoretical models to empirical data

It can be incredibly challenging to determine the empirical associations between land use and stream responses because of the covariation in anthropogenic and natural gradients within the landscape, mechanisms occurring across multiple spatial extents, non-linear responses to stress, and the difficulty of separating historical from present-day effects (Allan, 2004).

Similarly, the empirical data we collected shows the effect of total disturbance from insect outbreaks, logging, ATV trails, and other factors that we did not measure, making it virtually impossible to point to specific mechanisms behind the trends we found in the data. Simulating disturbance in our meta-

ecosystem model lets us parse out the relative and combined effects of multiple disturbances on different components of recipient stream ecosystems. Additionally, models allow us to calculate ecosystem properties that are time-consuming and challenging to measure accurately (such as rates of productivity).

By integrating empirical data (i.e., production and movement of resources within real ecosystems) into our meta-ecosystem model, we are not only answering important ecological questions about dynamics within boreal riparian ecosystems, but also contributing to the development of methods for studying these questions in other contexts (Gounand et al., 2018).

2.4.5 Integrating meta-ecosystem models and land use policy

The ultimate goal of integrating empirical and theoretical data is to encourage the use of meta-ecosystem modelling when developing policies for specific land use scenarios. As discussed, models allow us to have more indicators of ecosystem functions, have more insight into the mechanisms behind the outcomes of landscape change, and have the power to make predictions about future scenarios that are not practical to study in the field (see review in DeAngelis et al., 2021).

As the environment continues to rapidly change at a global scale, it becomes important to adapt ecosystem policies to match these changes. To do this we must also consider the dynamic nature of ecosystems rather than developing policies with static end points as the goal (Garmestani *et al.*, 2021). This is another area where theoretical models add value to policy making, as they allow for forecasting and predictions rather than relying on relationships and inferences from static data collected during a single field sampling event to develop new policies. Linking the two approaches allows for these predictions to be tailored to a specific landscape and mechanism of interest; we should be working to improve the integration of multiple fields not only in research but in environmental policy as well (Mayer *et al.*, 2016). It is also important to integrate policy for multiple disturbances (such as logging and road development) as they may have a synergistic effect on the recipient ecosystem.

Here, we developed a meta-ecosystem model that can incorporate the disturbances caused by logging, insect outbreaks, and ATV trail and logging road development that can be used to inform integrated

management decisions along with our general understanding of cross-ecosystem effects. These model predictions have an application to Newfoundland directly, informing landscape management, and trail development on the island, but following this framework can allow similar models to be used as a tool for a range of wildlife management decisions and policies. Including meta-ecosystem models in landscape management and policy making allows us to strike a balance between societal and ecological benefits and concerns, enabling more informed decision making and adding to our understanding of the indirect effects disturbances have across space and time.

2.5 Code and data availability

All code and data are available in the associated GitHub repository:

(https://github.com/hfadams/meta_ecosystem_model).

References

Akaike, H. (1998) 'Information Theory and an Extension of the Maximum Likelihood Principle', *Selected Papers of Hirotugu Akaike*, 29(6), pp. 655–662. Available at: https://doi.org/10.1007/978-1-4612-0919-5_38.

Allan, J.D. (2004) 'Landscapes and riverscapes: The influence of land use on stream ecosystems', *Annual Review of Ecology, Evolution, and Systematics*, 35(2002), pp. 257–284. Available at: https://doi.org/10.1146/annurev.ecolsys.35.120202.110122.

Arsenault, A. *et al.* (2016) 'Unravelling the past to manage Newfoundland's forests for the future', *Forestry Chronicle*, 92(4), pp. 487–502. Available at: https://doi.org/10.5558/tfc2016-085.

Baxter, C. V., Fausch, K.D. and Saunders, W.C. (2005) 'Tangled webs: Reciprocal flows of invertebrate prey link streams and riparian zones', *Freshwater Biology*, 50(2), pp. 201–220. Available at: https://doi.org/10.1111/j.1365-2427.2004.01328.x.

Bell, T. (2002) 'Ecoregions of Newfoundland', *Heritage Newfoundland and Labrador* [Preprint]. Available at: https://www.heritage.nf.ca/articles/environment/ecoregions-newfoundland.php.

Bellmore, J.R. *et al.* (2014) 'The response of stream periphyton to Pacific salmon: Using a model to understand the role of environmental context', *Freshwater Biology*, 59(7), pp. 1437–1451. Available at: https://doi.org/10.1111/fwb.12356.

Bilotta, G.S. and Brazier, R.E. (2008) 'Understanding the influence of suspended solids on water quality

and aquatic biota', *Water Research*, 42(12), pp. 2849–2861. Available at: https://doi.org/10.1016/j.watres.2008.03.018.

Campbell, J.L. *et al.* (2009) 'Consequences of climate change for biogeochemical cycling in forests of northeastern North America', *Canadian Journal of Forest Research*, 39(2), pp. 264–284. Available at: https://doi.org/10.1139/X08-104/ASSET/IMAGES/LARGE/X08-104F4.JPEG.

Cheong, A.L. *et al.* (1995) 'A discussion of suspended sediment in the Takla Lake region: the influence of water discharge and spawning salmon', *Canadian technical report of fisheries and aquatic sciences* [Preprint].

Chin, A. *et al.* (2004) 'Effects of all-terrain vehicles on stream dynamics', *Ouachita and Ozark Mountains symposium: ecosystem management research.*, pp. 292–296. Available at: http://www.treesearch.fs.fed.us/pubs/viewpub.jsp?index=6475.

Cobb, R.C., Meentemeyer, R.K. and Rizzo, D.M. (2010) 'Apparent competition in canopy trees determined by pathogen transmission rather than susceptibility', *Ecology*, 91(2), pp. 327–333. Available at: https://doi.org/10.1890/09-0680.1.

Crutzen, P.J. (2002) 'Geology of Mankind', *Nature* [Preprint], (415).

Crutzen, P.J. (2006) 'The "anthropocene"', in *Earth system science in the anthropocene*. Springer Berlin Heidelberg, pp. 13–18.

Dalby, S. (2013) 'Biopolitics and climate security in the Anthropocene', *Geoforum*, (49), pp. 184–192.

DeAngelis, D.L. *et al.* (2021) 'Towards Building a Sustainable Future: Positioning Ecological Modelling for Impact in Ecosystems Management', *Bulletin of Mathematical Biology*, 83, p. 107. Available at: https://doi.org/10.1007/s11538-021-00927-y.

Garmestani, A. *et al.* (2021) 'Panarchy: opportunities and challenges for ecosystem management', *Frontiers in Ecology and the Environment* [Preprint], (10). Available at: https://doi.org/10.1002/fee.2264.Submit.

Gounand, I. *et al.* (2018) 'Meta-Ecosystems 2.0: Rooting the Theory into the Field', *Trends in Ecology and Evolution*, 33(1), pp. 36–46. Available at: https://doi.org/10.1016/j.tree.2017.10.006.

Government of Newfoundland and Labrador and Nature Conservancy Canada (2013) 'Newfoundland and Labrador Human Footprint: A Snapshot of Human Influence on the Landscape', *Parks and Natural Areas Division, Department of Environment and Conservation*, p. 25.

Gravel, D. *et al.* (2010) 'Source and sink dynamics in meta-ecosystems', *Ecology*, 91(7), pp. 2172–2184. Available at: https://doi.org/10.1890/09-0843.1.

Guichard, F. and Marleau, J. (2021) *Meta-Ecosystem Dynamics: Understanding Ecosystems Through the Transformation and Movement of Matter*. Available at: http://www.springer.com/series/10049.

Gundersen, P. *et al.* (2010) 'Environmental services provided from riparian forests in the nordic countries', *Ambio*, 39(8), pp. 555–566. Available at: https://doi.org/10.1007/s13280-010-0073-9.

Harper, E.B., Stella, J.C. and Fremier, A.K. (2011) *Global sensitivity analysis for complex ecological models: a case study of riparian cottonwood population dynamics*, *Ecological Applications*.

Harvey, E. *et al.* (2017) 'Bridging ecology and conservation: from ecological networks to ecosystem function', *Journal of Applied Ecology*, 54(2), pp. 371–379. Available at: https://doi.org/10.1111/1365-2664.12769.

Harvey, E. *et al.* (2021) 'A general meta-ecosystem model to predict ecosystem function at landscape extents', *Authorea Preprints*, pp. 1–36.

Hernandez, O., Merritt, R.W. and Wipfli, M.S. (2005) 'Benthic invertebrate community structure is influenced by forest succession after clearcut logging in southeastern Alaska', *Hydrobiologia*, 533(1), pp. 45–59. Available at: https://doi.org/10.1007/s10750-004-2105-6.

Hipsey, M.R. *et al.* (2020) 'A system of metrics for the assessment and improvement of aquatic ecosystem models', *Environmental Modelling and Software*, 128(October 2019), p. 104697. Available at: https://doi.org/10.1016/j.envsoft.2020.104697.

Holt, R.D. (1977) 'Predation, apparent competition, and the structure of prey communities', *Theoretical Population Biology*, 12(2), pp. 197–229. Available at: https://doi.org/10.1016/0040-5809(77)90042-9.

Iwata, T., Nakano, S. and Inoue, M. (2003) 'Impacts of past Riparian Deforestation on Stream Communities in a Tropical Rain Forest in Borneo', *Ecological Applications*, 13(2), pp. 461–473.

Jacquet, Claire *et al.* (2022) 'Meta-ecosystem dynamics drive the spatial distribution of functional groups in river networks', *Oikos* [Preprint]. Available at: https://doi.org/10.1111/oik.09372.

Johnson, S.L. and Jones, J.A. (2000) 'Stream temperature responses to forest harvest and debris flows in western Cascades, Oregon', *Canadian Journal of Fisheries and Aquatic Sciences*, 57(SUPPL. 2), pp. 30–39. Available at: https://doi.org/10.1139/cjfas-57-s2-30.

Keenan, R.J. and van Dijk, A. (2010) 'Chapter 4: Planted forests and water', in J. Bauhaus, P. van der Meer, and M. Kanninen (eds) *Ecosystem Goods and Services from Plantation Forests*, pp. 77–95. Available at: https://doi.org/10.4324/9781849776417.

Kerekes, J.J. (1974) 'Limnological Conditions in Five Small Oligotrophic Lakes in Terra Nova National Park, Newfoundland', (August).

Kerekes, J.J. (1977) 'Factors Relating to Annual Planktonic Primary Production'.

Kiffney, P.M., Richardson, J.S. and Bull, J.P. (2003) 'Responses of periphyton and insects to experimental manipulation of riparian buffer width along forest streams', *Journal of Applied Ecology*, 40(6), pp. 1060–1076. Available at: https://doi.org/10.1111/J.1365-2664.2003.00855.X.

Larson, D.J. and Colbo, M.H. (1983) 'The aquatic insects: biogeographic considerations.', *Biogeography and ecology of the island of Newfoundland*, pp. 593–677.

Layman, Craig A *et al.* (2012) 'Applying stable isotopes to examine food-web structure: an overview of analytical tools Recommended Citation'. Available at: https://digitalcommons.fiu.edu/fce_lter_journal_articles/157 (Accessed: 27 July 2023).

Lecerf, A. and Richardson, J.S. (2010) 'Litter decomposition can detect effects of high and moderate levels of forest disturbance on stream condition', *Forest Ecology and Management*, 259(12), pp. 2433–2443. Available at: https://doi.org/10.1016/j.foreco.2010.03.022.

Leroux, S.J. *et al.* (2021) 'Cumulative effects of spruce budworm and moose herbivory on boreal forest ecosystems', *Functional Ecology*, 35, pp. 1448–1459. Available at: https://doi.org/10.1111/1365-2435.13805.

Leroux, S.J. and Loreau, M. (2012) 'Dynamics of Reciprocal Pulsed Subsidies in Local and Meta-Ecosystems', *Ecosystems*, 15(1), pp. 48–59. Available at: https://doi.org/10.1007/s10021-011-9492-0.

Leroux, S.J. and Loreau, M. (2015) 'Theoretical perspectives on bottom-up and top-down interactions across ecosystems', *Trophic Ecology: Bottom-Up and Top-Down Interactions Across Aquatic and Terrestrial Systems*, (May 2015), pp. 3–28. Available at: https://doi.org/10.1017/CBO9781139924856.002.

Leroux, S.J., Wiersma, Y.F. and Vander Wal, E. (2020) 'Herbivore Impacts on Carbon Cycling in Boreal Forests', *Trends in Ecology and Evolution*, 35(11), pp. 1001–1010. Available at: https://doi.org/10.1016/j.tree.2020.07.009.

Lloyd, D.S., Koenings, J.P. and Laperriere, J.D. (1987) 'Effects of Turbidity in Fresh Waters of Alaska', *North American Journal of Fisheries Management*, 7(1), pp. 18–33. Available at: https://doi.org/10.1577/1548-8659(1987)7<18:eotifw>2.0.co;2.

Loreau, M., Mouquet, N. and Holt, R.D. (2003) 'Meta-ecosystems: A theoretical framework for a spatial ecosystem ecology', *Ecology Letters*, 6(8), pp. 673–679. Available at: https://doi.org/10.1046/j.1461-0248.2003.00483.x.

MacLean, D.A. (1980) 'Vulnerability of Fir-Spruce Stands During Uncontrolled Spruce Budworm Outbreaks: A Review and Discussion', *The Forestry Chronicle*, 56(5), pp. 213–221. Available at: https://doi.org/10.5558/tfc56213-5.

MacLean, D.A. (1985) 'Effects of spruce budworm outbreaks on forest growth and yield', *Recent advances in spruce budworms research: proceedings of the CANUSA Spruce Budworms Research Symposium* [Preprint]. Available at: https://agris.fao.org/agris-search/search.do?recordID=US201302027941 (Accessed: 26 March 2022).

MacSween, J., Leroux, S.J. and Oakes, K.D. (2019) 'Cross-ecosystem effects of a large terrestrial herbivore on stream ecosystem functioning', *Oikos*, 128(1), pp. 135–145. Available at: https://doi.org/10.1111/oik.05331.

Marleau, J.N., Guichard, F. and Loreau, M. (2014) 'Meta-ecosystem dynamics and functioning on finite spatial networks', *Proceedings of the Royal Society B: Biological Sciences*, 281(1777). Available at: https://doi.org/10.1098/rspb.2013.2094.

Massol, F. *et al.* (2011) 'Linking community and ecosystem dynamics through spatial ecology', *Ecology Letters*, 14(3), pp. 313–323. Available at: https://doi.org/10.1111/j.1461-0248.2011.01588.x.

Mayer, A.L. *et al.* (2016) 'How Landscape Ecology Informs Global Land-Change Science and Policy', *BioScience*, 66(6). Available at: https://doi.org/10.1093/biosci/biw035.

Mori, A.S. and Kitagawa, R. (2014) 'Retention forestry as a major paradigm for safeguarding forest biodiversity in productive landscapes: A global meta-analysis', *Biological Conservation*, 175, pp. 65–73. Available at: https://doi.org/10.1016/j.biocon.2014.04.016.

Nuttle, T. *et al.* (2013) 'Historic disturbance regimes promote tree diversity only under low browsing regimes in eastern deciduous forest', *Ecological Monographs*, 83(1), pp. 3–17. Available at: https://doi.org/10.1890/11-2263.1.

Odum, E.P., Finn, J.T. and Franz, E.H. (1979) 'Perturbation Theory and the Subsidy-Stress Gradient',

BioScience, 29(6), pp. 349–352. Available at: https://doi.org/10.2307/1307690.

Oksanen, L. *et al.* (1981) 'Exploitation Ecosystems in Gradients of Primary Productivity', *The American Naturalist*, 118(2), pp. 240–261. Available at: https://doi.org/10.1086/283817.

Orrock, J.L., Holt, R.D. and Baskett, M.L. (2010) 'Refuge-mediated apparent competition in plant-consumer interactions', *Ecology Letters* [Preprint]. Available at: https://doi.org/10.1111/j.1461-0248.2009.01412.x.

Osakpolor, S.E. *et al.* (2021) 'Mini-review of process-based food web models and their application in aquatic-terrestrial meta-ecosystems', *Ecological Modelling*. Elsevier B.V. Available at: https://doi.org/10.1016/j.ecolmodel.2021.109710.

Pichon, B. *et al.* (2023) 'Quality matters: stoichiometry of resources modulates spatial feedbacks in aquatic-terrestrial meta-ecosystems', *Ecology Letters*, (June), pp. 1–14. Available at: https://doi.org/10.1111/ele.14284.

Piggott, J.J. *et al.* (2012) 'Multiple Stressors in Agricultural Streams: A Mesocosm Study of Interactions among Raised Water Temperature, Sediment Addition and Nutrient Enrichment', *PLoS ONE*, 7(11), p. 49873. Available at: https://doi.org/10.1371/journal.pone.0049873.

Pimlott, D.H. (1953) 'Newfoundland moose'.

Polis, G.A., Anderson, W.B. and Holt, R.D. (1997) 'Toward an integration of landscape and food web ecology: The dynamics of spatially subsidized food webs', *Annual Review of Ecology and Systematics*, 28, pp. 289–316. Available at: https://doi.org/10.1146/annurev.ecolsys.28.1.289.

Poudel, B.C. *et al.* (2012) 'Potential effects of intensive forestry on biomass production and total carbon balance in north-central Sweden', *Environmental Science and Policy*, 15(1), pp. 106–124. Available at: https://doi.org/10.1016/j.envsci.2011.09.005.

QGIS Development Team (2021) 'QGIS Geographic information system'. Open Source Geospatial Foundation Project.

R Core Team (2020) 'R: A language and environment for statistical computing'. Vienna, Austria: R Foundation for Statistical Computing.

Rasmussen, J.B. (2010) 'Estimating terrestrial contribution to stream invertebrates and periphyton using a gradient-based mixing model for δ13C', *Journal of Animal Ecology*, 79(2), pp. 393–402. Available at: https://doi.org/10.1111/J.1365-2656.2009.01648.X.

Régniè, J., St-Amant, R. and Duval, P. (2012) 'Predicting insect distributions under climate change from physiological responses: spruce budworm as an example', *Biological invasions*, 14, pp. 1571–1586. Available at: https://doi.org/10.1007/s10530-010-9918-1.

Richardson, J.S. and Béraud, S. (2014) 'Effects of riparian forest harvest on streams: A meta-analysis', *Journal of Applied Ecology*, 51(6), pp. 1712–1721. Available at: https://doi.org/10.1111/1365-2664.12332.

Roth, N.E., David Allan, J. and Erickson, D.L. (1996) 'Landscape influences on stream biotic integrity assessed at multiple spatial scales', *Landscape Ecology*, 11(3), pp. 141–156.

Ryan, P.A. (1991) 'Environmental effects of sediment on new zealand streams: A review', *New Zealand Journal of Marine and Freshwater Research*, 25(2), pp. 207–221. Available at: https://doi.org/10.1080/00288330.1991.9516472.

Schoen, E.R. *et al.* (2015) 'Temperature and depth mediate resource competition and apparent competition between Mysis diluviana and kokanee', *Ecological Applications*, 25(7), pp. 1962–1975. Available at: https://doi.org/10.1890/14-1822.1.

Scholl, E.A., Cross, W.F. and Guy, C.S. (2022) 'Geomorphology shapes relationships between animal communities and ecosystem function in large rivers', *Oikos* [Preprint]. Available at: https://doi.org/10.1111/oik.09431.

Steffen, W., Crutzen, P.J. and Mcneill, J.R. (2015) 'Royal Swedish Academy of Sciences The Anthropocene : Are Humans Now Overwhelming the Great Forces of Nature?', *Source: Ambio*, 36(8), pp. 614–621. Available at: http://www.jstor.org/stable/25547826%5Cnhttp://www.jstor.org/stable/25547826?seq=1&cid=pdf-reference#references_tab_contents%5Cnhttp://about.jstor.org/terms.

Stone, M.K. and Wallace, J.B. (1998) 'Long-term recovery of a mountain stream from clear-cut logging: The effects of forest succession on benthic invertebrate community structure', *Freshwater Biology*, 39(1), pp. 151–169. Available at: https://doi.org/10.1046/j.1365-2427.1998.00272.x.

Tanentzap, A.J. *et al.* (2014) 'Forests fuel fish growth in freshwater deltas', *Nature Communications* [Preprint]. Available at: https://doi.org/10.1038/ncomms5077.

'The Canadian Aquatic Biomonitoring Network Field Manual' (2009). Available at: http://www.unb.ca/cri/cabin_criweb.html (Accessed: 15 May 2022).

Vernier, P.R. *et al.* (2022) 'Comparing Global and Regional Maps of Intactness in the Boreal Region of

North America: Implications for Conservation Planning in One of the World's Remaining Wilderness Areas', *Frontiers in Forests and Global Change*, 5(March). Available at: https://doi.org/10.3389/ffgc.2022.843053.

Waight, C.F. (2014) 'Understanding all-terrain vehicle users : The human dimensions of ATV use on the island portion of Newfoundland and Labrador', *Memorial University Research Repository* [Preprint].

White, J.W. *et al.* (2014) 'Ecologists should not use statistical significance tests to interpret simulation model results', *Oikos*, 123(4), pp. 385–388. Available at: https://doi.org/10.1111/J.1600-0706.2013.01073.X.

Wipfli, M.S. and Musslewhite, J. (2004) 'Density of red alder (Alnus rubra) in headwaters influences invertebrate and detritus subsidies to downstream fish habitats in Alaska', *Hydrobiologia*, 520(1–3), pp. 153–163. Available at: https://doi.org/10.1023/B:HYDR.0000027734.95586.24.

Wolfram Research, I. (2022) 'Mathematica'. Champaign, Illinois: Wolfram Research, Inc. Available at: https://www.wolfram.com/mathematica.

Yang, L.H. (2004) 'Periodical cicadas as resource pulses in North American forests', *Science*, pp. 1565–1567. Available at: https://doi.org/10.1126/science.1103114.

Figures

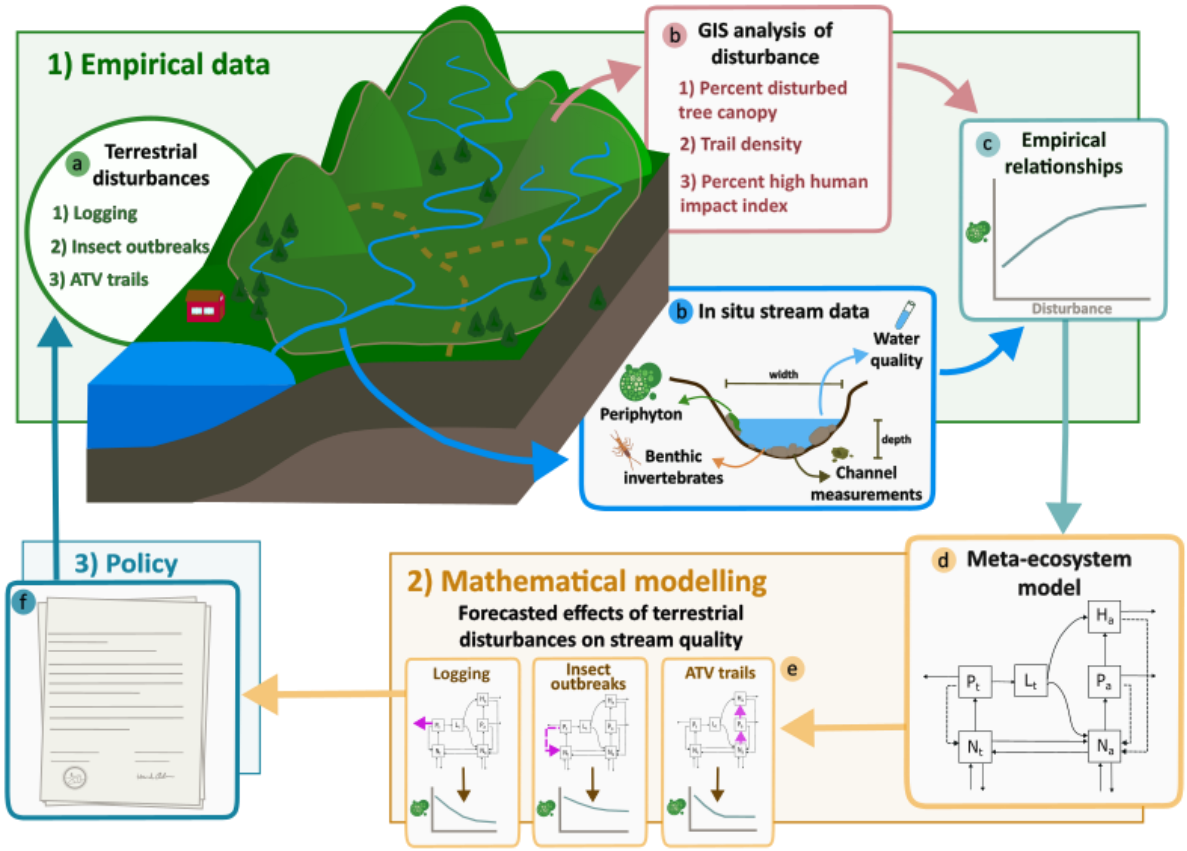

Figure 1: Conceptual diagram showing the workflow that connects empirical data collection and analysis to mathematical model development and forecasting. 1) (a) terrestrial disturbances (i.e., logging, insect outbreaks, and ATV trail development) occur in the catchment area of a stream. (b) In situ data collection is used to measure aspects of the stream structure and quality (i.e., productivity and biomass of differrent communitites, water chemistry, morphology of the stream bed) and GIS analysis is used to measure aspects of the surrounding terrestrial system (i.e., % open canopy from disturbance, trail density, land classes). (c) Empirical data is combined and statistically analyzed to determine relationships between the response variables in the stream and the predictor (disturbance) variables in the terrestrial ecosystem. 2) (d) Empirical relationships are used to inform the development of the meta-ecosystem model, which is (e) used to forecast the biomass and productivity of the meta-ecosystem under various disturbance simpulations. 3) (f) These outcomes forecasted by the model can be used to inform environmental policy put in place around the original terrestrial disturbances, ultimately reducing the undesired effects on both the stream and terrestrial ecosystems.

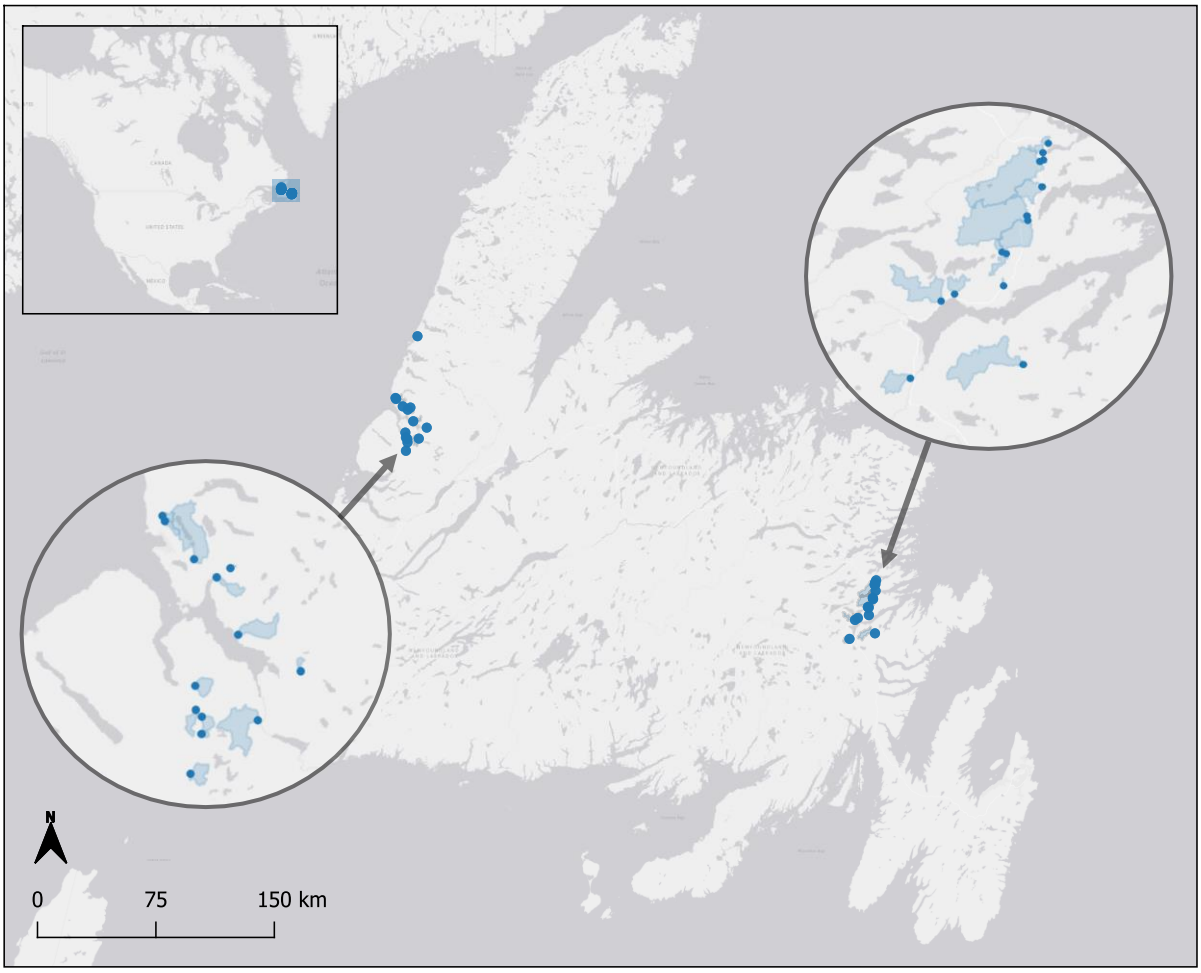

Figure 2: Map of study site sampling locations (blue dots) and catchments (light blue shaded areas) for the 28 stream sites on the island of Newfoundland, Canada. Sampling locations are grouped around Gros Morne National Park (left) and Terra Nova National Park (right). Base map credit: ESRI, 2017).

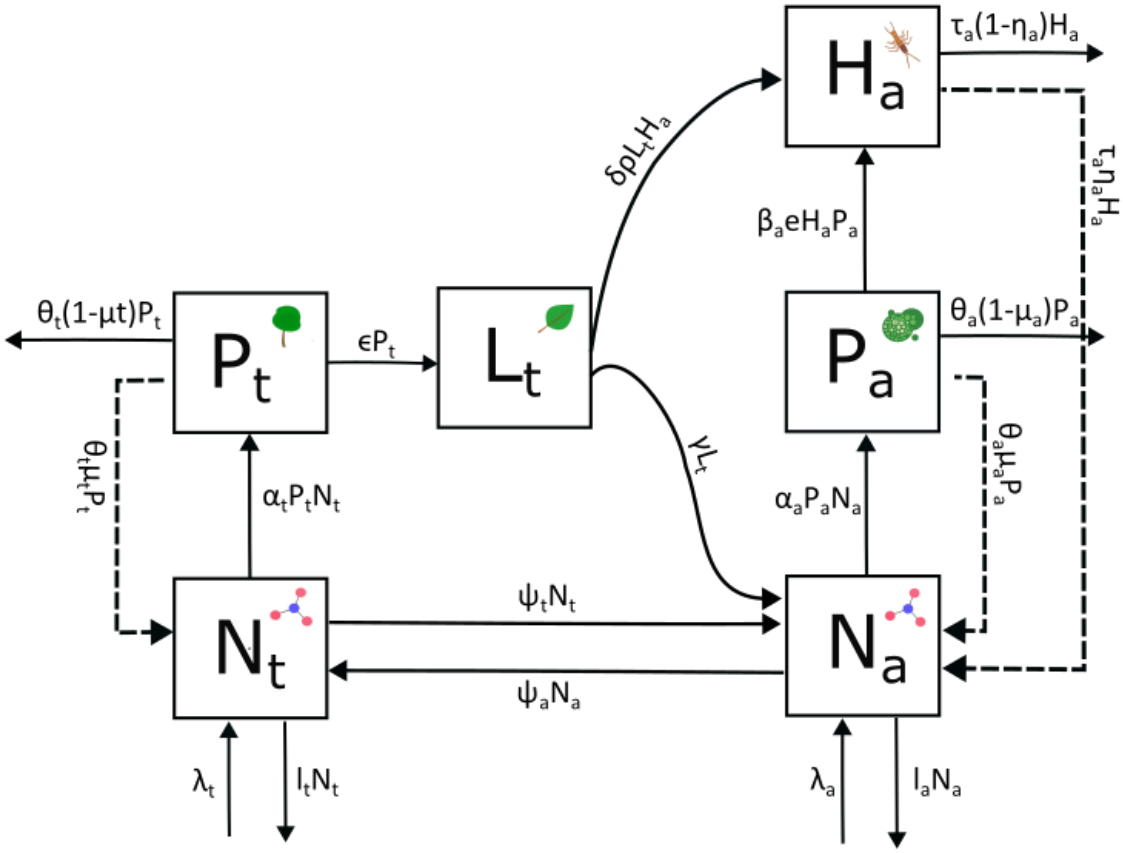

Figure 3: Box and arrow diagram of the meta-ecosystem model, representing the flow of limited nutrients between a terrestrial and aquatic ecosystem. The terrestrial ecosystem has three trophic levels: trees as primary producers (P_t), leaf litter from P_t that lands in the stream (L_t), and inorganic nutrients (N_t). The aquatic ecosystem has three trophic levels: benthic invertebrates as the primary herbivores (H_a), periphyton as the primary producer (P_a), and inorganic nutrients (N_a). A description of all variables and parameters can be found in tables 2 and 3.

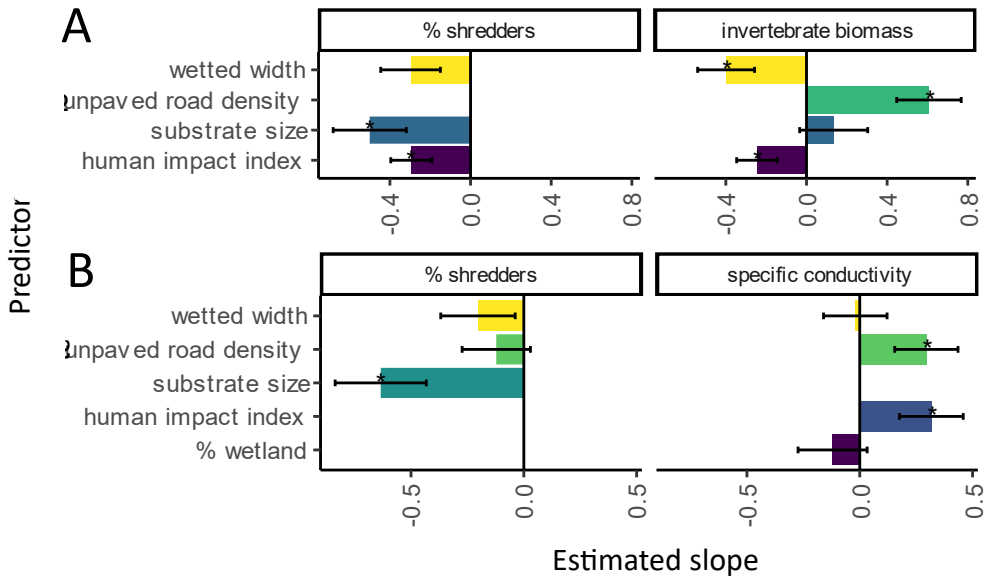

Figure 4: Magnitude and direction of relationships estimated by the "best" general liner models based on AICc for (a) local extent and (b) catchment extent. Data were rescaled from 0-1 using max-min scaling, so the estimated slopes for each predictor variable are comparable to each other and to other models. Columns show results for each model (stream metric response variable) and the rows separate out the results for each spatial extent (local, riparian, and catchment). Error bars show standard error for each slope estimate, and asterisks indicate slopes that were found to be statistically significant (α=0.05).

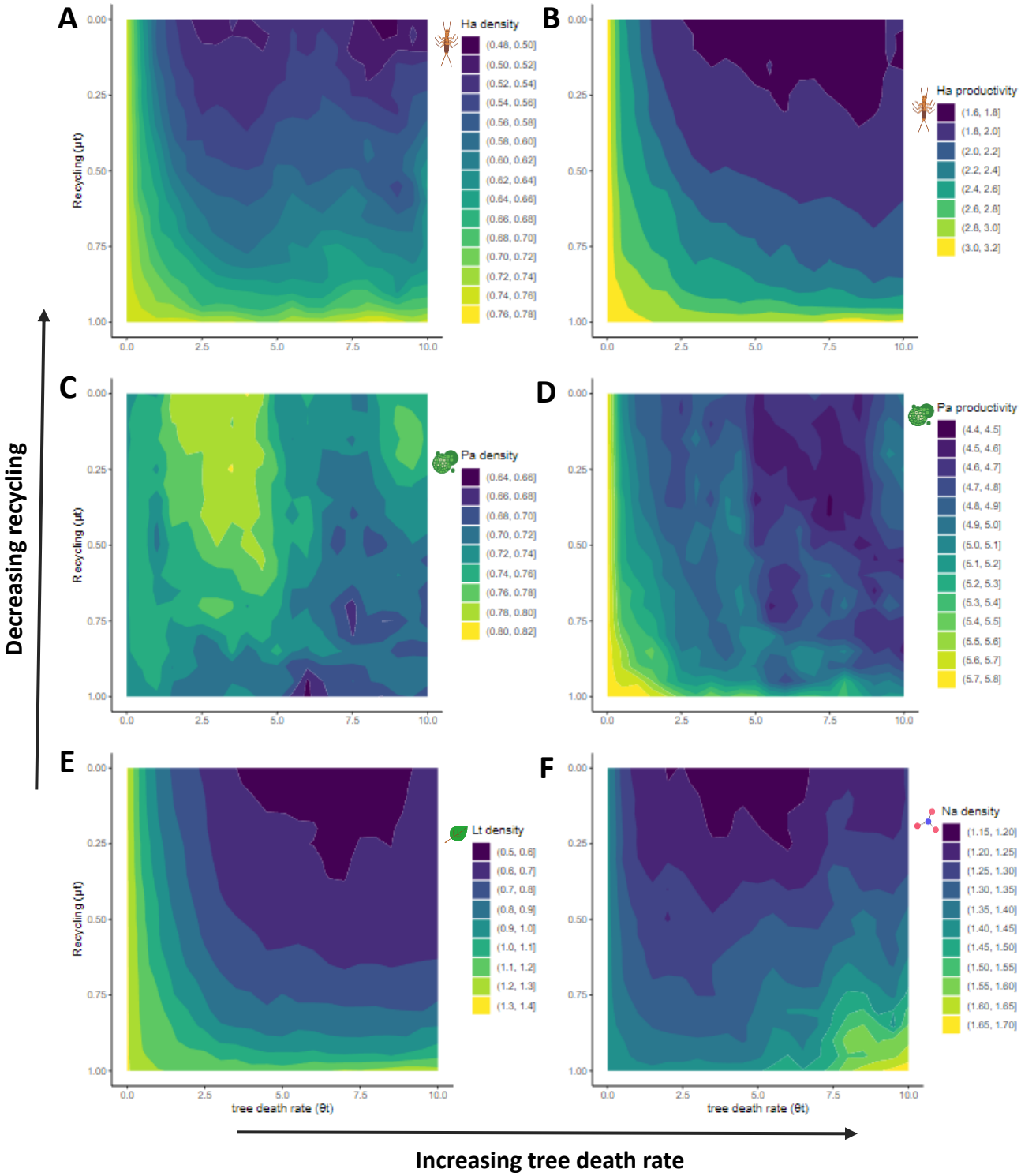

Figure 5: Surface plots of (a) benthic invertebrate biomass, (b) benthic invertebrate productivity, (c) periphyton biomass, (d) periphyton productivity, (e) litter biomass, and (f) limiting nutrients in the aquatic system across a range of mortality rates (θ_t) and tree biomass recycling (μ_t), simulating tree mortality and/or removal from insect outbreaks and logging in the meta-ecosystem model. An insect outbreak is represented by the moderate mortality rate and recycling rate found in the lower quadrant of each subplot, and logging is represented by the high mortality rate and low recycling rate found in the top quadrant. /Density and productivity data represent the median value from the 1000 disturbance simulations. The x and y axes increase by increments of 0.5 and 0.05 respectively. See Table B11 for a summary of the number of data points represented at each disturbance increments in the surface plots.

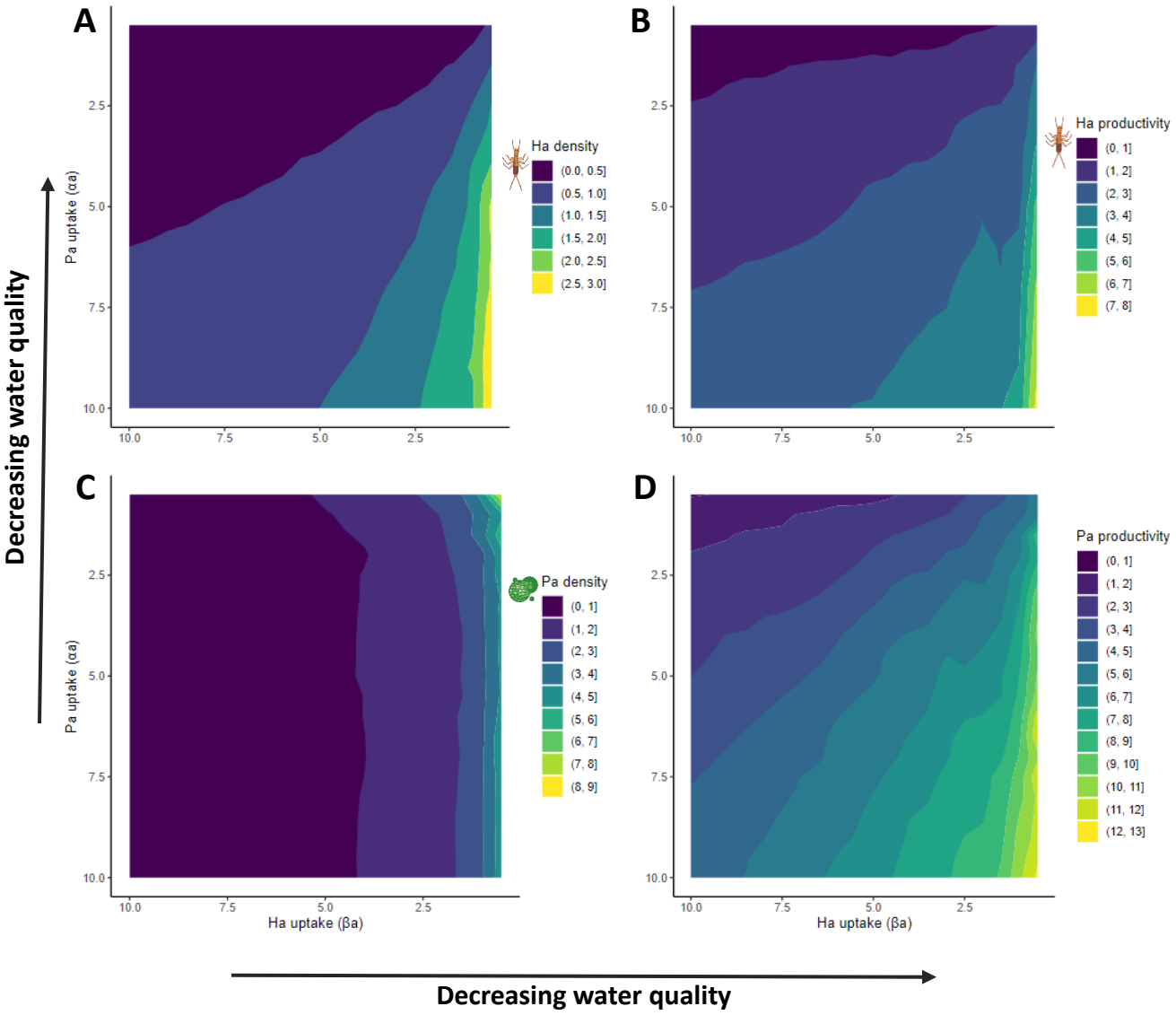

Figure 6: Surface plots of (a) benthic invertebrate biomass, (b) benthic invertebrate productivity, (c) periphyton biomass, and (d) periphyton productivity across a range of periphyton (α_i) and benthic invertebrate (β_i) uptake rates, simulating disturbance from ATV trail and logging road presence in the meta-ecosystem model. High ATV trail and logging road density is represented by the low periphyton and benthic invertebrate uptake rates found in the bottom left quadrant of each subplot. Plotted density and productivity data represent the median value from the 1000 disturbance simulations. Both the x and y axes increase by increments of 0.05. See Table B12 for a summary of the number of data points represented at each disturbance increments in the surface plots.

Tables

Table 1: Comparison of stream characteristics (depth, width, flow rate, temperature, and stream order) in Gros Morne National Park (GMNP) and Terra Nova National Park (TNNP). Mean values and standard deviation are provided as subtotals for each park and the total for all sites. We found the streams were similar enough between the two parks that all data were combined for analysis.

Park	Site name	Depth (m)	Wetted width (m)	Flow (ms^{-1})	Temperature (°C)	Strahler stream order
GMNP	BER	0.12	1.64	3.65	17.30	2
	BRY	0.17	1.87	1.81	16.77	2
	CCR	0.19	5.13	2.67	19.97	3
	GMS	0.09	0.55	0.94	13.47	1
	HCT	0.18	4.11	2.11	19.17	2
	HOR	0.12	3.82	1.74	16.73	3
	LOM	0.20	7.10	2.25	12.63	4
	MAC	0.10	2.34	3.15	18.07	3
	MAS	0.11	1.48	2.65	25.37	2
	MIT	0.23	4.39	1.88	16.33	3
	RHB	0.26	4.02	1.46	22.47	3
	SLA	0.21	5.02	1.32	18.10	1
	TUK	0.29	7.25	1.18	19.13	3
	WAT	0.12	2.98	3.68	18.30	3
	GM total	**0.17 ± 0.06**	**3.69 ± 2.03**	**2.18 ± 0.88**	**18.13 ± 3.24**	**2.5 ± 0.9**
TNNP	ARB	0.10	2.37	2.92	21.00	2
	BFF	0.10	7.37	3.66	24.47	4
	BIG	0.12	8.22	2.37	25.13	4
	BLD	0.11	2.27	4.06	16.70	3
	CHR	0.14	4.01	2.01	20.37	2
	DAV	0.07	1.51	7.94	15.90	2
	GTG	0.14	2.94	5.33	19.40	2
	JUS	0.09	2.75	2.62	23.23	4
	RPS	0.12	3.31	2.20	17.83	3
	SAL	0.14	3.43	2.81	20.67	3
	SPK	0.10	1.96	2.11	19.83	2
	SQR	0.08	1.55	6.40	16.90	2
	SWR	0.23	5.80	6.41	21.23	4
	TIC	0.15	3.64	5.19	19.57	3
	TN total	**0.12 ± 0.04**	**3.65 ± 2.08**	**4.00 ± 1.93**	**20.16 ± 2.80**	**2.9 ± 0.9**
TOTAL		**0.14 ± 0.06**	**3.67 ± 2.02**	**3.09 ± 1.74**	**19.14 ± 3.15**	**2.7 ± 0.9**

Table 2: Description and units of variables in the meta-ecosystem model, including trophic level densities and productivity rates.

Variable	Description	Units	Range
P_t	Terrestrial primary producers	g	>0
N_t	Terrestrial inorganic nutrients	g	>0
L_t	Leaf litter from P_t that enters the stream	g	>0
H_a	Aquatic herbivores (benthic invertebrates)	g	>0
P_a	Aquatic primary producers (periphyton)	g	>0
N_a	Aquatic inorganic nitrogen	g	>0
H_a productivity	Productivity of aquatic herbivores	$g \cdot t^{-1}$	>0
P_t productivity	Productivity of terrestrial primary producers	$g \cdot t^{-1}$	>0
P_a productivity	Productivity of aquatic primary producers	$g \cdot t^{-1}$	>0

Table 3: Description, units, and ranges of the parameters in the meta-ecosystem model. Note that some parameter symbology is denoted with "t" for terrestrial, "a" for aquatic, and "i" when shared by the same trophic level in both ecosystems.

Parameter	Description	Units	Range
$\boldsymbol{\alpha_i}$	P_i uptake rate	$g^{-1} \cdot t^{-1}$	>0
$\boldsymbol{\beta}$	H_a uptake rate	$g^{-1} \cdot t^{-1}$	>0
ρ	Feeding efficiency of H_a on L_t	unitless	0-1
e	Feeding efficiency of H_a on P_a	unitless	0-1
$\boldsymbol{\epsilon}$	rate of movement between P_t and L_t	t^{-1}	>0
$\boldsymbol{\delta}$	proportion of L_t partitioned to H_a rather than N_a	unitless	0-1
$\boldsymbol{\theta_i}$	P_i emigration rates (leaving the system)	t^{-1}	>0
τ	H_a emigration rates (leaving the system)	t^{-1}	>0
$\boldsymbol{\eta}$	Proportion H_a that is not recycled	unitless	0-1
$\boldsymbol{\mu_i}$	Proportion P_i that is not recycled	unitless	0-1
$\boldsymbol{\lambda_i}$	External input to N_i	$g \cdot t^{-1}$	>0
$\boldsymbol{\psi_i}$	Flow rate between N_t and N_a	t^{-1}	>0
$\boldsymbol{l_i}$	leaching rate from N_i	t^{-1}	>0

Table 4: Summary statistics (mean and standard deviation) for disturbance data and land classes at each spatial extent.

Variable	Local extent	Riparian extent	Catchment extent
Catchment area (km^2)	0.17 (0.08)	5.67 (8.39)	8.21 (11.80)
Insect outbreak (% area)	9.12 (12.07)	5.77 (6.42)	8.7 (10.97)
Logging (% area)	8.89 (13.68)	7.90 (10.64)	9.32 (12.64)
Cleared (% area)	3.29 (5.61)	1.16 (1.91)	1.24 (2.05)
Fire (% area)	3.57 (18.90)	0.19 (1.00)	0.17 (0.87)
ATV trail and logging road density ($m \cdot m^{-2}$)	34.45 (38.70)	24.01 (23.70)	24.36 (23.77)
High human impact (% area)	54.95 (40.83)	23.48 (29.05)	20.44 (26.69)
Barrens (% area)	0.02 (0.13)	3.87 (4.73)	4.84 (6.33)
Lake (% area)	0.3 (1.44)	3.57 (5.17)	2.78 (4.2)
Wetland (% area)	4.62 (7.05)	14.88 (15.77)	14.5 (15.07)

Table 5: Summary statistics (mean and standard deviation) for stream characteristics at the 28 study sites. See Tables A3-A4 in appendix A for site means.

Variable	Value
Reach length (m)	21.79 (8.84)
Canopy (%)	38.61 (28.79)
Depth (m)	0.14 (0.06)
Wetted width (m)	3.67 (2.02)
Flow ($m \cdot s^{-1}$)	3.09 (1.74)
Water pH	7.15 (0.56)
Alkalinity (mgL^{-1} $CaC0_3$)	34.89 (31.11)
Water temperature (°C)	19.14 (3.15)
Specific conductivity ($\mu S \cdot cm^{-1}$)	96.21 (97.44)
Total dissolved nitrogen ($mg \cdot L^{-1}$)	0.84 (0.39)
Substrate size (cm)	6.35 (1.09)
Embeddedness (%)	28.57 (10.82)
Periphyton biomass ($mg \cdot cm^{-2}$)	0.16 (0.14)
Invertebrate biomass ($mg \cdot cm^{-2}$)	2.1 (1.77)
Unique benthic invertebrate taxa	21.04 (4.89)
EPT index	43.94 (16.01)
Shredders (%)	6.76 (5.81)
Collectors (filterers) (%)	21.61 (18.54)
Collectors (gatherers) (%)	19.39 (10.95)
Grazers (%)	8.69 (7.51)
Predators (%)	43.55 (17.21)

Table 6: *Parameter estimates for the best performing general linear models fitted to empirical data at the catchment extent. Model performance is based on AICc, and we present all models within ΔAICc=2 of the best performing models. Top models are denoted with a double asterisk, and models within ΔAICc=2 of the top model are denoted with a double asterisk. Null models are provided for reference even if they are not within ΔAICc=2 of the best performing models. See appendix A for a full list of models tested at all spatial extents and for correlation plots between predictor variables.*

Response variable	**Model number**	**Predictors**	**k**	**ΔAICc**	**Log likelihood**	**Adjusted R2**
Percent shredders	2*	road density + wetted width + substrate size	4	0.00	5.36	0.30
	1**	disturbance + wetted width + substrate size	4	0.28	5.22	0.29
	3**	human impact + wetted width + substrate size	4	0.70	5.01	0.28
	8**	canopy + flow + wetted width + substrate size	5	1.80	6.10	0.30
	null		1	4.90	-1.21	0.00
Periphyton	null*		1	0.00	5.94	0.00
	1**	disturbance + wetted width + canopy	4	0.21	9.96	1.56
	2**	road density + wetted width + canopy	4	0.98	9.57	0.13
	3**	human impact + wetted width + canopy	4	1.15	9.48	0.13
Specific conductivity	4*	road density + human impact + wetted width + % wetland	5	0.00	9.65	0.29
	3**	human impact + wetted width + % wetland	4	1.66	7.18	0.19
	null		1	2.74	2.52	0.00
Embeddedness	null*		1	0.00	-1.63	0.00
EPT index	null*		1	0.00	-2.33	0.00
Invertebrate biomass	2*	road density + wetted width + substrate size	4	0.00	4.95	0.19
	3**	human impact + wetted width + substrate size	4	0.72	4.59	0.17
	1**	disturbance + wetted width + substrate size	4	0.77	4.57	0.17
	null**		1	1.12	0.27	0.00
Total nitrogen	null*		1	0.00	1.75	0.00

Chapter 3: Summary and discussion

As discussed in earlier chapters, land use change is affecting terrestrial ecosystems at a global scale and is a key driver of biodiversity loss, with negative consequences on the functioning of all ecosystems (Cardinale *et al.*, 2012). Anthropogenic habitat fragmentation and destruction may not only result in loss of species from the area, but the simplification of larger natural communities (Haddad *et al.*, 2015; Galiana *et al.*, 2022). A current goal of ecosystem ecology is to improve our mechanistic understanding of environmental dynamics, which will then improve our ability to understand and predict environmental change under current anthropogenic stressors (Loreau, 2010). Integrating this knowledge into natural resource management will allow us to adapt our policies to the rapidly changing environment.

In chapter 2 we provide an example of this process. We integrate empirical data collection and analysis with mathematical modelling to develop a riparian forest-small stream meta-ecosystem model based on data collected from stream catchments in Newfoundland. We use this model to forecast the effects of different disturbance types and intensities in our model ecosystem, with application to the real landscape making up these stream catchments.

In the following sections, we review results from our empirical data, model simulations, and provide suggestions for integrating both concepts in the context of natural resource management and conservation.

3.1 Empirical results

For the initial component of meta-ecosystem model development, we collected empirical data from 28 streams and their respective catchments to investigate relationships between terrestrial disturbances and stream quality using general linear models. These trends provided insight into the linkages between the terrestrial and aquatic ecosystems and were the basis for the structure of the meta-ecosystem model.

Local stream characteristics such as habitat, diversity, and productivity are influenced by the surrounding landscape through spatially nested mechanisms. Characteristics of the stream catchment (i.e., slope, soil and rock type, vegetation) influence local stream habitat and biota through many connected and complex

processes, and anthropogenic activity can therefore influence stream quality by changing components of these mechanisms (Allan, 2004). Based on this literature, we anticipated that different qualities of the terrestrial system surrounding our stream study sites (e.g., land class, logging, insect outbreaks, and ATV trails) would influence the local stream ecosystem.

The following results supported our predictions:

- Erosion indicators (i.e., specific conductivity) increased with road density in the stream catchment, supporting our prediction that unpaved roads increase erosion in the landscape and consequently increase sediment loading into the stream.
- Percent shredders in the benthic invertebrate sample (a proxy for leaf litter inputs) decreased with human impact and forest disturbance. This suggests reduction in canopy cover from logging, insect outbreaks, and land development reduce the particulate organic matter entering the stream.
- Benthic invertebrate biomass decreased with human impact index. We expected that through a variety of mechanisms (e.g., increased salinity in runoff, decreased canopy cover, increased "flushing" of streams during storm events) there would be poorer condition for the benthic invertebrates.

However, we also found results counter to our predictions (see chapter 2 and section 5 in the associated appendix). Key trends to highlight here are that benthic invertebrate biomass did not increase with forest disturbance in the catchment when we predicted that reduced riparian vegetation would increase primary productivity, thus increasing benthic invertebrate biomass (Stone and Wallace, 1998). In a similar study on the effects of moose mediated meadow on streams, MacSween et al. (2019) found that counter to their predictions, the benthic invertebrate community shifted to have a larger population of predators in areas with low moose impacts with no significant change to benthic invertebrate biomass. We found that shredders decreased at sites with greater forest disturbance, indicating a similar shift in the benthic invertebrate community without much change to its biomass. In a meta-analysis on the effects of forest harvest on streams, Richardson and Béraud (2014) found a wide range of responses by the benthic

invertebrate communities unique to the site, suggesting that we should adapt forest management (and model development) to the context of the specific area.

3.2 Model results

We then derived a meta-ecosystem model with a structure based on our empirical system and observed patterns. We used this model to isolate specific disturbances and simulate disturbance across a range of intensity that were not possible to isolate or measure at our field sites. Model results provide insight into the mechanisms connecting the meta-ecosystem, and how disturbances impact such connections. Key model predictions include:

- Logging has a negative effect on stream productivity and benthic invertebrate biomass and may be contributing to eutrophication of the aquatic ecosystem by weakening the mechanism of apparent competition between benthic invertebrates, leaf litter subsidies, and periphyton. Logging also may reduce the amount of energy in the system, ultimately reducing the biomass in all trophic compartments.
- Insect outbreaks have a positive effect on stream productivity and a negative effect on benthic invertebrate biomass. This may be in part because the mechanisms of apparent competition and energy flux were not weakened as the trees remained in the system.
- ATV trail and logging road simulations suggested that benthic invertebrates may be more sensitive to sediment loading than periphyton. They also suggest that the amount of sediment loading into the stream from these disturbances may be low enough that they act as a positive "stress" to the system, by increasing habitat heterogeneity bioavailable nutrients.

3.3 Model validation

Despite -or perhaps because of- the increasing number of ecosystem models being produced, there is no universal standard for validation of ecosystem models. Because of this lack in standards for validation, there is a tendency for models to "fail to fail" (Franks, 2009). However, attempting to create optimized parameter sets assumes that a single set of parameters are able to produce the full range of ecosystem

dynamics and that our empirical knowledge of the system is an adequate representation of the "real world" and can be used to objectively test our models (Hipsey *et al.*, 2020).

To properly assess ecosystem models we must take a more realistic approach. Hipsey et al. (2020) suggest a framework for model validation, a hierarchical assessment of a range of metrics and for aquatic ecosystem structure and function. In it, there are four levels of assessment:

0) Concept: ensure the model is consistent with ecological theory and is valid over the range of conditions in which it will be applied (e.g., is it relevant for a riparian forest-stream ecosystem)
1) State: comparison of simulated state variables with observed properties (e.g., measure of fit, skewness, and kurtosis of error)
2) Process: comparison of simulated energy and mass fluxes with measured process rates (e.g., compare flux of nitrogen in runoff from riparian to aquatic system or productivity of periphyton)
3) System: comparison of system-scale emergent properties, patterns, and relationships with observed and theorized phenomena (e.g., scaling relationships such as nutrient loading and the response in chlorophyll-a concentration)

We assessed our model at level 0 and informally at level 1, but we were using the model to predict levels 2 and 3. However, given enough empirical data it would be best practice to assess levels 2 and 3 with empirical data before making predictions.

Working toward a common framework and standards for assessing models will allow for the synthesis and transfer of knowledge between unique models (Hipsey *et al.*, 2020). Additionally, being able to compare which models are best under different circumstances and what level of complexity is required will also allow us to improve our application of these models in the context of natural resource management.

3.3 Application to natural resource management

Ecosystem management is often constrained by policies and laws that are already in place, but not equipped for handling the rapid environmental changes as well as social-ecological nuance that is now prevalent (Garmestani et al., 2021). Historically, natural resource laws were put in place assuming that ecosystems would fluctuate within a predictable range, and furthermore were meant for isolated ecosystems, disregarding the connectivity of the landscape. This has changed with developments in forest harvesting buffers, but is generally lacking across the range of natural resource extraction practices (Richardson and Béraud, 2014). Furthermore, much of the undeveloped northern land is protected through challenges in accessibility rather than as a permanent conservation goal, and will become sources for natural resource extraction as high-latitude areas become more easily accessed (Andrew, Wulder and Coops, 2012). We are working towards the integration of empirically based meta-ecosystem models into environmental policy to develop ecosystem-based management (Gounand *et al.*, 2018; McCann *et al.*, 2021).

Our model results can be used to inform environmental management policies. For example, given model predictions on the effects of forest disturbance, clear cutting could be limited in riparian areas as suggested by Richardson Béraud (2014) -especially where there are aquatic species at risk. However, these model predictions should be used in an adaptive management framework (sensu Walters, 1986), where we make predictions, monitor and test the application of the management techniques, change the model, and make new predictions (see McCarthy and Possingham, 2007; Walters, 1986). Continued data collection after implementing management techniques is a necessary component of this process, and in our case would involve monitoring benthic invertebrate and periphyton biomass, water quality, and changes to tree density in the stream catchment. Additionally, it is best practice to use response variables with greater diagnostic value (i.e., combine many mechanisms of influence) such as EPT index when using these data for long-term environmental monitoring (Allan, 2004). It is also beneficial to use

established protocols such as the CABIN method (CABIN field manual, 2009) and allowing the data to be publicly available for transparency and reproducibility.

Many stream characteristics, such as habitat heterogeneity, may be most important at the local scale (Strayer *et al.*, 2003). Thus, monitoring and developing policy for a variety of spatial extents is valuable. The spatial extent being sampled and modelled should match the policy being developed (and therefore it is important to understand at which scale these policies work; Mayer et al., 2016). Marini et al. (2019) point out a gap in network ecology applications where we are lacking the information required to manage landscapes in a way that optimizes conservation of biodiversity, and moreover, incorporating overly complex models into applied ecology can be unrealistic. Using the approach outlined here, developing simple models based on empirical data at multiple spatial extents will move us towards more adaptable and informed environmental policy.

3.4 Limitations and future directions

As with all theoretical models, there are limitations with meta-ecosystem modelling as there is a necessary simplification of the compartments and processes found in the real ecosystem. We selected and developed the trophic levels and nutrient flows to a level of complexity that could be solved with the computing power that was accessible to us, inherently building in assumptions about how the system operates. We were working with short-term empirical data collected from one season, and relatively few study sites and these data are a snapshot of our system dynamics. We used trends in our empirical data to inform our simplified ecosystem model, but future work should aim to fit the meta-ecosystem model to empirical data as discussed above. This, however, is not a trivial task as such an exercise would require long term monitoring data for one or multiple sites. The Long Term Ecological Research Network in the United States (LTER Network Office, 2023) and distributed experiments (e.g., Celldex; Tiegs et al., 2019) are two examples where data for building empirically parameterized meta-ecosystem models may be possible in the near term.

Below are some suggestions for future models:

- A similar model could incorporate more nuanced interaction equations between ecosystems where needed. For example, our model simulated logging by removing tree biomass, but we did not simulate the increase in soil leaching and initial subsidy of woody debris to the stream (Stone and Wallace, 1998). We also simplified the effect of sediment loading on streams, making it a negative, linear relationship with uptake rate when there are other known effects, such as increasing habitat heterogeneity at low levels (Piggott *et al.*, 2012). Depending on the intended application for the model, it could be valuable to increase the complexity of specific mechanisms.
- A unique model could be developed for different spatial extents to better represent the mechanisms occurring at various spatial scales (see Jacquet et al., 2022). The model we present simulated a stream with a 100 m riparian buffer, but incorporating a local and catchment scale model would allow for a more holistic management application.
- Similarly, a series of models could be created to represent expected changes to the system over time, such as the recovery of the stream after an initial terrestrial disturbance.
- Isotope analysis of $\delta^{13}C$ and $\delta^{15}N$ could be used to verify assumptions about foraging behaviour of benthic invertebrate foraging on allochthonous compared to autochthonous material (among other food web characteristics) before incorporating into the model; Coat et al. (2009) were able to distinguish trophic guilds in aquatic consumers and differentiate allochthonous and autochthonous carbon sources using this approach.
- With more detailed food web data, distinct trophic levels and feeding groups could be incorporated into the model where relevant to the research question. However, these additional complexities should be included selectively as they can quickly create a level of complexity that is challenging to model.
- Detecting shifts in ecosystem function is a valuable application for ecosystem models (see Skerratt et al., 2013; Trolle et al., 2008). Assessing regime shifts and changes to the resilience of

the ecosystem under varying degrees of disturbance would be an ideal next step for our meta-ecosystem model to expand its scope of application and improve our ability to validate its structure (Hipsey *et al.*, 2020).

Essentially, there are always trade-offs between conceptual complexity, spatial resolution, empirical data, and computing power when it comes to model development (Hipsey *et al.*, 2020). Here, we integrated empirical data from freshwater streams in Newfoundland to develop a simplified meta-ecosystem model that can predict how the riparian forest and stream ecosystems will respond to environmental change. While validation of the model is required before it can be applied in natural resource management, it is a step towards making informed decisions about how we use the land, such as working towards preserving biodiversity and meeting the challenges of ecosystem management (Schiesari *et al.*, 2019; Guichard and Marleau, 2021).

References

Allan, J.D. (2004) 'Landscapes and riverscapes: The influence of land use on stream ecosystems', *Annual Review of Ecology, Evolution, and Systematics*, 35(2002), pp. 257–284. Available at: https://doi.org/10.1146/annurev.ecolsys.35.120202.110122.

Andrew, M.E., Wulder, M.A. and Coops, N.C. (2012) 'Identification of de facto protected areas in boreal Canada', *Biological Conservation*, 146(1), pp. 97–107.

Cardinale, B.J. *et al.* (2012) 'Biodiversity loss and its impact on humanity'. Available at: https://doi.org/10.1038/nature11148.

Coat, S. *et al.* (2009) 'Trophic relationships in a tropical stream food web assessed by stable isotope analysis', *Freshwater Biology*, 54(5), pp. 1028–1041. Available at: https://doi.org/10.1111/j.1365-2427.2008.02149.x.

Franks, P.J.S. (2009) 'Planktonic ecosystem models: perplexing parameterizations and a failure to fail', *Journal of Plankton Research*, 31(11), pp. 1299–1306. Available at: https://doi.org/10.1093/PLANKT/FBP069.

Galiana, N. *et al.* (2022) 'Ecological network complexity scales with area', *Nature Ecology and Evolution*, 6(3), pp. 307–314. Available at: https://doi.org/10.1038/s41559-021-01644-4.

Gounand, I. *et al.* (2018) 'Meta-Ecosystems 2.0: Rooting the Theory into the Field', *Trends in Ecology and Evolution*, 33(1), pp. 36–46. Available at: https://doi.org/10.1016/j.tree.2017.10.006.

Guichard, F. and Marleau, J. (2021) *Meta-Ecosystem Dynamics: Understanding Ecosystems Through the Transformation and Movement of Matter*. Available at: http://www.springer.com/series/10049.

Haddad, N.M. *et al.* (2015) 'Habitat fragmentation and its lasting impact on Earth's ecosystems', *Science Advances*, 1(2), pp. 1–10. Available at: https://doi.org/10.1126/sciadv.1500052.

Hipsey, M.R. *et al.* (2020) 'A system of metrics for the assessment and improvement of aquatic ecosystem models', *Environmental Modelling and Software*, 128(October 2019), p. 104697. Available at: https://doi.org/10.1016/j.envsoft.2020.104697.

Jacquet, C., Carraro, L. and Altermatt, F. (2022) 'Meta-ecosystem dynamics drive the spatial distribution of functional groups in river networks', *Oikos*, 2022(11). Available at: https://doi.org/10.1111/oik.09372.

Loreau, M. (2010) *From populations to ecosystems: Theoretical foundations for a new ecological synthesis*. Princeton University Press.

LTER Network Office (2023) *Long Term Ecological Research Network*. Available at: https://lternet.edu/.

MacSween, J., Leroux, S.J. and Oakes, K.D. (2019) 'Cross-ecosystem effects of a large terrestrial herbivore on stream ecosystem functioning', *Oikos*, 128(1), pp. 135–145. Available at: https://doi.org/10.1111/oik.05331.

Marini, L. *et al.* (2019) 'Species–habitat networks: A tool to improve landscape management for conservation', *Journal of Applied Ecology*, 56(4), pp. 923–928. Available at: https://doi.org/10.1111/1365-2664.13337.

Mayer, A.L. *et al.* (2016) 'How Landscape Ecology Informs Global Land-Change Science and Policy', *BioScience*, 66(6). Available at: https://doi.org/10.1093/biosci/biw035.

McCann, K.S. *et al.* (2021) 'Landscape modification and nutrient-driven instability at a distance', *Ecology Letters*, 24(3), pp. 398–414. Available at: https://doi.org/10.1111/ele.13644.

McCarthy, M.A. and Possingham, H.P. (2007) 'Active adaptive management for conservation', *Conservation Biology*, 21(4), pp. 956–963. Available at: https://doi.org/10.1111/j.1523-1739.2007.00677.x.

Piggott, J.J. *et al.* (2012) 'Multiple Stressors in Agricultural Streams: A Mesocosm Study of Interactions

among Raised Water Temperature, Sediment Addition and Nutrient Enrichment', *PLoS ONE*, 7(11), p. 49873. Available at: https://doi.org/10.1371/journal.pone.0049873.

Richardson, J.S. and Béraud, S. (2014) 'Effects of riparian forest harvest on streams: A meta-analysis', *Journal of Applied Ecology*, 51(6), pp. 1712–1721. Available at: https://doi.org/10.1111/1365-2664.12332.

Schiesari, L. *et al.* (2019) 'Towards an applied metaecology', *Perspectives in Ecology and Conservation*, 17(4), pp. 172–181. Available at: https://doi.org/10.1016/j.pecon.2019.11.001.

Skerratt, J. *et al.* (2013) 'Use of a high resolution 3D fully coupled hydrodynamic, sediment and biogeochemical model to understand estuarine nutrient dynamics under various water quality scenarios'. Available at: https://doi.org/10.1016/j.ocecoaman.2013.05.005.

Stone, M.K. and Wallace, J.B. (1998) 'Long-term recovery of a mountain stream from clear-cut logging: The effects of forest succession on benthic invertebrate community structure', *Freshwater Biology*, 39(1), pp. 151–169. Available at: https://doi.org/10.1046/j.1365-2427.1998.00272.x.

Strayer, D.L. *et al.* (2003) 'Effects of Land Cover on Stream Ecosystems : Roles of Empirical Models and Scaling Issues', (September 2002), pp. 407–423. Available at: https://doi.org/10.1007/s10021-002-0170-0.

'The Canadian Aquatic Biomonitoring Network Field Manual' (2009). Available at: http://www.unb.ca/cri/cabin_criweb.html (Accessed: 15 May 2022).

Trolle, D., Skovgaard, H. and Jeppesen, E. (2008) 'The Water Framework Directive: Setting the phosphorus loading target for a deep lake in Denmark using the 1D lake ecosystem model DYRESM-CAEDYM'. Available at: https://doi.org/10.1016/j.ecolmodel.2008.08.005.

Walters, C.J. (1986) *Adaptive management of renewable resources*. Macmillan Publishers Ltd.

Appendix

Corresponding to the thesis chapter entitled: "Chapter 2: Integrating field data and a meta-ecosystem model to study the effects of multiple terrestrial disturbances on small stream ecosystem function."

Table of Contents

List of Figures

List of tables

Appendix A: Empirical data collection and analysis

1 Predictions

In our empirical study, we test the following predictions: i) we expect sites experiencing disturbance from either logging or natural disturbances (i.e., insect outbreaks and forest fire) followed by moose herbivory to have an increase in specific conductivity and total dissolved nitrogen (Richardson and Béraud, 2014), higher benthic invertebrate biomass, periphyton biomass, and EPT index (percent of Ephemeroptera, Plecoptera, and Tripchoptera taxa in a sample as a measure of water quality; Kiffney et al., 2003), and lower proportion of shredders due to reduced allochthonous plant material inputs (Richardson and Béraud, 2014); and ii) sites with higher unpaved road density will have an increase in total suspended solids, substrate embeddedness, specific conductivity, and total dissolved nitrogen, along with reduced benthic invertebrate and periphyton biomass due to increased erosion and runoff (Chin *et al.*, 2004). We use a meta-ecosystem model that captures key food web structure in our empirical system to untangle specific mechanisms or explanations for the patterns in our empirical data.

2 Empirical data collection

The following sections expand on the methods used to collect qualitative and quantitative data at the 28 stream sites in Gros Morne National Park and Terra Nova National Park.

2.1 Qualitative site assessment

Before entering each stream, we recorded qualitative data, including a site sketch, photographs, of the stream and substrate, and categories for stream bank integrity, relative water level, and water clarity. We randomly selected areas within the appropriate stream habitat (riffle or run) along the study reach to collect water samples, benthic invertebrates, and periphyton to minimize bias in where we collected samples within the stream. After determining the location for each measurement and sample, we began collecting samples and taking measurements beginning at the downstream end of the study reach and moving upstream to avoid contaminating the samples with stirred up sediment (*CABIN Field Manual*, 2009) (Figure A1). See Figures A2-A4 for site photos.

2.2 Channel measurements

At three randomly selected cross-sections of the stream, we measured the depth, width, and flow, along with a 100-pebble count to determine the mean substrate size, an estimate of embeddedness for 10% of the pebbles, and an estimate of the substrate matrix size, all following CABIN guidelines for wadable streams. We also measured the percent canopy cover at five meter intervals along the centre of the stream using the "canopy cover" android app (Healson, 2016).

2.3 Water quality

Using a pH probe (Hanna HI98129, Hanna instruments) we measured water temperature, specific conductivity, pH, and total dissolved solids from three samples of water collected in a high-density polyethylene (HDPE) cup immediately after removing it from the stream.

To collect samples for dissolved organic carbon (DOC) and total dissolved nitrogen (TDN) analysis, we filled three 250 mL amber HDPE bottles, filtered the water from each bottle through a 0.45 µm glass fibre syringe filter (37C-3216-OEM, Foxx Life Sciences) into a pre-combusted and acid-washed 15 mL glass vial (one for DOC and one for TDN analysis from each sample), preserved each filtered sample with three drops of 15 M phosphoric acid to bring the sample to a pH of 2, and placed in ice until it could be refrigerated and analyzed in the lab (adapted from Longnecker; 2021 and Bowering et al.; 2022). We measured DOC by high temperature combustion analysis (Shimadzu TOC-V) And TDN by chemiluminescence detection. Data below the method detection limit (DOC: MDL=4.10 mgL^{-1}, n=3; TDN: MDL=0.36 mgL^{-1}, n=5) were removed from the analysis.

We collected three litres of water to measure total suspended solids (TSS) at each site. We filtered the stream water onto a 0.45 µm glass fibre filter using a vacuum hand pump, noting the precise amount of water filtered (Hauer and Lamberti, 2007). We wrapped the filters in aluminum foil and stored them in the freezer to avoid degradation of the organic portion of the sample. In the lab we measured TSS by drying the filtered samples at 90°C for 24 hours and measured the mass of the dry samples using an analytical scale and subtracted the mass of the glass fiber filters (Hauer and Lamberti, 2007). Due to the nature of

our sampling methods and low balance precision, we found all but four samples to be below the limit of detection (LOD= 0.002 g) and removed the TSS data from our analysis.

We measured alkalinity using a direct reading titrator (Alkalinity Test Kit 4491-DR-01, Lamotte) and turbidity using a visual test (Turbidity test kit TTM 7509-01, Lamotte).

2.4 Periphyton

We collected periphyton samples by randomly selecting one rock sample from each of the three (randomly selected) sampling blocks in the stream, for a total of three rock samples per site. Following Hauer and Lamberti (2007), we removed all periphyton from the rocks by scrubbing with a coarse-bristled brush and transferred the periphyton into a sample container by rinsing with ultrapure water. We stored the periphyton samples in ice and away from light while in the field and refrigerated them as soon as possible. We then filtered the samples onto a 0.45 μm glass fiber filter (Whatman) using a hand pump vacuum filter. We wrapped the filters in aluminum foil and stored in the freezer to minimize degradation of the chlorophyll in each sample until further lab analysis. We used the aluminum foil method to measure the surface area of the rocks sampled at each site, following the procedure from Hauer and Lamberti (2007). We wrapped each rock in aluminum foil so that it was fully covered with no overlapping edges. The mass of aluminum foil required to cover the surface area of all rocks collected from each site was converted to cm^2 of surface area by comparing to the mass of a 100 cm^2 section of aluminum foil, using the following equation:

$$total\ substrate\ area = \frac{known\ foil\ area}{known\ foil\ mass} \times total\ mass\ of\ foil\ from\ the\ site$$

In the lab, we reserved half of each filter for ash-free dry mass analysis and extracted chlorophyll from the other half filter by placing them in 90% buffered acetone solution (10% magnesium carbonate) for 24 hours (Axler and Owen, 1994; Hauer and Lamberti, 2007) and centrifuging them at 4000 rpm for 20 minutes (Axler and Owen, 1994). We then measured chlorophyll *a* content using a Genesys 10S UV-Vis spectrophotometer, measuring the absorbance of the sample at 664 nm before and after acidifying with 0.1 mL of 0.1 N hydrochloric acid for 90 seconds, and subtracting the absorbance at 750 nm to account

for turbidity in the sample and 665 nm to account for the presence of pheophytins as the chlorophyll in the samples degraded (Hauer and Lamberti, 2007). We used the monochromatic equation with an acidification step (Lorenzen, 1967):

$$\text{Chlorophyll } a \text{ } (\mu g/cm^2) = \frac{26.7(E_{664b} - E_{665a}) \times V_{ext}}{area\ of\ substrate\ (cm^2) \times \text{L } (cm)}$$

Where $E_{664b} = [(\text{absorbance of sample at 664 nm} - \text{ absorbance of blank at 664 nm}) -$ $(\text{absorbance of sample at 750 nm} - \text{ absorbance of blank at 750 nm})]$ before acidification;

$E_{665b} = [(\text{absorbance of sample at 665 nm} - \text{ absorbance of blank at 665 nm}) -$ $(\text{absorbance of sample at 750 nm} - \text{ absorbance of blank at 750 nm})]$ after acidification;

$V_{ext} = \text{volume of 90\% acetone used in the extraction (mL)};$

$\text{L} = \text{cuvette length (cm)}$; and

$26.7 = \text{ absorbance correction.}$

We removed all chlorophyll a data (n=2) below the method detection limit (MDL = 0.07 mg·cm^{-2}).

We determined the ash-free dry mass (AFDM) for the second half of the periphyton samples by combusting the filtered at 500°Celsius for 4 hours in a muffle furnace and weighing before and after to determine the amount of organic material that was combusted (Hauer and Lamberti, 2007). Nearly all samples (n=64) were below the method detection limit (MDL = 0.002 g), so we removed the AFDM data from our analysis and used chlorophyll a as a proxy for periphyton biomass.

2.5 Benthic invertebrates

We collected one benthic invertebrate sample from each of the three sampling blocks using a 12”x12” Surber sampler with a 500 µm mesh. We collected each sample by placing the Surber sampler on the stream bed and gently removing invertebrates from the substrate and loose sediment by hand. While in the field, we removed large pieces of substrate after inspecting for invertebrates and stored the samples in

70% ethanol (Barbour, 1999). We replaced the ethanol 24 hours after the sample was initially collected to remove the excess water in the sample that would have diluted the ethanol and caused the sample to degrade and stored them until they could be further analyzed in the lab.

We picked benthic invertebrate individuals from the substrate using forceps under a dissecting microscope and placed them in 90% ethanol. For large samples with many individuals, we divided the sample by mass (or area when very little substrate in sample) following the benthic invertebrate subsampling protocol from Environment Canada (2002). We had the invertebrates identified to the family level by taxonomic specialists at BioTech and had 10% of the samples verified by taxonomic specialists at Entomogen Inc.

To estimate the biomass of the invertebrates, we used length data from the United States Geological Survey (USGS) invertebrate database (Vieira *et al.*, 2016) to convert the mean length of an individual from each invertebrate order to dry mass using the power law: $dry\ mass = ax^b$, where x is the length of the organism in cm (Burgherr and Meyer, 1997). We used coefficient from (Benke *et al.*, 1999) for these equations, using the "all insect" category for orders where no other coefficients were available (i.e., *collembola, oligochaeta, gastropoda, hirudinea, acarina, neuropteran, lepidoptera*, and *bivalvia*). Additionally, we used the USGS database to assign functional feeding groups to all taxa to analyze how these functional groups differed between sites.

Using these benthic invertebrate data (and the known 30.48 cm^2 area of the Surber sampler), we calculated Ephemeroptera, Plecoptera, and Trichoptera (EPT) index (a bioindicator of water quality), biomass per cm^2, and the proportion of three main functional feeding groups (i.e., predators, collectors, and shredders). We use the percent of shredders in the stream as an indicator for allochthonous inputs as shredders are the dominant feeding group in sections of streams with more course particulate organic matter (Vannote *et al.*, 1980). See Table A1 for a list of all site locations and Table A2 for a summary of all data collected.

3 Geospatial data collection and processing

The following sections provide details on geospatial data analysis performed in both R (ver. 4.2.2; R Core Team, 2020) and QGIS (ver. 3.26.3; QGIS Development Team, 2021) to delineate the catchment, riparian buffer, and local extent at each stream site and to determine the magnitude of disturbances along with the proportion of different land classes represented within these extents.

3.1 Calculating stream catchment, riparian buffer, and local extents

We calculated the catchment for each stream site in QGIS from a 5 m resolution digital elevation model (DEM) from the CanElevation series (Government of Canada, 2022). First, we breached the gaps in the DEM using Whitebox "BreachDepressions" tool, then converted the DEM to a PC Raster format using the PCRaster tool. We then made a local drain direction map using "lddcreate" (PCRaster) and created a stream layer using "streamorder" (PCRaster). We classified this layer into 10 categories based on accumulated flow and retained the highest six categories as our stream orders. We then used a D8 pointer layer (created by the Whitebox tool "D8Pointer") and a layer of pour points (site sampling locations snapped to the digital stream using Whitebox tool "JensonSnapPourPoints"), to create catchments using the "watershed" tool (Whitebox) and converted to a vector to use in further disturbance analysis of the catchments. The watershed tool calculates the catchment as the region of land upstream of the sampling point that would drain into the stream. The riparian and local extent were calculated using base vector tools in QGIS (Figure A5).

3.2 Digitizing disturbance layers

We classified disturbances into four categories: insect outbreak, forestry, cleared (i.e., trees removed from the shoulder of the highway or from private property), and forest fire (present at one site). Using the Google satellite base map (2021) in QGIS, we manually outlined clearings in the forest greater than 10m at the 1:2500 scale, classified them into these general disturbance categories.

3.3 Quantifying disturbance with geospatial data

To quantify the terrestrial disturbances occurring in the catchment of each study stream, we used geospatial data within each catchment area above the sampling point in the stream (Table A3).

Referencing the Google satellite base map (2021) in QGIS, we manually outlined clearings in the forest greater than 10 m at the 1:2500 scale and classified them into four categories: insect outbreak, forestry, cleared (i.e., trees removed from the shoulder of the highway or from private property), and forest fire (present at one site). Along with the satellite imagery, we used land classifications from the Forest Resource Inventory at the provincial scale (Government of Newfoundland and Labrador, 2010), disturbance data from GMNP and TNNP (e.g., history of insect outbreaks, timber harvest, forest fires, moose density, and other land changes) to validate our disturbance classifications. Finally, the disturbance layer was additionally vetted by park ecologists to further validate our disturbance classifications. Similarly, we manually digitized trails and paved roads using the Google satellite base map (2021) at the 1:2500 scale, referencing shapefiles of highways, snowmobile paths, and hiking trails provided by the parks.

From these data we created the three metrics for quantifying terrestrial disturbances at each spatial extent described in the main text: 1) Percent disturbed area (forest that had been cleared, logged, or experienced severe defoliation from an insect outbreak, and forest fire); 2) unpaved road density (ATV trails and logging roads); and 3) percent high human impact index (area with a human impact intensity ranking of 7-10 on a scale from 0-10). These metrics were determined using raster (Hijmans, 2022), rgdal (Bivand and Keitt, 2022), sf (Pebesma, 2018), elevatr (Hollister, 2021), and lwgeom (Pebesma, 2022) packages in R and base vector tools in QGIS.

4 Statistical analysis of empirical data

The following figures and tables are provided to provide detail and transparency for the statistical analysis of the empirical data. We compared general linear models (GLMs) for each response variable (Table A4), using Akaike Information Criterion for small sample sizes (AICc) to determine the "best" model, which is the model with the lowest AICc value. For each set of models, we checked for models within ΔAICc=2 of the best model and considered them to have the same goodness of fit. We checked for high correlation between predictor variables before choosing our predictor variables and covariates (Figure A7; Table A5).

Covariates were selected based on *a priori* assumptions about which stream variables would be influential to the response variable (i.e., substrate size would influence the abundance and genera of benthic invertebrates). We used mean values for each site in the statistical analysis where applicable and rescaled the data to range between 0-1 so the estimated slopes from the GLM could be compared to each other.

See Figure A6 for a summary of the models that were compared for each response variable and Tables A7-A9 for the results from all models at each spatial extent.

5 Factors affecting mechanisms linking terrestrial and aquatic ecosystems

Cross-ecosystem mechanisms are not discrete, rather they change across gradients of space, time, biotic community composition, and abiotic resource availability. In this section, we discuss some of these factors and how they impact our empirical results.

5.1 Spatial scale

Local stream characteristics such as habitat, diversity, and productivity are influenced by the surrounding landscape through spatially nested mechanisms. A study by Allan and Fay (1997) found that local stream habitat quality and organic inputs are determined primarily by local factors such as riparian vegetation, whereas nutrient and sediment inputs, hydrology, and channel morphology are influenced by factors at the catchment scale, such as landscape features and land use. Other studies have found local habitat and biotic assemblages to be most highly correlated to landscape metrics at the catchment scale and land use within the riparian zone (Roth, David Allan and Erickson, 1996; Townsend *et al.*, 2003).

The cascading influences of anthropogenic land use changes on stream quality, including periphyton and benthic invertebrate communities, both influence and are diluted by the local environment (i.e., substrate, canopy, allochthonous material, stream width), but can ultimately degrade the habitat quality and heterogeneity over time (Allan, 2004). Thus, it remains crucial to understand the mechanisms behind environmental change across scales (Guichard and Marleau, 2021). Landscape management policies have transitioned from focusing on the local (1-300 m) scale to focusing processes occurring at the catchment

scale (Allan, 2004). However, it is still important to consider local factors as they are not only the result of larger-scale mechanisms.

In our empirical data we found unique relationships at different spatial extents (Figure A6; Tables A9-A11):

- Benthic invertebrate biomass was most impacted by disturbance at the local extent (positive relationship with road density and a negative relationship with human impact index).
- Specific conductivity (an indicator of erosion) was the most strongly related to road density when measured at the riparian and catchment extents. Specific conductivity also had a positive relationship with human impact at the riparian and catchment extents.
- Percent shredders (a proxy for allochthonous inputs) strongly decreased with human impact index at the local extent, forest disturbance at the riparian extent, and unpaved road density at the catchment extent.

Our findings from the effect of ATV trails and forest disturbance on streams agree with findings in literature that factors such as sediment and nutrient loading can be important to biota at a local scale, with mechanisms occurring across multiple scales. This highlights how it is important to consider these spatial extents throughout meta-ecosystem model development. In future applications, models could be developed for each spatial extent of interest by implementing the unique mechanisms found in the empirical data at each extent.

5.2 Temporal scale

Mechanisms linking terrestrial and aquatic systems change throughout the year. For example, heavy rain during the spring increases runoff and sediment loading into streams (Larson and Colbo, 1983). Leaf litter accumulates throughout the summer season, and deciduous leaf litter subsidies are greatest in the fall. Insects with an aquatic juvenile stage tend to mature and move to the terrestrial system in the late summer and fall, acting as a subsidy for terrestrial and aerial consumers (Kawaguchi, Taniguchi and Nakano, 2018). In boreal systems, summer is the most productive season with the most movement of organisms

and matter, while winter is a time of low productivity and less movement between systems (Larson and Colbo, 1983).

Aside from annual cycles, time after an event or disturbance will change the mechanisms in place and the measurable effect on the recipient ecosystem as it goes through the process of succession (Stone and Wallace, 1998). A well-researched example is the change in nutrient leaching from soil in the years following a clear-cutting event (Reuss, Stottlemyer and Troendle, 1997). Initially there is an increase in nutrients and dissolved solids, but as vegetation and early successional trees begin to grow back, the concentration of these ions returns to approximately baseline conditions (Reuss, Stottlemyer and Troendle, 1997). There is also more overland and under land flow of water when there is a higher canopy cover (Zimmermann, Elsenbeer and De Moraes, 2006), so disturbed forest is skewed towards overland flow. Additionally, grass has lower retention of nitrogen than common tree species such as balsam fir, and alder species fix nitrogen, increasing nitrates in the groundwater and local streams (Callahan *et al.*, 2017).

Moose also play a role in the succession of forest following a disturbance. By maintaining an early successional "grassland" stage, there is an increase in water temperature, total nitrogen, and specific conductivity (MacSween, Leroux and Oakes, 2019). This was found to have a negative effect on periphyton biomass, possibly because predatory invertebrates may be lower in streams with high moose impacts, reducing predation on grazing invertebrates (Allan and Flecker, 1988) as they have been shown to exert a strong influence on prey abundance (Wooster, 1994) and reducing the periphyton biomass through foraging.

Temporal scale could be incorporated into meta-ecosystem models by being explicit about the stage of succession being modelled and comparing between successional stages if relevant to the research question.

5.3 Biological response

Varying biological response to different intensities and mechanisms of stress may be responsible for part of the variation in response of streams to terrestrial disturbances.

As discussed in chapter 2, an example of this is the effect of sediment loading on benthic invertebrates. In experiments by Piggott et al. (2012), sediment loading had a positive effect on benthic invertebrate and periphyton biomass up to intermediate levels before it began to notably reduce nutrient uptake and light availability, with benthic invertebrates being more tolerant of suspended sediment. However, the sediment type, associated nutrient subsidy, water temperature, and species present in the system strongly affected the nuance of these relationships (Piggott *et al.*, 2012). Synergistic effects were at play as well: the effect of sediment was much stronger when combined with increased water temperature, notably reducing biodiversity and biomass (Piggott *et al.*, 2012). At our sites, benthic invertebrate biomass increased with unpaved road density. Therefore, the density of ATV trails and logging roads we measured may provide only a small increase in sediment loading to streams whereas greater road density (and in closer proximity to the streams) may result in high enough sediment loading to have a negative effect on benthic invertebrates and periphyton (see threshold ranges in Bilotta & Brazier, 2008).

Similarly, organisms may view certain stressors as a subsidy or a stress (Odum, Finn and Franz, 1979) depending on the intensity of the disturbance. Quinn (2000) found that low to moderate amounts of stress (i.e., increases in solar irradiance and nutrient inputs in agricultural areas) have a net positive impact on benthic invertebrate and algal growth in temperate freshwater streams, but increases to these inputs resulted in eutrophication of the stream, displacing sensitive benthic invertebrate taxa due to poor light penetration of the water and fluctuations in dissolved oxygen and pH (Quinn, 2000).

5.4 Resource availability

If fewer resources are available, the overall effect of a disturbance may be net positive where in resource-rich ecosystems it would have an overall negative effect (see Canning-Clode et al., 2008). Streams in Newfoundland are nutrient-poor, so subsidies of nutrients associated with sediment loading or soil leaching may be meeting the nutrient limitation of primary production, whereas in a eutrophic system the addition of nutrients would have little effect. However, research by Smith et al. (2013) suggest that

benthic invertebrate communities can be used to indicate anthropogenic impacts, despite possible differences in the strength or type of response due to their resource poor environment.

Figures

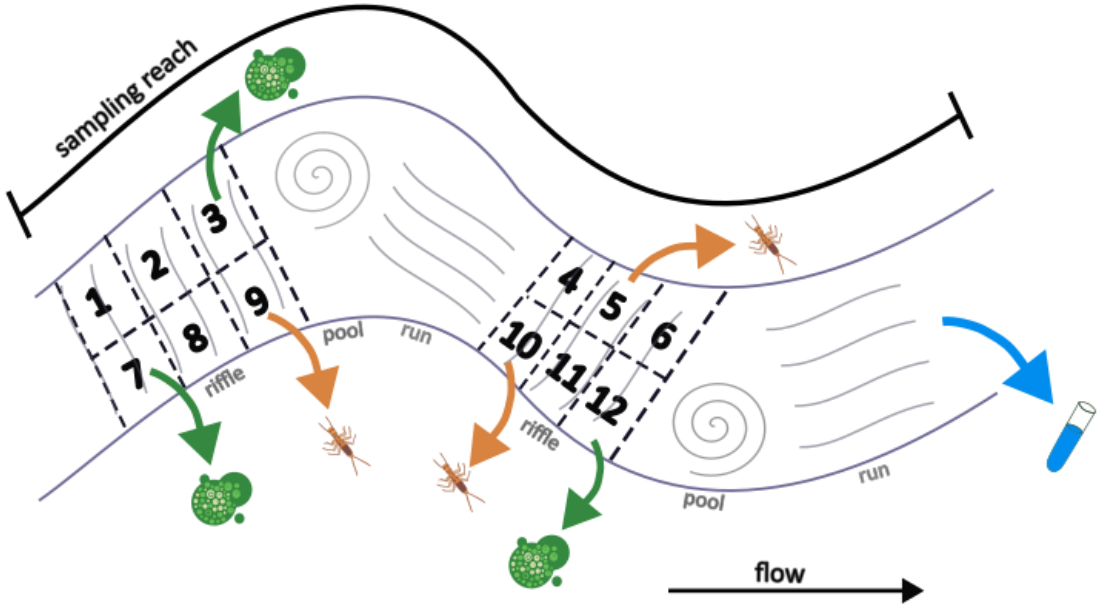

Figure A7: Example setup and sampling procedure for each stream site. Periphyton and benthic invertebrate samples were taken from randomly selected "sampling blocks" in riffle sections along the sampling reach (numbered 1-12 in this example), and water samples were taken from a run along the sampling reach. Samples were collected beginning at the downstream end to avoid disturbing the stream bed in the sections being sampled; in this case, water samples would be collected first, then periphyton and benthic invertebrates from the sampling blocks in decreasing order. Canopy cover measurements would be taken from the centre of the stream at 5-meter intervals along the sampling reach.

Figure A8: Site photos for streams sampled in Gros Morne National Park(a) GM-MIT, (b) GM-SLA, (c) GM-RHB, (d) GM-GMS, (e) GM-TUK, (f) GM-LOM, (g) GM-MAC, (h) GM-MAS, and (i) GM-HOR. See Table A1 for locations of each stream sampling location.

Figure A9: Site photos for streams sampled in Gros Morne National Park: (a) GM-BER, (b) GM-CCR, (c) GM-WAT, (d) GM-HCT, (e) GM-BRY and Terra Nova National Park: (f) TN-SPK, (g) TN-RPS, (h) TN-BIG, (i) TN-BLD. See Table A1 for locations of each stream sampling location.

Figure A10: Site photos for streams sampled in Terra Nova National Park. (a) TN-JUS, (b) TN-TIC, (c) TN-BFF, (d) TN-CHR, (e) TN-SAL, (f) TN-ARB, (g) TN-DAV, (h) TN-SWR, (i) TN-SQR, (j) TN-GTG. See Table A1 for locations of each stream sampling location.

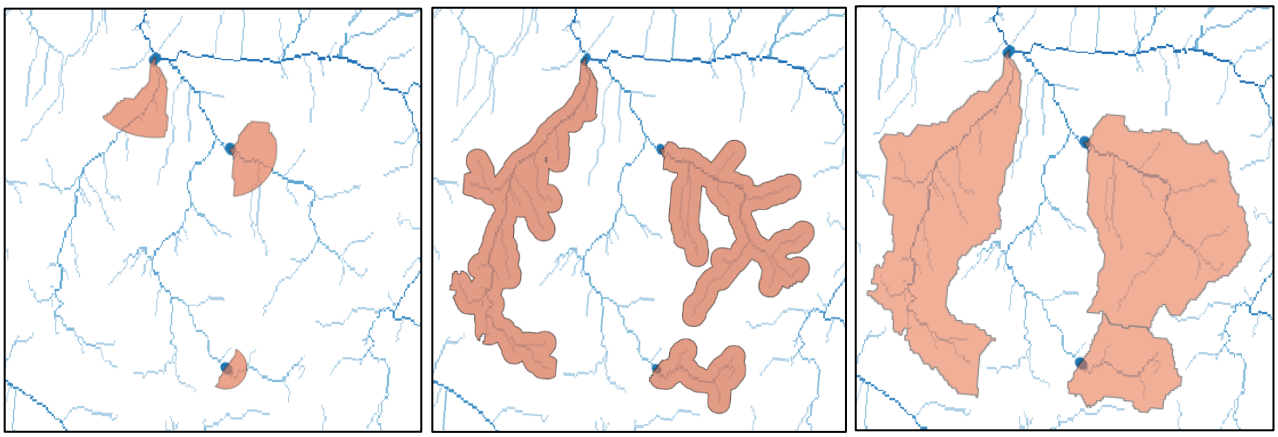

Figure A11: Three spatial extents generated in QGIS: (a) local extent (the closest 10% of the catchment area upstream of the sampling location) (b) riparian extent (100 m buffer on either side of the upstream tributaries), and (c) catchment extent calculated with the Whitebox "watershed" tool.

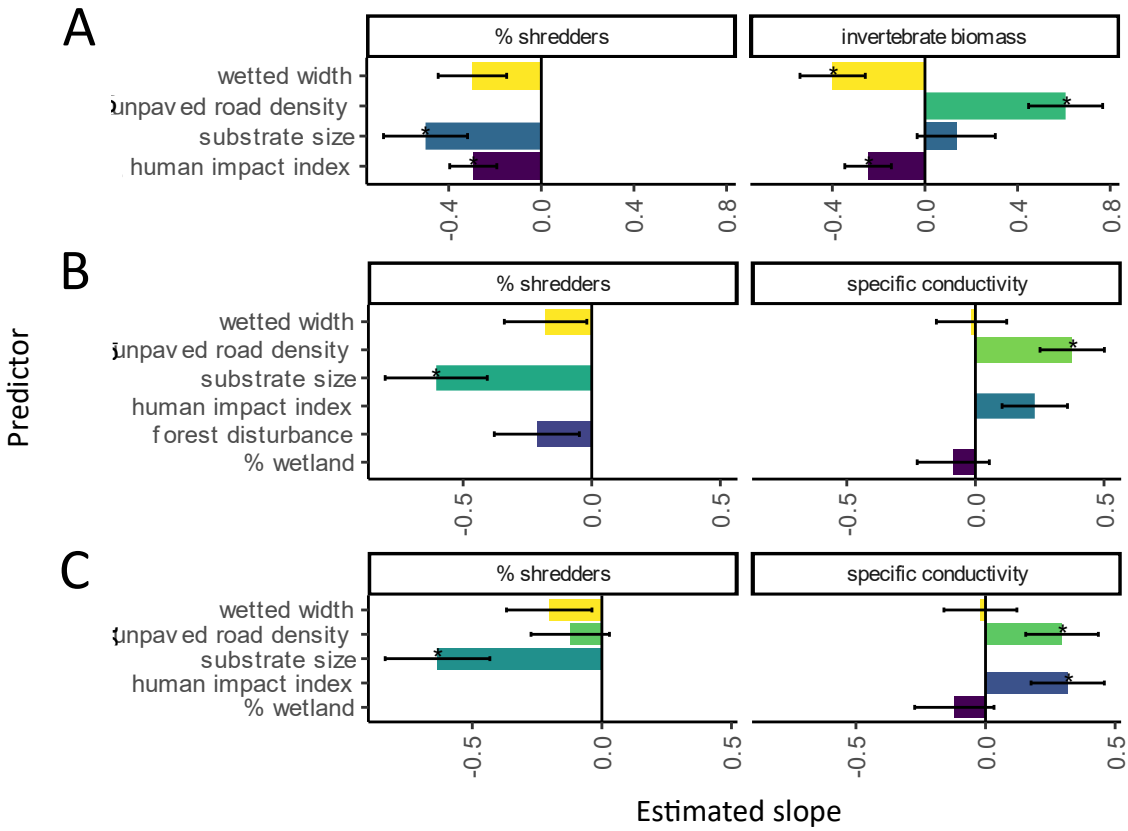

Figure A12: Magnitude and direction of relationships estimated by the "best" general liner models based on AICc. Data were rescaled from 0-1 using max-min scaling, so the estimated slopes for each predictor variable are comparable to each other and to other models. Columns show results for each model (stream response variable) and the rows separate out the results for each spatial extent (a) local, (b) riparian, and (c) catchment. Error bars show standard error for each slope estimate.

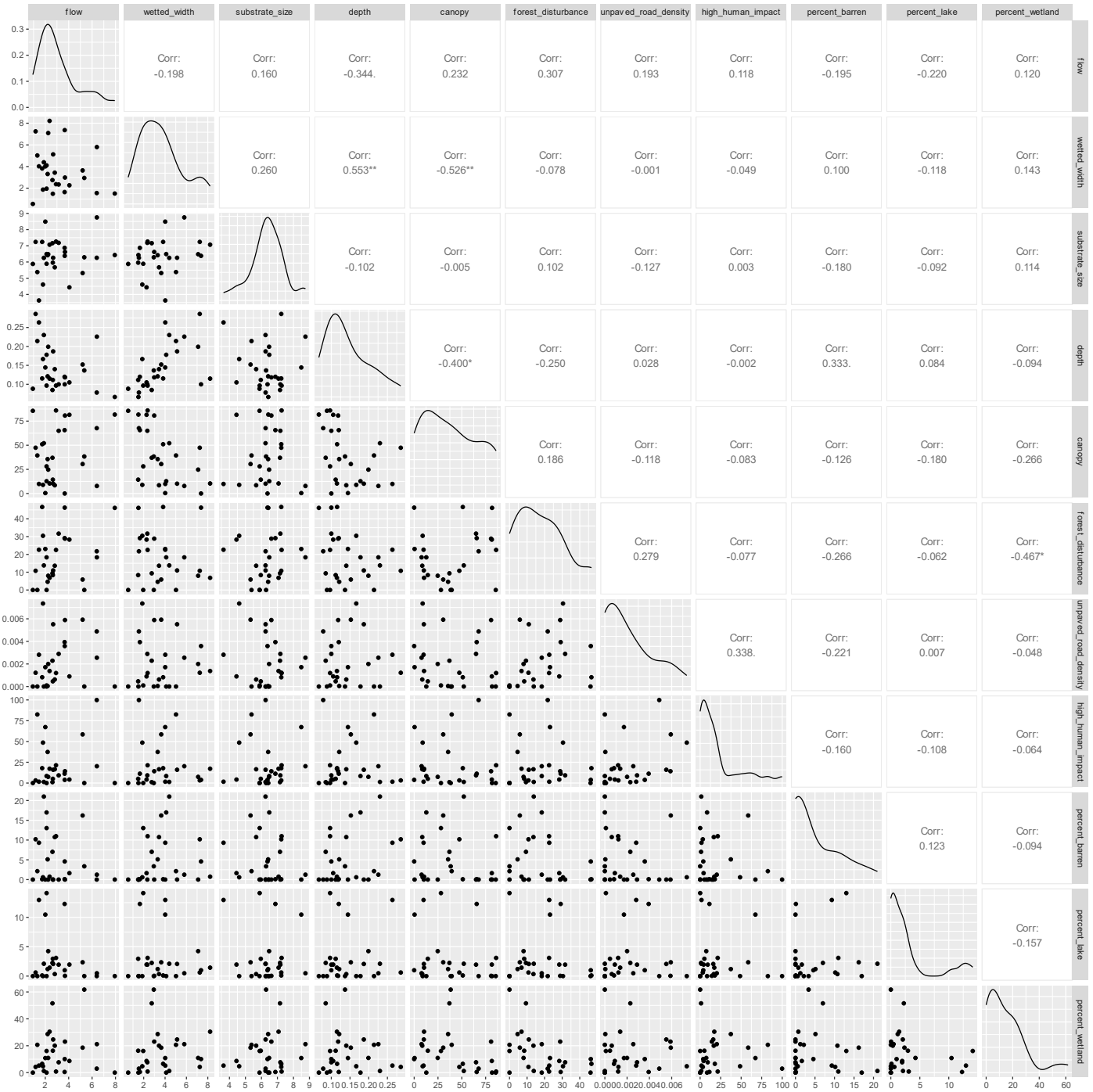

Figure A13: Correlogram of predictor variables used in the statistical models on empirical data at the catchment extent. We used this correlogram to ensure there was no significant correlation between model predictors.

Tables

Table A7: Coordinates and sampling date for each stream site, grouped by park: Gros Morne National Park (GMNP) or Terra Nova National Park (TNNP). Coordinates indicate the downstream end of the sampling reach. Note that some stream sampling locations are outside of the park boundaries.

Park	Site	Sampling date (yyyy-mm-dd)	Latitude (decimal degrees)	Longitude (decimal degrees)
Gros Morne National Park (GMNP)	GMS	2022-07-11	49.571	-57.806
	MAC	2022-07-12	49.403	-57.832
	LOM	2022-07-12	49.404	-57.736
	MAS	2022-07-13	49.384	-57.830
	HOR	2022-07-13	49.437	-57.848
	BER	2022-07-15	49.650	-57.883
	WAT	2022-07-18	49.410	-57.843
	CCR	2022-07-18	49.338	-57.843
	BRY	2022-07-19	49.617	-57.924
	HCT	2022-07-19	49.463	-57.671
	MIT	2022-07-05	49.559	-57.828
	SLA	2022-07-08	49.951	-57.748
	RHB	2022-07-08	49.577	-57.869
	TUK	2022-07-11	49.497	-57.782
Terra Nova National Park (TNNP)	ARB	2022-07-27	48.624	-53.970
	CHR	2022-07-27	48.446	-54.021
	SAL	2022-07-27	48.580	-53.965
	SQR	2022-07-28	48.636	-53.961
	SWR	2022-07-28	48.612	-53.974
	DAV	2022-07-28	48.615	-53.967
	SPK	2022-07-29	48.488	-54.022
	RPS	2022-08-01	48.534	-53.986
	BIG	2022-08-01	48.540	-53.989
	JUS	2022-08-02	48.420	-54.135
	BLD	2022-08-02	48.431	-54.112
	BFF	2022-08-03	48.346	-53.970
	TIC	2022-08-03	48.316	-54.181
	GTG	2022-08-04	48.491	-54.030

Table A8: Description and units for all empirical data collected at the 28 stream sites. We took all measurements in triplicate and calculated the mean values for each site when using the data in further statistical analysis.

Name	Description	Units
Reach length	Length of the sampling reach (5x the bankfull width)	m
Canopy cover	Percent of the area above the stream shaded by a canopy of vegetation.	%
Depth	Mean depth of the stream taken at approximately 1-meter intervals along the three cross-sections	m
Wetted width	Mean width of the stream at the three cross-sections	m
Bankfull width	Mean width of stream at maximum height of the stream bank	
Flow	Mean flow rate measured at three randomly selected cross-sections along the stream	$m \cdot s^{-1}$
Water pH	Mean pH of three water samples (Hanna combo probe)	pH units
Water temperature	Mean temperature of three water samples (Hanna combo probe)	℃
Specific conductivity (SC)	Mean SC of three water samples (Hanna combo probe)	$\mu S \cdot cm^{-1}$
Alkalinity	Mean alkalinity of three water samples (Lamotte test kit)	$mg \cdot L^{-1}$ CaC03
WolmanD50	Mean secondary axis length in 100 randomly selected pieces of substrate	m
Embeddedness	Mean percent embeddedness of 10 randomly selected pieces of substrate	%
Periphyton biomass	Biomass of periphyton using chlorophyll a as a proxy	$g \cdot cm^{-2}$
EPT index	Proportion of Ephemeroptera, Plecoptera, and Trichoptera (EPT) individuals in the total sample	%
Dissolved organic carbon (DOC)	Mean DOC from three water samples, measured using high temperature combustion analysis	$mg \cdot L^{-1}$
Total dissolved nitrogen (TDN)	Mean TDN from three water samples, measured using chemiluminescence detection	$mg \cdot L^{-1}$
Proportion of each functional group	Proportion of four main functional feeding groups in the total sample (i.e., shredders, collectors, predators, and scrapers)	%
Benthic invertebrate biomass	Biomass of benthic invertebrates in the sample, converted from number of individuals per cm^2 using the power law allometric equation (Burgherr and Meyer, 1997) and coefficients from Benke et al. (1999)	$gc \cdot m^{-2}$

Table A9: Mean data for stream morphology and water chemistry at each of the 28 study sites. Refer to associated GitHub repository (https://github.com/hfadams/meta_ecosystem_model) for individual replicate samples and standard deviations.

Park	Site	Reach length (m)	Canopy cover (%)	Depth (m)	Wetted Width (m)	Flow ($m \cdot s^{-1}$)	pH	Temperature (°C)	Specific conductivity ($\mu S \cdot cm^{-1}$)	Alkalinity ($mg \cdot L^{-1}$ $CaC0_3$)	Substrate axis length (cm)	Embeddedness (%)
GM	BER	10	65.6	0.12	1.64	3.65	7.62	17.30	140.33	64	6.9	46
	BRY	10	8.9	0.17	1.87	1.81	7.89	16.77	217.67	125	4.6	20
	CCR	30	10.2	0.19	5.13	2.67	7.13	19.97	39.67	25	6.3	15
	GMS	10	85.6	0.09	0.55	0.94	5.38	13.47	20.33	20	5.9	33
	HCT	30	12.7	0.18	4.11	2.11	7.18	19.17	40.00	40	6.5	25
	HOR	30	51.0	0.12	3.82	1.74	7.96	16.73	239.33	60	7.2	28
	LOM	30	24.7	0.20	7.10	2.25	8.20	12.63	243.00	95	6.5	33
	MAC	20	64.9	0.10	2.34	3.15	7.37	18.07	72.00	23	7.2	42
	MAS	10	14.3	0.11	1.48	2.65	6.46	25.37	44.67	17	6.0	35
	MIT	30	52.1	0.23	4.39	1.88	6.79	16.33	26.67	13	6.3	23
	RHB	15	9.9	0.26	4.02	1.46	8.01	22.47	181.00	95	3.6	35
	SLA	25	39.4	0.21	5.02	1.32	7.43	18.10	92.33	30	5.4	37
	TUK	35	47.4	0.29	7.25	1.18	6.57	19.13	52.00	30	7.2	35
	WAT	25	80.7	0.12	2.98	3.68	7.84	18.30	152.00	90	6.6	28
TN	ARB	15	86.0	0.10	2.37	2.92	7.30	21.00	64.33	20	7.3	45
	BFF	35	0.0	0.10	7.37	3.66	7.11	24.47	49.67	18	6.4	40
	BIG	35	10.4	0.12	8.22	2.37	6.95	25.13	45.33	17	7.1	25
	BLD	20	81.5	0.11	2.27	4.06	6.91	16.70	46.00	21	4.4	15
	CHR	25	0.4	0.14	4.01	2.01	7.00	20.37	30.33	11	8.5	28
	DAV	15	81.8	0.07	1.51	7.94	7.01	15.90	60.00	19	6.4	35
	GTG	15	38.3	0.14	2.94	5.33	6.98	19.40	38.00	17	6.3	28
	JUS	20	37.0	0.09	2.75	2.62	6.81	23.23	37.33	17	7.2	18
	RPS	20	35.6	0.12	3.31	2.20	7.14	17.83	153.67	14	6.4	38
	SAL	20	8.5	0.14	3.43	2.81	6.99	20.67	42.67	15	5.7	5
	SPK	10	28.1	0.10	1.96	2.11	6.66	19.83	24.67	9	5.9	40
	SQR	10	67.7	0.08	1.55	6.40	7.34	16.90	453.00	45	6.3	30
	SWR	35	7.8	0.23	5.80	6.41	7.09	21.23	56.67	17	8.8	10
	TIC	25	30.5	0.15	3.64	5.19	7.15	19.57	31.33	16	5.3	13

Table A10: Mean data for nutrient concentrations and biotic samples at each of the 28 study sites. Refer to associated GitHub repository (https://github.com/hfadams/meta_ecosystem_model) for individual replicate samples and standard deviations.

Park	Site	Dissolved organic carbon ($mg \cdot L^{-1}$)	Total dissolved nitrogen ($m \cdot gL^{-1}$)	Periphyton biomass ($g \cdot cm^{-2}$)	Invertebrate biomass ($g \cdot cm^{-2}$)	Collector/ filterer (% of sample)	Collector/ gatherer (% of sample)	Predator (% of sample)	Scraper/ grazer (% of sample)	Shredder (% of sample)	EPT Index (%)
GM	BER	19.340	0.950	0.15	7.53	2.6	39.7	36.8	15.7	5.2	38.6
	BRY	8.997	0.519	0.12	0.92	42.9	11.6	12.6	22.1	10.7	24.6
	CCR	39.091	0.479	0.08	1.98	20.2	26.0	43.4	4.1	6.4	43.6
	GMS	13.315	0.641	0.16	5.94	8.1	12.6	57.6	1.2	20.5	24.8
	HCT	8.752	0.558	0.10	1.33	10.1	51.8	36.9	0.7	0.5	77.9
	HOR	23.773	2.095	0.03	0.35	1.2	32.1	61.2	3.0	2.4	77.0
	LOM	6.705	0.437	0.33	0.32	2.7	27.5	65.3	0.0	4.5	63.5
	MAC	11.255	0.465	0.06	1.38	5.2	26.4	51.3	12.6	4.6	74.5
	MAS	13.682	0.548	0.08	1.64	8.3	15.3	52.8	4.2	19.4	37.5
	MIT	11.566	0.671	0.02	2.76	5.9	9.4	78.6	0.3	5.9	32.0
	RHB	11.297	0.730	0.13	1.97	1.5	6.1	48.3	21.1	23.0	44.0
	SLA	20.580	0.977	0.17	1.96	2.1	14.6	53.7	15.3	14.3	32.9
	TUK	11.579	0.439	0.74	0.28	5.2	12.0	78.1	0.8	4.0	43.4
	WAT	9.730	0.425	0.06	1.10	4.5	26.4	65.7	1.7	1.7	69.0
TN	ARB	22.512	1.173	0.19	0.84	27.7	16.8	28.6	23.4	3.6	42.9
	BFF	11.467	0.752	0.33	2.29	25.4	31.1	31.4	8.6	3.5	58.2
	BIG	10.693	0.569	0.06	0.97	61.0	9.4	23.3	2.3	4.1	39.3
	BLD	18.008	0.993	0.25	1.07	60.2	9.2	25.3	1.6	3.7	18.1
	CHR	17.530	1.072	0.07	0.91	13.5	9.2	63.2	11.6	2.4	28.4
	DAV	11.905	1.539	0.07	4.55	5.2	21.6	49.0	14.4	9.8	32.0
	GTG	13.176	0.633	0.11	1.30	41.7	11.3	34.5	7.7	5.0	30.6
	JUS	25.940	1.103	0.12	2.42	26.8	30.7	33.5	6.1	2.9	45.5
	RPS	11.554	0.691	0.33	3.69	33.3	24.2	31.3	7.1	4.0	39.7
	SAL	16.336	1.149	0.07	1.40	37.5	14.5	32.9	9.5	5.6	36.0
	SPK	11.850	0.725	0.23	3.57	39.5	7.8	20.8	24.4	7.5	44.0
	SQR	23.124	1.322	0.15	4.58	36.2	13.0	31.2	11.8	7.7	51.0
	SWR	18.586	1.123	0.21	0.64	39.3	12.3	39.0	6.4	3.1	35.9
	TIC	13.135	0.824	0.15	1.10	37.2	20.3	33.2	6.0	3.3	45.8

Table A11: Geospatial data generated and collected for statistical analysis with empirical stream quality metrics.

Name	Source	Description
Disturbance	Digitized from Google satellite image (2021)	Manually digitized based on satellite imagery, local land classes, and personal communication with park ecologists. Categories include insect outbreak, logging, cleared, and forest fire
Trails	Digitized from Google satellite image (2021)	Manually digitized based on satellite imagery, local land classes, and personal communication with park ecologists. Categories include paved roads, unpaved roads and ATV trails, and hiking paths
Human impact index	Government of Newfoundland and Labrador and Nature Conservancy Canada (2013)	Raster data ranking human impact on a scale from 0-10 based on distance to anthropogenic infrastructure (i.e., paved road, building, etc.). See referenced material for full description.
Land classes	Forest Resource Inventory (Government of Newfoundland and Labrador, 2010)	Major land classes and dominant vegetation data provided at a provincial scale by the Forest Resource Inventory (see cited FRI technical document for further details)
Gros Morne National Park disturbance data	Park ecologist	Layer of major disturbances from wind, insect outbreaks, logging, and forest fire within the last 15 years

Table A12: Response variables tested using general linear models.

Variable	Units
Benthic invertebrate biomass	$g \cdot cm^{-2}$
EPT index	% of EPT in benthic invertebrate sample
% shredders	% of benthic invertebrate sample
Periphyton biomass	$g \cdot cm^{-2}$
Specific conductivity	$\mu S \cdot cm^{-2}$
Total dissolved nitrogen	$mg \cdot L^{-1}$
Embeddedness	% of substrate area

Table A13: Predictor variables and covariates in the general linear models (covariates denoted in bold). Note that not all variables shown in this table were used in each set of models.

Variable	Units
Total disturbance	% area
Total road density	$m \cdot km^{-2}$
Human impact index	% area
Wetted width/depth/flow	$m; m; m \cdot s^{-1}$
Substrate size	m
Percent barrens/lakes/wetlands	% area

Table A14: Summary of predictor variables used for the eight sets of models compared within each model category (i.e., for each response variable). Results are provided in Tables C7-C9 below.

Response variable	Model number	Predictor variables
Invertebrate biomass, EPT index, % shredders	null	
	1	forest disturbance + wetted width + substrate size
	2	road density + wetted width + substrate size
	3	human impact + wetted width + substrate size
	4	road density + human impact + wetted width + substrate size
	5	forest disturbance + road density + wetted width + substrate size
	6	forest disturbance + human impact + wetted width + substrate size
	7	forest disturbance + road density + human impact + wetted width + substrate size
	8	wetted width + substrate size + canopy + flow
Periphyton biomass	null	
	1	forest disturbance + wetted width + canopy
	2	road density + wetted width + canopy
	3	human impact + wetted width + canopy
	4	road density + human impact + wetted width + canopy
	5	forest disturbance + road density + wetted width + canopy
	6	forest disturbance + human impact + wetted width + canopy
	7	forest disturbance + road density + human impact + wetted width + canopy
	8	wetted width + % wetland + substrate size + canopy
Total nitrogen, specific conductivity	null	
	1	forest disturbance + wetted width + % wetland
	2	road density + wetted width + % wetland
	3	human impact + wetted width + % wetland
	4	road density + human impact + wetted width + % wetland
	5	forest disturbance + road density + wetted width + % wetland
	6	forest disturbance + human impact + wetted width + % wetland
	7	forest disturbance + road density + human impact + wetted width + % wetland
	8	wetted width + canopy + % lake + % wetland
Embeddedness	null	
	1	forest disturbance + substrate size + % lake
	2	road density + substrate size + % lake
	3	human impact + substrate size + % wetland
	4	road density + human impact + substrate size + % lake
	5	forest disturbance + road density + substrate size + % lake
	6	forest disturbance + human impact + substrate size + % lake
	7	forest disturbance + road density + human impact + substrate size + % lake
	8	wetted width + substrate size + % lake + flow

Table A15: Model output for analysis at the catchment extent. Top models are marked with an asterisk, and models within ΔAICc=2 of the top model are denoted with two asterisks. Standard error is shown in brackets for each estimate.

response variable	model number	k	Δ AIC_c	log likelihood	adjusted R^2	intercept	forest disturbance	road density	human impact	wetted width	substrate size	canopy	flow	% lake	% wetland
% shredders	2*	4	0.000	5.365	0.296	0.73 (0.13)		-0.12 (0.15)		-0.2 (0.16)	-0.63 (0.2)				
	1**	4	0.285	5.222	0.289	0.73 (0.14)	-0.1 (0.16)			-0.21 (0.17)	-0.61 (0.2)				
	3**	4	0.704	5.013	0.279	0.7 (0.12)			-0.03 (0.16)	-0.19 (0.17)	-0.63 (0.2)				
	8**	5	1.802	6.100	0.303	0.8 (0.15)				-0.3 (0.2)	-0.55 (0.21)	-0.1 (0.15)	-0.2 (0.18)		
	5	5	3.117	5.442	0.270	0.75 (0.14)	-0.06 (0.17)	-0.1 (0.17)		-0.21 (0.17)	-0.62 (0.21)				
	4	5	3.272	5.365	0.266	0.73 (0.13)		-0.12 (0.16)	0 (0.16)	-0.2 (0.17)	-0.63 (0.21)				
	6	5	3.446	5.278	0.261	0.74 (0.15)	-0.11 (0.16)		-0.05 (0.16)	-0.21 (0.17)	-0.61 (0.21)				
	null	1	4.897	-1.208	0.000	0.28 (0.05)									
	7	6	6.708	5.447	0.237	0.75 (0.15)	-0.07 (0.18)	-0.09 (0.18)	-0.02 (0.18)	-0.21 (0.17)	-0.62 (0.21)				
specific conductivity	4*	5	0.000	9.650	0.295	0.06 (0.09)		0.3 (0.14)	0.32 (0.14)	-0.02 (0.14)					-0.12 (0.15)
	3**	4	1.664	7.181	0.194	0.16 (0.08)			0.4 (0.15)	-0.05 (0.15)					-0.18 (0.16)
	2	4	2.263	6.881	0.176	0.11 (0.1)		0.38 (0.15)		-0.02 (0.15)					-0.12 (0.17)
	null	1	2.740	2.519	0.000	0.18 (0.04)									
	7	6	3.545	9.677	0.264	0.05 (0.13)	0.04 (0.18)	0.28 (0.16)	0.33 (0.15)	-0.02 (0.14)					-0.1 (0.18)
	6	5	3.835	7.732	0.191	0.05 (0.14)	0.16 (0.17)		0.43 (0.15)	-0.04 (0.15)					-0.09 (0.19)
	5	5	5.236	7.031	0.150	0.15 (0.13)	-0.09 (0.18)	0.4 (0.16)		-0.03 (0.15)					-0.17 (0.19)
	1	4	9.128	3.449	-0.053	0.22 (0.14)	0.06 (0.19)			-0.06 (0.17)					-0.17 (0.21)
	8	5	12.247	3.526	-0.092	0.25 (0.18)				-0.06 (0.21)		0.02 (0.17)		-0.06 (0.16)	-0.21 (0.2)
embeddedness	null*	1	0.000	-1.628	0.000	0.57 (0.05)									
	1	4	3.011	0.991	0.067	0.37 (0.15)	0.18 (0.18)				0.11 (0.23)			0.33 (0.16)	
	2	4	4.009	0.492	0.033	0.45 (0.15)		-0.05 (0.18)			0.12 (0.23)			0.33 (0.17)	

	3	4	4.052	0.470	0.032	0.45 (0.15)			-0.04 (0.19)		0.13 (0.23)		0.32 (0.17)
	5	5	5.619	1.323	0.049	0.39 (0.16)	0.23 (0.2)	-0.14 (0.19)			0.09 (0.23)		0.35 (0.17)
	8	5	6.104	1.081	0.033	0.53 (0.16)				-0.17 (0.2)	0.21 (0.25)	-0.17 (0.21)	0.28 (0.17)
	6	5	6.277	0.994	0.027	0.38 (0.17)	0.17 (0.19)		-0.01 (0.19)		0.11 (0.23)		0.33 (0.17)
	4	5	7.257	0.504	-0.008	0.46 (0.16)		-0.05 (0.19)	-0.03 (0.2)		0.12 (0.24)		0.32 (0.17)
	7	6	9.149	1.358	0.008	0.38 (0.17)	0.25 (0.21)	-0.16 (0.22)	0.05 (0.21)		0.09 (0.24)		0.36 (0.17)
EPT index	null*	1	0.000	-2.331	0.000	0.43 (0.05)							
	1	4	4.105	-0.260	0.030	0.13 (0.16)	0.22 (0.19)			0.21 (0.2)	0.23 (0.25)		
	2	4	4.430	-0.422	0.018	0.15 (0.16)		0.19 (0.19)		0.2 (0.2)	0.27 (0.25)		
	3	4	5.373	-0.894	-0.015	0.24 (0.15)			-0.09 (0.19)	0.16 (0.2)	0.26 (0.25)		
	5	5	6.880	-0.011	0.005	0.11 (0.17)	0.17 (0.21)	0.13 (0.2)		0.22 (0.21)	0.24 (0.25)		
	4	5	6.952	-0.047	0.003	0.17 (0.16)		0.23 (0.2)	-0.16 (0.2)	0.19 (0.2)	0.28 (0.25)		
	6	5	7.275	-0.209	-0.009	0.15 (0.18)	0.21 (0.2)		-0.06 (0.2)	0.21 (0.21)	0.23 (0.25)		
	8	5	8.414	-0.778	-0.051	0.19 (0.2)				0.21 (0.25)	0.27 (0.27)	0.1 (0.19)	-0.1 (0.22)
	7	6	10.083	0.187	-0.025	0.13 (0.18)	0.13 (0.22)	0.17 (0.22)	-0.12 (0.21)	0.21 (0.21)	0.25 (0.26)		
invertebrate biomass	2*	4	0.000	4.953	0.195	0.38 (0.13)		0.13 (0.15)		-0.47 (0.17)	0.04 (0.2)		
	3**	4	0.725	4.591	0.174	0.44 (0.13)			-0.03 (0.16)	-0.49 (0.17)	0.03 (0.21)		
	1**	4	0.769	4.569	0.172	0.43 (0.14)	0.01 (0.16)			-0.48 (0.17)	0.03 (0.21)		
	null**	1	1.116	0.272	0.000	0.25 (0.05)							
	4	5	3.030	5.074	0.167	0.39 (0.14)		0.15 (0.16)	-0.07 (0.17)	-0.47 (0.17)	0.04 (0.21)		
	5	5	3.201	4.989	0.162	0.4 (0.14)	-0.04 (0.17)	0.14 (0.17)		-0.47 (0.17)	0.05 (0.21)		
	8	5	3.266	4.956	0.160	0.35 (0.16)				-0.39 (0.2)	0 (0.22)	0.11 (0.15)	0.04 (0.18)
	6	5	3.996	4.592	0.138	0.43 (0.15)	0.01 (0.17)		-0.03 (0.17)	-0.48 (0.18)	0.03 (0.21)		
	7	6	6.438	5.170	0.135	0.42 (0.15)	-0.07 (0.19)	0.18 (0.18)	-0.1 (0.18)	-0.48 (0.18)	0.06 (0.22)		
	null*	1	0.000	5.935	0.000	0.2 (0.04)							

periphyton biomass	1**	4	0.206	9.956	0.156	-0.01 (0.12)	-0.12 (0.13)			0.41 (0.16)		0.2 (0.13)			
	2**	4	0.977	9.571	0.132	-0.03 (0.12)		-0.06 (0.13)		0.41 (0.16)		0.18 (0.13)			
	3**	4	1.153	9.482	0.127	-0.05 (0.12)			-0.03 (0.14)	0.42 (0.16)		0.17 (0.13)			
	6	5	3.351	10.020	0.123	0.01 (0.13)	-0.13 (0.14)		-0.04 (0.14)	0.41 (0.16)		0.19 (0.13)			
	5	5	3.467	9.962	0.120	-0.01 (0.13)	-0.12 (0.15)	-0.01 (0.14)		0.41 (0.16)		0.2 (0.13)			
	8	5	3.825	9.783	0.108	0 (0.14)				0.44 (0.17)	-0.08 (0.18)	0.17 (0.13)		-0.08 (0.15)	
	4	5	4.243	9.574	0.095	-0.03 (0.13)		-0.05 (0.14)	-0.01 (0.14)	0.41 (0.17)		0.17 (0.13)			
	7	6	6.950	10.020	0.083	0.01 (0.14)	-0.13 (0.16)	0 (0.15)	-0.05 (0.15)	0.41 (0.17)		0.19 (0.13)			
total dissolved nitrogen	null*	1	0.000	1.754	0.000	0.25 (0.04)									
	7	6	2.508	8.060	0.218	0.07 (0.14)	0.53 (0.19)	-0.31 (0.17)	0.37 (0.16)	-0.16 (0.15)				0.15 (0.19)	
	1	4	2.935	4.410	0.069	0.16 (0.14)	0.33 (0.18)			-0.16 (0.17)				0.08 (0.2)	
	6	5	3.058	5.985	0.132	0.06 (0.15)	0.39 (0.18)		0.26 (0.16)	-0.14 (0.16)				0.13 (0.2)	
	3	4	4.963	3.396	-0.001	0.31 (0.1)			0.19 (0.17)	-0.18 (0.17)				-0.09 (0.18)	
	5	5	4.975	5.026	0.071	0.19 (0.14)	0.39 (0.19)	-0.17 (0.17)		-0.17 (0.17)				0.08 (0.2)	
	2	4	6.227	2.764	-0.047	0.38 (0.11)		-0.07 (0.17)		-0.2 (0.18)				-0.12 (0.19)	
	4	5	7.615	3.706	-0.021	0.35 (0.11)		-0.12 (0.17)	0.22 (0.17)	-0.19 (0.17)				-0.11 (0.19)	
	8	5	9.131	2.948	-0.078	0.31 (0.18)				-0.15 (0.21)		0.08 (0.18)	-0.06 (0.17)	-0.09 (0.2)	

Table A16: Model output for analysis at the riparian extent. Top models are marked with an asterisk, and models within ΔAICc=2 of the top model are denoted with two asterisks. Standard error is shown in brackets for each estimate.

response variable	model number	k	Δ AIC_c	log likelihood	adjusted R^2	intercept	forest disturbance	road density	human impact	wetted width	substrate size	canopy	flow	% lake	% wetland
% shredders	1*	4	0	5.929	0.324	0.75 (0.13)	-0.21 (0.17)			-0.18 (0.16)	-0.6 (0.2)				
	2**	4	0.648	5.605	0.308	0.74 (0.13)		-0.15 (0.14)		-0.2 (0.16)	-0.64 (0.2)				
	3**	4	1.834	5.012	0.279	0.7 (0.12)			-0.03 (0.15)	-0.19 (0.17)	-0.62 (0.2)				
	8	5	2.931	6.1	0.303	0.8 (0.15)				-0.3 (0.2)	-0.55 (0.21)	-0.1 (0.15)	-0.2 (0.18)		
	5	5	3.036	6.048	0.301	0.77 (0.13)	-0.17 (0.2)	-0.07 (0.17)		-0.19 (0.16)	-0.62 (0.2)				
	6	5	3.111	6.01	0.299	0.77 (0.13)	-0.22 (0.17)		-0.05 (0.14)	-0.19 (0.16)	-0.6 (0.2)				
	4	5	3.919	5.606	0.278	0.74 (0.13)		-0.15 (0.15)	0.01 (0.15)	-0.2 (0.17)	-0.64 (0.21)				
	null	1	6.026	-1.208	0	0.28 (0.05)									
	7	6	6.573	6.079	0.271	0.77 (0.14)	-0.18 (0.21)	-0.06 (0.18)	-0.04 (0.16)	-0.19 (0.17)	-0.61 (0.21)				
specific conductivity	4*	5	0	10.46	0.334	0.04 (0.09)		0.38 (0.13)	0.23 (0.13)	-0.02 (0.14)					-0.09 (0.14)
	2**	4	0.477	8.585	0.271	0.1 (0.09)		0.42 (0.13)		-0.02 (0.14)					-0.13 (0.14)
	5	5	2.966	8.977	0.26	0.13 (0.1)	-0.15 (0.19)	0.48 (0.15)		0 (0.15)					-0.17 (0.15)
	7	6	3.548	10.486	0.305	0.05 (0.11)	-0.04 (0.19)	0.39 (0.15)	0.22 (0.14)	-0.01 (0.14)					-0.1 (0.16)
	null	1	4.361	2.519	0	0.18 (0.04)									
	3	4	6.014	5.817	0.111	0.15 (0.09)			0.31 (0.14)	-0.05 (0.16)					-0.12 (0.16)
	6	5	7.175	6.873	0.14	0.04 (0.12)	0.24 (0.18)		0.35 (0.14)	-0.07 (0.16)					-0.03 (0.17)
	1	4	10.188	3.73	-0.032	0.19 (0.12)	0.15 (0.19)			-0.08 (0.17)					-0.14 (0.18)
	8	5	14.082	3.419	-0.101	0.21 (0.17)				-0.04 (0.21)		0.05 (0.17)		0 (0.18)	-0.18 (0.19)
embeddedness	null*	1	0	-1.628	0	0.57 (0.05)									
	1	4	2.233	1.38	0.092	0.35 (0.15)	0.12 (0.19)				0.18 (0.23)			0.41 (0.18)	
	2	4	2.433	1.28	0.086	0.41 (0.15)		-0.08 (0.17)			0.19 (0.23)			0.43 (0.18)	
	3	4	2.607	1.192	0.08	0.38 (0.15)			0.04 (0.17)		0.2 (0.23)			0.43 (0.19)	

	8	5	4.444	1.91	0.088	0.48 (0.16)				-0.19 (0.2)	0.28 (0.24)		-0.17 (0.21)	0.38 (0.19)
	5	5	4.545	1.86	0.085	0.37 (0.16)	0.22 (0.23)	-0.17 (0.19)			0.15 (0.23)			0.44 (0.18)
	6	5	5.383	1.441	0.057	0.33 (0.17)	0.13 (0.2)		0.06 (0.17)		0.18 (0.24)			0.43 (0.19)
	4	5	5.54	1.362	0.052	0.4 (0.16)		-0.09 (0.18)	0.07 (0.18)		0.19 (0.24)			0.44 (0.19)
	7	6	7.484	2.19	0.066	0.34 (0.17)	0.28 (0.24)	-0.23 (0.21)	0.14 (0.19)		0.14 (0.24)			0.48 (0.19)
EPT index	null*	1	0	-2.331	0	0.43 (0.05)								
	1**	4	1.026	1.28	0.131	0.1 (0.15)	0.4 (0.2)			0.16 (0.19)	0.22 (0.23)			
	2	4	3.687	-0.051	0.044	0.14 (0.16)		0.23 (0.17)		0.19 (0.2)	0.28 (0.25)			
	5	5	4.145	1.356	0.098	0.09 (0.16)	0.36 (0.23)	0.07 (0.2)		0.16 (0.19)	0.23 (0.24)			
	6	5	4.163	1.347	0.097	0.12 (0.16)	0.4 (0.2)		-0.06 (0.17)	0.15 (0.19)	0.23 (0.24)			
	3	4	5.271	-0.843	-0.012	0.25 (0.15)			-0.1 (0.18)	0.16 (0.21)	0.27 (0.25)			
	4	5	6.01	0.424	0.036	0.16 (0.16)		0.26 (0.18)	-0.16 (0.18)	0.18 (0.2)	0.3 (0.25)			
	7	6	7.457	1.5	0.067	0.11 (0.16)	0.33 (0.25)	0.1 (0.21)	-0.09 (0.19)	0.16 (0.2)	0.25 (0.25)			
	8	5	8.414	-0.778	-0.051	0.19 (0.2)				0.21 (0.25)	0.27 (0.27)	0.1 (0.19)	-0.1 (0.22)	
invertebrate biomass	1*	4	0	4.784	0.185	0.46 (0.13)	-0.11 (0.17)			-0.48 (0.17)	0.05 (0.21)			
	2**	4	0.151	4.709	0.181	0.4 (0.13)		0.07 (0.15)		-0.48 (0.17)	0.04 (0.21)			
	3**	4	0.354	4.607	0.175	0.44 (0.13)			-0.04 (0.15)	-0.49 (0.17)	0.04 (0.21)			
	null**	1	0.777	0.272	0	0.25 (0.05)								
	5	5	2.199	5.321	0.182	0.43 (0.14)	-0.2 (0.2)	0.16 (0.17)		-0.46 (0.17)	0.07 (0.21)			
	8	5	2.928	4.956	0.16	0.35 (0.16)				-0.39 (0.2)	0 (0.22)	0.11 (0.15)	0.04 (0.18)	
	6	5	3.13	4.855	0.154	0.48 (0.14)	-0.11 (0.18)		-0.05 (0.15)	-0.49 (0.17)	0.05 (0.21)			
	4	5	3.247	4.797	0.15	0.41 (0.14)		0.09 (0.15)	-0.06 (0.15)	-0.48 (0.17)	0.05 (0.21)			
	7	6	5.165	5.638	0.163	0.45 (0.14)	-0.25 (0.21)	0.21 (0.18)	-0.11 (0.16)	-0.47 (0.17)	0.09 (0.21)			
periphyton biomass	null*	1	0	5.935	0	0.2 (0.04)								
	1**	4	0.629	9.744	0.143	-0.03 (0.12)	-0.1 (0.14)			0.43 (0.16)		0.19 (0.13)		

	2**	4	0.975	9.571	0.132	-0.04 (0.12)		-0.05 (0.12)		0.41 (0.16)		0.18 (0.13)		
	3**	4	1.098	9.51	0.129	-0.04 (0.12)			-0.04 (0.12)	0.41 (0.16)		0.17 (0.13)		
	6	5	3.741	9.825	0.111	-0.01 (0.13)	-0.11 (0.15)		-0.05 (0.13)	0.42 (0.16)		0.18 (0.13)		
	5	5	3.892	9.749	0.106	-0.02 (0.12)	-0.09 (0.17)	-0.01 (0.15)		0.43 (0.17)		0.19 (0.13)		
	8	5	3.941	9.725	0.104	0 (0.14)				0.45 (0.17)	-0.09 (0.18)	0.18 (0.13)		-0.06 (0.15)
	4	5	4.202	9.594	0.096	-0.03 (0.13)		-0.05 (0.13)	-0.03 (0.13)	0.41 (0.17)		0.17 (0.13)		
	7	6	7.341	9.825	0.07	-0.01 (0.13)	-0.11 (0.18)	0 (0.16)	-0.05 (0.14)	0.43 (0.17)		0.18 (0.13)		
total dissolved nitrogen	null*	1	0	1.754	0	0.25 (0.04)								
	3	4	4.418	3.668	0.019	0.29 (0.1)			0.2 (0.16)	-0.17 (0.17)				-0.06 (0.17)
	1	4	5.789	2.983	-0.03	0.3 (0.12)	0.13 (0.2)			-0.2 (0.18)				-0.06 (0.19)
	2	4	6.239	2.758	-0.047	0.37 (0.11)		-0.04 (0.16)		-0.19 (0.18)				-0.11 (0.18)
	6	5	6.521	4.253	0.018	0.2 (0.13)	0.19 (0.2)		0.23 (0.16)	-0.19 (0.17)				0.01 (0.19)
	4	5	7.327	3.85	-0.011	0.31 (0.11)		-0.09 (0.16)	0.22 (0.16)	-0.18 (0.17)				-0.07 (0.18)
	7	6	7.807	5.41	0.055	0.19 (0.13)	0.37 (0.23)	-0.26 (0.19)	0.32 (0.17)	-0.23 (0.17)				0.05 (0.19)
	5	5	8.466	3.281	-0.053	0.31 (0.12)	0.21 (0.23)	-0.13 (0.18)		-0.22 (0.18)				-0.05 (0.19)
	8	5	8.674	3.177	-0.06	0.33 (0.18)				-0.15 (0.21)		0.06 (0.17)	-0.12 (0.18)	-0.11 (0.19)

Table A17: Model output for analysis at the local extent. Top models are marked with an asterisk, and models within ΔAICc=2 of the top model are denoted with two asterisks. Standard error is shown in brackets for each estimate.

response variable	model number	k	Δ AIC_c	log likelihood	adjusted R^2	intercept	forest disturbance	road density	human impact	wetted width	substrate size	canopy	flow	% lake	% wetland
% shredders	3*	4	0	9.172	0.464	0.79 (0.11)			-0.29 (0.1)	-0.3 (0.15)	-0.5 (0.18)				
	4**	5	0.172	10.722	0.499	0.73 (0.11)		0.27 (0.17)	-0.35 (0.1)	-0.24 (0.15)	-0.48 (0.18)				
	6	5	3.159	9.229	0.443	0.81 (0.12)	-0.05 (0.15)		-0.28 (0.11)	-0.29 (0.16)	-0.5 (0.19)				
	7	6	3.591	10.813	0.48	0.75 (0.12)	-0.06 (0.15)	0.28 (0.17)	-0.34 (0.12)	-0.23 (0.15)	-0.48 (0.18)				
	1	4	6.491	5.926	0.324	0.76 (0.13)	-0.2 (0.16)			-0.16 (0.16)	-0.61 (0.2)				
	2	4	8.167	5.088	0.282	0.67 (0.13)		0.08 (0.19)		-0.16 (0.17)	-0.63 (0.2)				
	5	5	9.256	6.18	0.307	0.73 (0.14)	-0.22 (0.16)	0.12 (0.19)		-0.12 (0.17)	-0.61 (0.2)				
	8	5	9.416	6.1	0.303	0.8 (0.15)				-0.3 (0.2)	-0.55 (0.21)	-0.1 (0.15)	-0.2 (0.18)		
	null	1	12.511	-1.208	0	0.28 (0.05)									
specific conductivity	null*	1	0	2.519	0	0.18 (0.04)									
	3	4	5.473	3.906	-0.019	0.17 (0.11)			0.14 (0.12)	-0.06 (0.17)					-0.14 (0.18)
	2	4	5.505	3.891	-0.02	0.16 (0.12)		0.24 (0.21)		-0.03 (0.18)					-0.09 (0.19)
	1	4	6.036	3.625	-0.04	0.19 (0.11)	0.15 (0.17)			-0.12 (0.17)					-0.18 (0.18)
	4	5	7.99	4.285	-0.035	0.12 (0.13)		0.18 (0.22)	0.1 (0.13)	-0.02 (0.18)					-0.09 (0.19)
	5	5	8.29	4.135	-0.046	0.13 (0.13)	0.11 (0.18)	0.2 (0.22)		-0.06 (0.18)					-0.11 (0.19)
	6	5	8.512	4.023	-0.054	0.15 (0.12)	0.08 (0.19)		0.11 (0.14)	-0.08 (0.18)					-0.15 (0.18)
	8	5	9.44	3.559	-0.09	0.27 (0.19)				-0.1 (0.22)		-0.03 (0.19)		-0.16 (0.21)	-0.19 (0.22)
	7	6	11.436	4.361	-0.076	0.11 (0.13)	0.07 (0.19)	0.17 (0.23)	0.08 (0.14)	-0.03 (0.19)					-0.1 (0.2)
embeddedness	null*	1	0	-1.628	0	0.57 (0.05)									
	2**	4	0.156	2.418	0.157	0.47 (0.13)		0.24 (0.2)			0.16 (0.22)			-0.52 (0.21)	
	1**	4	1.571	1.71	0.114	0.56 (0.14)	-0.09 (0.18)				0.15 (0.22)			-0.52 (0.21)	
	3**	4	1.728	1.632	0.109	0.54 (0.13)			-0.04 (0.13)		0.15 (0.23)			-0.51 (0.22)	

	4	5	2.457	2.904	0.151	0.49 (0.13)		0.32 (0.22)	-0.13 (0.14)		0.2 (0.22)		-0.48 (0.21)
	5	5	2.927	2.669	0.136	0.51 (0.15)	-0.12 (0.18)	0.25 (0.2)			0.18 (0.22)		-0.52 (0.21)
	8	5	4.619	1.823	0.083	0.57 (0.15)				-0.13 (0.2)	0.19 (0.24)	-0.06 (0.23)	-0.48 (0.24)
	6	5	4.819	1.723	0.076	0.56 (0.15)	-0.08 (0.2)		-0.02 (0.14)		0.15 (0.23)		-0.52 (0.22)
	7	6	5.897	2.984	0.117	0.51 (0.15)	-0.07 (0.19)	0.32 (0.22)	-0.11 (0.15)		0.2 (0.23)		-0.48 (0.22)
EPT index	null*	1	0	-2.331	0	0.43 (0.05)							
	1**	4	0.458	1.563	0.148	0.08 (0.15)	0.4 (0.18)			0.12 (0.19)	0.22 (0.23)		
	5	5	3.47	1.694	0.119	0.06 (0.16)	0.39 (0.19)	0.1 (0.22)		0.15 (0.2)	0.22 (0.24)		
	6	5	3.716	1.571	0.112	0.08 (0.15)	0.39 (0.2)		0.02 (0.15)	0.13 (0.2)	0.21 (0.24)		
	3	4	4.663	-0.539	0.01	0.18 (0.15)			0.13 (0.14)	0.22 (0.21)	0.21 (0.26)		
	2	4	4.93	-0.673	0.001	0.17 (0.16)		0.18 (0.23)		0.22 (0.21)	0.26 (0.25)		
	7	6	7.069	1.694	0.079	0.06 (0.16)	0.39 (0.21)	0.1 (0.24)	-0.01 (0.16)	0.15 (0.21)	0.22 (0.25)		
	4	5	7.649	-0.395	-0.022	0.15 (0.17)		0.12 (0.25)	0.11 (0.16)	0.24 (0.22)	0.22 (0.26)		
	8	5	8.414	-0.778	-0.051	0.19 (0.2)				0.21 (0.25)	0.27 (0.27)	0.1 (0.19)	-0.1 (0.22)
invertebrate biomass	4*	5	0	11.9	0.488	0.34 (0.11)		0.61 (0.16)	-0.25 (0.1)	-0.4 (0.14)	0.14 (0.17)		
	2	4	3.185	8.671	0.383	0.29 (0.12)		0.47 (0.16)		-0.35 (0.15)	0.03 (0.18)		
	7	6	3.32	12.04	0.47	0.36 (0.11)	-0.07 (0.14)	0.61 (0.16)	-0.23 (0.11)	-0.38 (0.15)	0.13 (0.17)		
	5	5	4.645	9.577	0.396	0.34 (0.12)	-0.18 (0.14)	0.51 (0.17)		-0.31 (0.15)	0.05 (0.18)		
	3	4	10.355	5.086	0.202	0.47 (0.13)			-0.11 (0.12)	-0.53 (0.17)	0.08 (0.21)		
	1	4	10.949	4.789	0.185	0.47 (0.13)	-0.1 (0.16)			-0.47 (0.17)	0.04 (0.21)		
	null	1	11.736	0.272	0	0.25 (0.05)							
	6	5	13.544	5.128	0.17	0.48 (0.14)	-0.05 (0.18)		-0.1 (0.13)	-0.51 (0.18)	0.08 (0.21)		
	8	5	13.887	4.956	0.16	0.35 (0.16)				-0.39 (0.2)	0 (0.22)	0.11 (0.15)	0.04 (0.18)
periphyton biomass	null*	1	0	5.935	0	0.2 (0.04)							
	1**	4	0.841	9.639	0.136	-0.01 (0.14)	-0.08 (0.14)			0.42 (0.16)		0.16 (0.13)	

	3**	4	1.154	9.482	0.127	-0.04 (0.13)			-0.02 (0.1)	0.41 (0.16)		0.18 (0.13)			
	2**	4	1.187	9.466	0.126	-0.05 (0.12)		-0.01 (0.16)		0.42 (0.16)		0.18 (0.13)			
	8	5	3.562	9.914	0.117	-0.07 (0.15)				0.5 (0.19)	-0.13 (0.18)	0.25 (0.16)			0.12 (0.18)
	5	5	4.112	9.639	0.099	-0.01 (0.14)	-0.08 (0.15)	0.01 (0.17)		0.42 (0.17)		0.16 (0.14)			
	6	5	4.112	9.639	0.099	-0.01 (0.14)	-0.08 (0.16)		0 (0.11)	0.42 (0.17)		0.16 (0.13)			
	4	5	4.426	9.482	0.089	-0.04 (0.13)		0 (0.18)	-0.02 (0.11)	0.41 (0.17)		0.18 (0.13)			
	7	6	7.711	9.64	0.058	-0.01 (0.15)	-0.08 (0.16)	0.01 (0.18)	0 (0.12)	0.42 (0.17)		0.16 (0.14)			
total dissolved nitrogen	null*	1	0	1.754	0	0.25 (0.04)									
	2	4	4.293	3.731	0.023	0.46 (0.12)		-0.27 (0.21)		-0.29 (0.18)					-0.22 (0.19)
	1	4	6.032	2.861	-0.039	0.38 (0.11)	-0.06 (0.17)			-0.2 (0.17)					-0.12 (0.18)
	3	4	6.102	2.826	-0.042	0.34 (0.12)			0.03 (0.12)	-0.2 (0.18)					-0.12 (0.18)
	4	5	7.026	4.001	0	0.42 (0.13)		-0.32 (0.23)	0.09 (0.13)	-0.27 (0.18)					-0.22 (0.19)
	5	5	7.564	3.732	-0.019	0.46 (0.13)	-0.01 (0.18)	-0.27 (0.22)		-0.28 (0.19)					-0.22 (0.2)
	8	5	8.928	3.05	-0.07	0.28 (0.19)				-0.16 (0.22)		0.09 (0.2)		0.11 (0.21)	-0.07 (0.22)
	6	5	9.111	2.958	-0.077	0.36 (0.12)	-0.09 (0.2)		0.06 (0.14)	-0.17 (0.19)					-0.11 (0.19)
	7	6	10.498	4.065	-0.041	0.43 (0.13)	-0.06 (0.19)	-0.31 (0.23)	0.1 (0.14)	-0.26 (0.19)					-0.21 (0.2)

References

Allan, J.D. (2004) 'Landscapes and riverscapes: The influence of land use on stream ecosystems', *Annual Review of Ecology, Evolution, and Systematics*, 35(2002), pp. 257–284. Available at: https://doi.org/10.1146/annurev.ecolsys.35.120202.110122.

Allan, J.D., Erickson, D.L. and Fay, J. (1997) 'The influence of catchment land use on stream integrity across multiple spatial scales', *Freshwater Biology*, 37(1), pp. 149–161. Available at: https://doi.org/10.1046/J.1365-2427.1997.D01-546.X.

Allan, J.D. and Flecker, A.S. (1988) 'Prey preference in stoneflies: a comparative analysis of prey vulnerability', *Oecologia*, 76, pp. 496–503.

Axler, R.P. and Owen, C.J. (1994) 'Measuring chlorophyll and phaeophytin: Whom should you believe?', *Lake and Reservoir Management*, 8(2), pp. 143–151. Available at: https://doi.org/10.1080/07438149409354466.

Barbour, M.T. (1999) *Rapid bioassessment protocols for use in wadeable streams and rivers: periphyton, benthic macroinvertebrates and fish*. Second edi. Washington: US Environmental Protection Agency.

Benke, A.C. *et al.* (1999) *Length-Mass Relationships for Freshwater Macroinvertebrates in North America with Particular Reference to the Southeastern United States*, *Source: Journal of the North American Benthological Society*.

Bilotta, G.S. and Brazier, R.E. (2008) 'Understanding the influence of suspended solids on water quality and aquatic biota', *Water Research*, 42(12), pp. 2849–2861. Available at: https://doi.org/10.1016/j.watres.2008.03.018.

Bivand, R. and Keitt, T. (2022) 'rgdal: Bindings for the "Geospatial" Data Abstraction Library'. Available at: https://cran.r-project.org/package=rgdal.

Bowering, K.L. *et al.* (2022) 'Dissolved Organic Carbon Mobilization Across a Climate Transect of Mesic Boreal Forests Is Explained by Air Temperature and Snowpack Duration', *Ecosystems*, 26, pp. 55–71. Available at: https://doi.org/10.1007/s10021-022-0074.

Burgherr, P. and Meyer, E.I. (1997) 'Regression analysis of linear body dimensions vs. dry mass in stream macroinvertebrates', *Archiv für Hydrobiologie*, 139(1), pp. 101–112. Available at: https://doi.org/10.1127/archiv-hydrobiol/139/1997/101.

Callahan, M.K. *et al.* (2017) 'Nitrogen Subsidies from Hillslope Alder Stands to Streamside Wetlands

and Headwater Streams, Kenai Peninsula, Alaska', *JAWRA Journal of the American Water Resources Association*, 53(2), pp. 478–492. Available at: https://doi.org/10.1111/1752-1688.12508.

Canning-Clode, J. *et al.* (2008) 'Influence of disturbance and nutrient enrichment on early successional fouling communities in an oligotrophic marine system', *Marine Ecology*, 29(1), pp. 115–124. Available at: https://doi.org/10.1111/j.1439-0485.2007.00210.x.

Chin, A. *et al.* (2004) 'Effects of all-terrain vehicles on stream dynamics', *Ouachita and Ozark Mountains symposium: ecosystem management research.*, pp. 292–296. Available at: http://www.treesearch.fs.fed.us/pubs/viewpub.jsp?index=6475.

Government of Canada (2022) *High Resolution Digital Elevation Model (HRDEM) - CanElevation Series*.

Government of Newfoundland and Labrador (2010) 'Forest resource inventory', *Department of Natural Resources* [Preprint].

Guichard, F. and Marleau, J. (2021) *Meta-Ecosystem Dynamics: Understanding Ecosystems Through the Transformation and Movement of Matter*. Available at: http://www.springer.com/series/10049.

Hauer, F.R. and Lamberti, G.A. (2007) *Methods in stream ecology*. Elsevier Inc.

Healson (2016) 'Canopy cover free'.

Hijmans, R. (2022) 'raster: Geographic Data Analysis and Modeling'. Available at: https://cran.r-project.org/package=raster.

Hollister, J.W. (2021) 'elevatr: Access Elevation Data from Various APIs'. Available at: https://cran.r-project.org/package=elevatr/.

Kawaguchi, Y., Taniguchi, Y. and Nakano, S. (2018) 'Terrestrial Invertebrate Inputs Determine the Local Abundance of Stream Fishes in a Forested Stream', *Ecological Society of America*, 84(3), pp. 701–708.

Kiffney, P.M., Richardson, J.S. and Bull, J.P. (2003) 'Responses of periphyton and insects to experimental manipulation of riparian buffer width along forest streams', *Journal of Applied Ecology*, 40(6), pp. 1060–1076. Available at: https://doi.org/10.1111/J.1365-2664.2003.00855.X.

Larson, D.J. and Colbo, M.H. (1983) 'The aquatic insects: biogeographic considerations.', *Biogeography and ecology of the island of Newfoundland*, pp. 593–677.

Longnecker, K. (2021) ‘Collecting samples for dissolved organic carbon (DOC) analysis V.1’, *Woods Hole Oceanographic institute* [Preprint].

Lorenzen, J. (1967) ‘Determination of chlorophyll and pheo-pigments : spectrophotometric equations’, *Limnol. Oceanogr.*, 12, pp. 343–346. Available at: https://cir.nii.ac.jp/crid/1570854175550119936.bib?lang=en (Accessed: 9 May 2023).

MacSween, J., Leroux, S.J. and Oakes, K.D. (2019) ‘Cross-ecosystem effects of a large terrestrial herbivore on stream ecosystem functioning’, *Oikos*, 128(1), pp. 135–145. Available at: https://doi.org/10.1111/oik.05331.

Odum, E.P., Finn, J.T. and Franz, E.H. (1979) ‘Perturbation Theory and the Subsidy-Stress Gradient’, *BioScience*, 29(6), pp. 349–352. Available at: https://doi.org/10.2307/1307690.

Pebesma, E. (2018) ‘Simple Features for R: Standardized Support for Spatial Vector Data’, *The R Journal*, 10(1), pp. 439–446. Available at: https://doi.org/10.32614/RJ-2018-009.

Pebesma, E. (2022) ‘lwgeom: Bindings to Selected “liblwgeom” Functions for Simple Features’. Available at: https://cran.r-project.org/package=lwgeom.

Piggott, J.J. *et al.* (2012) ‘Multiple Stressors in Agricultural Streams: A Mesocosm Study of Interactions among Raised Water Temperature, Sediment Addition and Nutrient Enrichment’, *PLoS ONE*, 7(11), p. 49873. Available at: https://doi.org/10.1371/journal.pone.0049873.

QGIS Development Team (2021) ‘QGIS Geographic information system’. Open Source Geospatial Foundation Project.

Quinn, J.M. (2000) ‘Effects of pastoral development’, *New Zealand Stream Invertebrates: Ecology and Implications for Management*, (October), pp. 208–229.

R Core Team (2020) ‘R: A language and environment for statistical computing’. Vienna, Austria: R Foundation for Statistical Computing.

Reuss, J.O., Stottlemyer, R. and Troendle, C.A. (1997) ‘Effect of clear cutting on nutrient fluxes in a subalpine forest at Fraser, Colorado’, *Hydrology and Earth System Sciences*, 1(2), pp. 333–344. Available at: https://doi.org/10.5194/HESS-1-333-1997.

Richardson, J.S. and Béraud, S. (2014) ‘Effects of riparian forest harvest on streams: A meta-analysis’, *Journal of Applied Ecology*, 51(6), pp. 1712–1721. Available at: https://doi.org/10.1111/1365-2664.12332.

Roth, N.E., David Allan, J. and Erickson, D.L. (1996) 'Landscape influences on stream biotic integrity assessed at multiple spatial scales', *Landscape Ecology*, 11(3), pp. 141–156.

Smith, E.L., Coté, D. and Colbo, M.H. (2013) 'An Impoverished Benthic Community Shows Regional Distinctions', *https://doi.org/10.1656/045.020.0107*, 20(1), pp. 91–102. Available at: https://doi.org/10.1656/045.020.0107.

Stone, M.K. and Wallace, J.B. (1998) 'Long-term recovery of a mountain stream from clear-cut logging: The effects of forest succession on benthic invertebrate community structure', *Freshwater Biology*, 39(1), pp. 151–169. Available at: https://doi.org/10.1046/j.1365-2427.1998.00272.x.

'The Canadian Aquatic Biomonitoring Network Field Manual' (2009). Available at: http://www.unb.ca/cri/cabin_criweb.html (Accessed: 15 May 2022).

Townsend, C.R. *et al.* (2003) 'The influence of scale and geography on relationships between stream community composition and landscape variables: description and prediction', *Freshwater Biology*, 48(5), pp. 768–785. Available at: https://doi.org/10.1046/J.1365-2427.2003.01043.X.

Vannote, R.L. *et al.* (1980) 'The River Continuum Concept', *Canadian Journal of Fisheries and Aquatic Sciences*, 37(1).

Vieira, N.K.M. *et al.* (2016) 'A Database of Lotic Invertebrate Traits for North America', *U.S. Geological Survey Data Series*, 187, pp. 1–15.

Wooster, D. (1994) 'Predator impacts on stream benthic prey', *Oecologia*, 99(1–2), pp. 7–15. Available at: https://doi.org/10.1007/BF00317077/METRICS.

Zimmermann, B., Elsenbeer, H. and De Moraes, J.M. (2006) 'The influence of land-use changes on soil hydraulic properties: Implications for runoff generation', *Forest ecology and management*, 222(1–3). Available at: https://doi.org/10.1016/j.foreco.2005.10.070.

Appendix B: Meta-ecosystem model

1 Model development

1.1 Selecting feasible and stable equilibria

We used Mathematica (Wolfram Research, 2022) to generate the analytical equilibrium equations for the meta-ecosystem model and found two (equilibrium 9 and 10 listed in section 3) to be have the potential for feasible equilibrium states (i.e., where all trophic level densities can be greater than zero), and selected equilibrium 10 as it was feasible more frequently than equilibrium 9. All ten equilibria generated in Mathematica for our model are provided in section 3 below.

We then generated 300,000 random parameter combinations within a range of 0-10 (or between 0-1 if they were a proportion) using lhs (version 1.1.6; Carnell, 2022) and filtered for feasibility and stability: we selected for parameter combinations that lead to feasible equilibrium states (non-negative trophic level densities) for all state variables (see Jacquet et al., 2022), and used Mathematica to find the Jacobian matrix and the base "eigen" function in R to determine the leading eigenvalue of the Jacobian matrix evaluated for each parameter set to determine local stability. From this we retained the first 1000 feasible and locally stable parameter combinations to be used in the disturbance simulations (see Table B10 for median values of key parameters and state variables in these 1000 "undisturbed" meta-ecosystems).

Jacobian matrix:

$$\begin{bmatrix} N_t\alpha_t - \epsilon - \theta_t & P_t\alpha_t & 0 & 0 & 0 & 0 \\ -(N_t\alpha_t) + \theta_t\mu_t & -l_t - P_t\alpha_t - \psi_t & 0 & 0 & 0 & \psi_a \\ \epsilon & 0 & -\gamma - H_a\delta & -(L_t\delta) & 0 & 0 \\ 0 & 0 & H_a\delta\rho & eP_a\beta_a + L_t\delta\rho - \tau_a & eH_a\beta_a & 0 \\ 0 & 0 & 0 & -(P_a\beta_a) & N_a\alpha_a - H_a\beta_a - \theta_a & P_a\alpha_a \\ 0 & \psi_t & \gamma & \eta_a\tau_a & -(N_a\alpha_a) + \theta_a\mu_a & -l_a - P_a\alpha_a - \psi_a \end{bmatrix}$$

1.2 Global sensitivity analysis

We performed a global sensitivity analysis (GSA) on each trophic level and productivity metric of the model and on the entire model to identify the parameters creating the most uncertainty in the model (i.e., the most important parameters). Following Bellmore et al. (2014) and Harper et al. (2011), we used the Random Forest statistical method to rank parameters based on importance. We applied the RandomForest package from Liaw and Wiener (2001) to the same 1000 random parameter combinations (Figure B8). We used the relative importance of each parameter to determine how to create effective disturbance simulations in the terrestrial ecosystem.

2 Simulating disturbance

We simulated disturbance from logging, insect outbreaks, and ATV trails/logging roads by taking the 1000 feasible and stable parameters and increasing the following parameters in the model across their ranges, while keeping all other parameters the same:

1) **Tree density disturbance (logging and insect outbreaks)**

   We tested θ_t (tree death) across the range of 0-10 in increments of 0.5 to simulate increasing tree death from either logging or insect outbreaks, and tested tree recycling (μ_t) across the range of 0-1 in increments of 0.05 to simulating either high proportion of dead tree biomass recycling (normal conditions) or low proportion of tree biomass recycling (abnormal conditions where trees are removed from the ecosystem). Insect outbreaks are therefore represented by the simulations with high recycling (μ_t=0.7-1) and moderate tree death (θ_t=3-7), depending on the insect population, and logging is represented by the simulations with low recycling (μ_t=0-0.3) and high tree death (θ_t=3-7), depending on how many trees are logged.

2) **Unpaved road density (ATV trails and logging roads)**

   We tested β_a and α_a across the range of 0-10 in increments of 0.5 to simulate increasing water turbidity, which is expected to influence the ability of both benthic invertebrates and periphyton to undergo their respective processes of taking up nutrients and increasing their biomass. Poor water conditions are represented by low uptake rates for both β_a and α_a.

This resulted in 441 “disturbance scenarios” for each of the 1000 initial "undisturbed" parameter sets, creating 441,000 total disturbance scenarios (Figure B9). We took the median value at each combination of the parameters being manipulated and used that generate surface plots for the meta-ecosystem properties of interest, retaining only the disturbance simulations that had stable and feasible equilibria (see Tables B11 and B12 for the number of meta-ecosystem simulations that were stable at each increment of disturbance). Results for inorganic nutrient stock in each disturbance simulation (not included in the main text) are provided in Figures B10 and B11.

3 Equilibria for the meta-ecosystem model

Equilibrium 1:

$$\left\{Pt \to 0,\ Nt \to \frac{la\,\delta\,\lambda t\,\rho + \delta\,(\lambda a + \lambda t)\,\rho\,\psi a + \gamma\,(1 - \eta a\,\rho)\,\tau a\,\psi a}{\delta\,\rho\,(lt\,\psi a + la\,(lt + \psi t))},\ Lt \to \frac{\tau a}{\delta\,\rho},\ Ha \to -\frac{\gamma}{\delta},\ Pa \to 0,\ Na \to \right.$$

$$\left.\frac{lt\,\delta\,\lambda a\,\rho + lt\,\gamma\,(1 - \eta a\,\rho)\,\tau a + \delta\,(\lambda a + \lambda t)\,\rho\,\psi t + \gamma\,(1 - \eta a\,\rho)\,\tau a\,\psi t}{\delta\,\rho\,(lt\,\psi a + la\,(lt + \psi t))}\right\}$$

Equilibrium 2:

$$\left\{Pt \to 0,\ Nt \to \frac{\alpha a\,\lambda t + \theta a\,\psi a}{lt\,\alpha a + \alpha a\,\psi t},\ Lt \to 0,\ Ha \to 0,\ Pa \to \frac{lt\,(-\alpha a\,\lambda a + \theta a\,\psi a) - \alpha a\,(\lambda a + \lambda t)\,\psi t + la\,\theta a\,(lt + \psi t)}{\alpha a\,\theta a\,(-1 + \mu a)\,(lt + \psi t)},\ Na \to \frac{\theta a}{\alpha a}\right\}$$

Equilibrium 3

$$\left\{Pt \to \frac{-lt\,\alpha a\,(\epsilon + \partial t) + \alpha a\,\alpha t\,\lambda t + \alpha t\,\partial a\,\psi a - \alpha a\,(\epsilon + \partial t)\,\psi t}{\alpha a\,\alpha t\,(\epsilon + \partial t - \partial t\,\mu t)},\ Nt \to \frac{\epsilon + \partial t}{\alpha t},\ Lt \to -\frac{\epsilon\,(lt\,\alpha a\,(\epsilon + \partial t) - \alpha a\,\alpha t\,\lambda t - \alpha t\,\partial a\,\psi a + \alpha a\,(\epsilon + \partial t)\,\psi t)}{\alpha a\,\alpha t\,\gamma\,(\epsilon + \partial t - \partial t\,\mu t)},\ Ha \to 0,\ Pa \to \right.$$

$$\frac{lt\,\alpha a\,\epsilon\,(\epsilon + \partial t) - \alpha a\,\alpha t\,\epsilon\,\lambda a - \alpha a\,\alpha t\,\partial t\,\lambda a - \alpha a\,\alpha t\,\epsilon\,\lambda t + \alpha a\,\alpha t\,\partial t\,\lambda a\,\mu t + la\,\alpha t\,\partial a\,(\epsilon + \partial t - \partial t\,\mu t) + \alpha t\,\partial a\,\partial t\,\psi a - \alpha t\,\partial a\,\partial t\,\mu t\,\psi a - \alpha a\,\epsilon\,\partial t\,\psi t - \alpha a\,\partial t^2\,\psi t + \alpha a\,\epsilon\,\partial t\,\mu t\,\psi t + \alpha a\,\partial t^2\,\mu t\,\psi t}{\alpha a\,\alpha t\,\partial a\,(-1 + \mu a)\,(\epsilon + \partial t - \partial t\,\mu t)},$$

$$\left.Na \to \frac{\partial a}{\alpha a}\right\}$$

Equilibrium 4:

$$\left\{Pt \to 0,\ Nt \to \frac{\alpha a\,\delta\,\lambda t - \beta a\,\gamma\,\psi a + \delta\,\partial a\,\psi a}{lt\,\alpha a\,\delta + \alpha a\,\delta\,\psi t},\right.$$

$$Lt \to \frac{\alpha a\,(\beta a\,\gamma + \delta\,\partial a\,(-1 + \mu a))\,\tau a\,(lt + \psi t) + e\,\beta a\,(lt\,(\alpha a\,\delta\,\lambda a - \alpha a\,\gamma\,\eta a\,\tau a + \beta a\,\gamma\,\psi a - \delta\,\partial a\,\psi a) + \alpha a\,(\delta\,(\lambda a + \lambda t) - \gamma\,\eta a\,\tau a)\,\psi t + la\,(\beta a\,\gamma - \delta\,\partial a)\,(lt + \psi t))}{\alpha a\,\delta\,(-e\,\beta a\,\gamma + \beta a\,\gamma\,\rho + \delta\,\partial a\,(-1 + \mu a)\,\rho)\,(lt + \psi t)},$$

$$Ha \to -\frac{\gamma}{\delta},\ Pa \to \frac{lt\,\alpha a\,(\delta\,\lambda a\,\rho + \gamma\,(1 - \eta a\,\rho)\,\tau a) + lt\,(\beta a\,\gamma - \delta\,\partial a)\,\rho\,\psi a + \alpha a\,\delta\,(\lambda a + \lambda t)\,\rho\,\psi t + \alpha a\,\gamma\,(1 - \eta a\,\rho)\,\tau a\,\psi t + la\,(\beta a\,\gamma - \delta\,\partial a)\,\rho\,(lt + \psi t)}{\alpha a\,(e\,\beta a\,\gamma - (\beta a\,\gamma + \delta\,\partial a\,(-1 + \mu a))\,\rho)\,(lt + \psi t)},\ Na \to \left.\frac{-\beta a\,\gamma + \delta\,\partial a}{\alpha a\,\delta}\right\}$$

Equilibrium 5:

$$\left\{Pt \to 0,\ Nt \to \frac{la\,\lambda t + (\lambda a + \lambda t)\,\psi a}{lt\,\psi a + la\,(lt + \psi t)},\ Lt \to 0,\ Ha \to 0,\ Pa \to 0,\ Na \to \frac{lt\,\lambda a + (\lambda a + \lambda t)\,\psi t}{lt\,\psi a + la\,(lt + \psi t)}\right\}$$

Equilibrium 6:

$$\left\{Pt \to 0,\ Nt \to \frac{\tau a\,(\alpha a\,\lambda t + \theta a\,\mu a\,\psi a) + e\,(la\,\beta a\,\lambda t - \alpha a\,\eta a\,\lambda t\,\tau a + \beta a\,\lambda a\,\psi a + \beta a\,\lambda t\,\psi a - \eta a\,\theta a\,\tau a\,\psi a)}{\alpha a\,\tau a\,(lt + \psi t) + e\,(-lt\,\alpha a\,\eta a\,\tau a + lt\,\beta a\,\psi a - \alpha a\,\eta a\,\tau a\,\psi t + la\,\beta a\,(lt + \psi t))},\ Lt \to 0,\ Ha \to \right.$$

$$\frac{\alpha a\,\theta a\,(-1 + \mu a)\,\tau a\,(lt + \psi t) + e\,\beta a\,(lt\,(\alpha a\,\lambda a - \theta a\,\psi a) + \alpha a\,(\lambda a + \lambda t)\,\psi t - la\,\theta a\,(lt + \psi t))}{\beta a\,(\alpha a\,\tau a\,(lt + \psi t) + e\,(-lt\,\alpha a\,\eta a\,\tau a + lt\,\beta a\,\psi a - \alpha a\,\eta a\,\tau a\,\psi t + la\,\beta a\,(lt + \psi t)))},\ Pa \to \frac{\tau a}{e\,\beta a},\ Na \to$$

$$\left.\frac{\theta a\,\mu a\,\tau a\,(lt + \psi t) + e\,(lt\,(\beta a\,\lambda a - \eta a\,\theta a\,\tau a) + \beta a\,(\lambda a + \lambda t)\,\psi t - \eta a\,\theta a\,\tau a\,\psi t)}{\alpha a\,\tau a\,(lt + \psi t) + e\,(-lt\,\alpha a\,\eta a\,\tau a + lt\,\beta a\,\psi a - \alpha a\,\eta a\,\tau a\,\psi t + la\,\beta a\,(lt + \psi t))}\right\}$$

Equilibrium 7:

$$\left\{Pt \to \frac{\left(lt\,\delta\,(\epsilon + \varpi t)\,\rho - \alpha t\left(\delta\,(\lambda a + \lambda t)\,\rho + \gamma\left(1 - \eta a\,\rho\right)\,\tau a\right)\right)\psi a + la\,\delta\,\rho\left(lt\,(\epsilon + \varpi t) - \alpha t\,\lambda t + (\epsilon + \varpi t)\,\psi t\right)}{\alpha t\,\delta\,\rho\left(-la\left(\epsilon + \varpi t - \varpi t\,\mu t\right) + \varpi t\,(-1 + \mu t)\,\psi a + \epsilon\left(-1 + \eta a\,\rho\right)\,\psi a\right)},\ Nt \to \frac{\epsilon + \varpi t}{\alpha t},\ Lt \to \frac{\tau a}{\delta\,\rho},\right.$$

$$Ha \to \frac{\left(-lt\,\delta\,\epsilon\,(\epsilon + \varpi t)\,\rho + \alpha t\,\delta\,\epsilon\,(\lambda a + \lambda t)\,\rho + \alpha t\,\gamma\,\varpi t\,(-1 + \mu t)\,\tau a\right)\psi a - la\left(lt\,\delta\,\epsilon\,(\epsilon + \varpi t)\,\rho - \alpha t\,\delta\,\epsilon\,\lambda t\,\rho + \alpha t\,\gamma\left(\epsilon + \varpi t - \varpi t\,\mu t\right)\,\tau a + \delta\,\epsilon\,(\epsilon + \varpi t)\,\rho\,\psi t\right)}{\alpha t\,\delta\,\tau a\left(la\left(\epsilon + \varpi t - \varpi t\,\mu t\right) + \left(\epsilon + \varpi t - \varpi t\,\mu t - \epsilon\,\eta a\,\rho\right)\,\psi a\right)},$$

$$\left.Pa \to 0,\ Na \to \frac{\alpha t\left(\delta\,\rho\left(\varpi t\,\lambda a\,(-1 + \mu t) - \epsilon\left(\lambda a + \eta a\,\lambda t\,\rho\right)\right) + \gamma\left(\epsilon + \varpi t - \varpi t\,\mu t\right)\left(-1 + \eta a\,\rho\right)\,\tau a\right) + \delta\,(\epsilon + \varpi t)\,\rho\left(lt\,\epsilon\,\eta a\,\rho + \varpi t\,(-1 + \mu t)\,\psi t + \epsilon\left(-1 + \eta a\,\rho\right)\,\psi t\right)}{\alpha t\,\delta\,\rho\left(-la\left(\epsilon + \varpi t - \varpi t\,\mu t\right) + \varpi t\,(-1 + \mu t)\,\psi a + \epsilon\left(-1 + \eta a\,\rho\right)\,\psi a\right)}\right\}$$

Equilibrium 8:

$$\left\{Pt \to \frac{-la\,lt\,(\epsilon+\theta t)+la\,\alpha t\,\lambda t-lt\,(\epsilon+\theta t)\,\psi a+\alpha t\,(\lambda a+\lambda t)\,\psi a-la\,(\epsilon+\theta t)\,\psi t}{\alpha t\,(la\,(\epsilon+\theta t-\theta t\,\mu t)-\theta t\,(-1+\mu t)\,\psi a)},\ Nt \to \frac{\epsilon+\theta t}{\alpha t},\ Lt \to \right.$$

$$-\frac{\epsilon\,(la\,lt\,(\epsilon+\theta t)-la\,\alpha t\,\lambda t+lt\,(\epsilon+\theta t)\,\psi a-\alpha t\,(\lambda a+\lambda t)\,\psi a+la\,(\epsilon+\theta t)\,\psi t)}{\alpha t\,\gamma\,(la\,(\epsilon+\theta t-\theta t\,\mu t)-\theta t\,(-1+\mu t)\,\psi a)},\ Ha \to 0,\ Pa \to 0,\ Na \to$$

$$\left.-\frac{lt\,\epsilon\,(\epsilon+\theta t)-\alpha t\,\epsilon\,(\lambda a+\lambda t)+\alpha t\,\theta t\,\lambda a\,(-1+\mu t)+\theta t\,(\epsilon+\theta t)\,(-1+\mu t)\,\psi t}{\alpha t\,(la\,(\epsilon+\theta t-\theta t\,\mu t)-\theta t\,(-1+\mu t)\,\psi a)}\right\}$$

Equilibrium 9:

$$\left\{Pt \to -\left(\left(-2\,e\,la\,lt\,\alpha a\,\beta a\,\delta\,\epsilon^2-4\,e\,la\,lt\,\alpha a\,\beta a\,\delta\,\epsilon\,\theta t-2\,e\,la\,lt\,\alpha a\,\beta a\,\delta\,\theta t^2+2\,e\,la\,\alpha a\,\alpha t\,\beta a\,\delta\,\epsilon\,\lambda t+2\,e\,la\,\alpha a\,\alpha t\,\beta a\,\delta\,\theta t\,\lambda t+2\,e\,la\,lt\,\alpha a\,\beta a\,\delta\,\epsilon\,\theta t\,\mu t+2\,e\,la\,lt\,\alpha a\,\beta a\,\delta\,\theta t^2\,\mu t-\right.\right.\right.$$
$$2\,e\,la\,\alpha a\,\alpha t\,\beta a\,\delta\,\theta t\,\lambda t\,\mu t-2\,lt\,\alpha a^2\,\delta\,\epsilon^2\,\tau a+2\,e\,lt\,\alpha a^2\,\delta\,\epsilon^2\,\eta a\,\tau a-4\,lt\,\alpha a^2\,\delta\,\epsilon\,\theta t\,\tau a+4\,e\,lt\,\alpha a^2\,\delta\,\epsilon\,\eta a\,\theta t\,\tau a-2\,lt\,\alpha a^2\,\delta\,\theta t^2\,\tau a+2\,e\,lt\,\alpha a^2\,\delta\,\eta a\,\theta t^2\,\tau a+$$
$$2\,\alpha a^2\,\alpha t\,\delta\,\epsilon\,\lambda t\,\tau a-2\,e\,\alpha a^2\,\alpha t\,\delta\,\epsilon\,\eta a\,\lambda t\,\tau a+2\,\alpha a^2\,\alpha t\,\delta\,\theta t\,\lambda t\,\tau a-2\,e\,\alpha a^2\,\alpha t\,\delta\,\eta a\,\theta t\,\lambda t\,\tau a+2\,lt\,\alpha a^2\,\delta\,\epsilon\,\theta t\,\mu t\,\tau a-2\,e\,lt\,\alpha a^2\,\delta\,\epsilon\,\eta a\,\theta t\,\mu t\,\tau a+2\,lt\,\alpha a^2\,\delta\,\theta t^2\,\mu t\,\tau a-$$
$$2\,e\,lt\,\alpha a^2\,\delta\,\eta a\,\theta t^2\,\mu t\,\tau a-2\,\alpha a^2\,\alpha t\,\delta\,\theta t\,\lambda t\,\mu t\,\tau a+2\,e\,\alpha a^2\,\alpha t\,\delta\,\eta a\,\theta t\,\lambda t\,\mu t\,\tau a-e\,la\,\alpha t\,\beta a^2\,\gamma\,\epsilon\,\psi a-2\,e\,lt\,\alpha a\,\beta a\,\delta\,\epsilon^2\,\psi a+e\,la\,\alpha t\,\beta a\,\delta\,\epsilon\,\alpha a\,\psi a-$$
$$e\,la\,\alpha t\,\beta a^2\,\gamma\,\theta t\,\psi a-4\,e\,lt\,\alpha a\,\beta a\,\delta\,\epsilon\,\theta t\,\psi a+e\,la\,\alpha t\,\beta a\,\delta\,\alpha a\,\theta t\,\psi a-2\,e\,lt\,\alpha a\,\beta a\,\delta\,\theta t^2\,\psi a+e\,\alpha a\,\alpha t\,\beta a\,\delta\,\epsilon\,\lambda a\,\psi a+e\,\alpha a\,\alpha t\,\beta a\,\delta\,\theta t\,\lambda a\,\psi a+2\,e\,\alpha a\,\alpha t\,\beta a\,\delta\,\epsilon\,\lambda t\,\psi a+$$
$$2\,e\,\alpha a\,\alpha t\,\beta a\,\delta\,\theta t\,\lambda t\,\psi a+e\,la\,\alpha t\,\beta a^2\,\gamma\,\theta t\,\mu t\,\psi a+2\,e\,lt\,\alpha a\,\beta a\,\delta\,\epsilon\,\theta t\,\mu t\,\psi a-e\,la\,\alpha t\,\beta a\,\delta\,\alpha a\,\theta t\,\mu t\,\psi a+2\,e\,lt\,\alpha a\,\beta a\,\delta\,\theta t^2\,\mu t\,\psi a-e\,\alpha a\,\alpha t\,\beta a\,\delta\,\theta t\,\lambda a\,\mu t\,\psi a-$$
$$2\,e\,\alpha a\,\alpha t\,\beta a\,\delta\,\theta t\,\lambda t\,\mu t\,\psi a+lt\,\alpha a\,\beta a\,\delta\,\epsilon^2\,\rho\,\psi a+lt\,\alpha a\,\beta a\,\delta\,\epsilon\,\theta t\,\rho\,\psi a-\alpha a\,\alpha t\,\beta a\,\delta\,\epsilon\,\lambda t\,\rho\,\psi a-\alpha a\,\alpha t\,\beta a\,\gamma\,\epsilon\,\tau a\,\psi a+e\,\alpha a\,\alpha t\,\beta a\,\gamma\,\epsilon\,\eta a\,\tau a\,\psi a+\alpha a\,\alpha t\,\delta\,\epsilon\,\theta a\,\tau a\,\psi a-$$
$$2\,e\,\alpha a\,\alpha t\,\delta\,\epsilon\,\eta a\,\theta a\,\tau a\,\psi a-\alpha a\,\alpha t\,\beta a\,\gamma\,\theta t\,\tau a\,\psi a+e\,\alpha a\,\alpha t\,\beta a\,\gamma\,\eta a\,\theta t\,\tau a\,\psi a+\alpha a\,\alpha t\,\delta\,\theta a\,\theta t\,\tau a\,\psi a-2\,e\,\alpha a\,\alpha t\,\delta\,\eta a\,\theta a\,\theta t\,\tau a\,\psi a+\alpha a\,\alpha t\,\delta\,\epsilon\,\theta a\,\mu a\,\tau a\,\psi a+$$
$$\alpha a\,\alpha t\,\delta\,\theta a\,\theta t\,\mu a\,\tau a\,\psi a+\alpha a\,\alpha t\,\beta a\,\gamma\,\theta t\,\mu t\,\tau a\,\psi a-e\,\alpha a\,\alpha t\,\beta a\,\gamma\,\eta a\,\theta t\,\mu t\,\tau a\,\psi a-\alpha a\,\alpha t\,\delta\,\theta a\,\theta t\,\mu t\,\tau a\,\psi a+2\,e\,\alpha a\,\alpha t\,\delta\,\eta a\,\theta a\,\theta t\,\mu t\,\tau a\,\psi a-\alpha a\,\alpha t\,\delta\,\theta a\,\theta t\,\mu a\,\mu t\,\tau a\,\psi a+$$
$$e\,\alpha t\,\beta a\,\delta\,\epsilon\,\theta a\,\psi a^2-e\,\alpha t\,\beta a^2\,\gamma\,\theta t\,\psi a^2+e\,\alpha t\,\beta a\,\delta\,\theta a\,\theta t\,\psi a^2+e\,\alpha t\,\beta a^2\,\gamma\,\theta t\,\mu t\,\psi a^2-e\,\alpha t\,\beta a\,\delta\,\theta a\,\theta t\,\mu t\,\psi a^2-\alpha t\,\beta a\,\delta\,\epsilon\,\theta a\,\mu a\,\rho\,\psi a^2-2\,e\,la\,\alpha a\,\beta a\,\delta\,\epsilon^2\,\psi t-$$
$$4\,e\,la\,\alpha a\,\beta a\,\delta\,\epsilon\,\theta t\,\psi t-2\,e\,la\,\alpha a\,\beta a\,\delta\,\theta t^2\,\psi t+2\,e\,la\,\alpha a\,\beta a\,\delta\,\epsilon\,\theta t\,\mu t\,\psi t+2\,e\,la\,\alpha a\,\beta a\,\delta\,\theta t^2\,\mu t\,\psi t-2\,\alpha a^2\,\delta\,\epsilon^2\,\tau a\,\psi t+2\,e\,\alpha a^2\,\delta\,\epsilon^2\,\eta a\,\tau a\,\psi t-4\,\alpha a^2\,\delta\,\epsilon\,\theta t\,\tau a\,\psi t+$$
$$4\,e\,\alpha a^2\,\delta\,\epsilon\,\eta a\,\theta t\,\tau a\,\psi t-2\,\alpha a^2\,\delta\,\theta t^2\,\tau a\,\psi t+2\,e\,\alpha a^2\,\delta\,\eta a\,\theta t^2\,\tau a\,\psi t+2\,\alpha a^2\,\delta\,\epsilon\,\theta t\,\mu t\,\tau a\,\psi t-2\,e\,\alpha a^2\,\delta\,\epsilon\,\eta a\,\theta t\,\mu t\,\tau a\,\psi t+2\,\alpha a^2\,\delta\,\theta t^2\,\mu t\,\tau a\,\psi t-2\,e\,\alpha a^2\,\delta\,\eta a\,\theta t^2\,\mu t\,\tau a\,\psi t-$$
$$e\,\alpha a\,\beta a\,\delta\,\epsilon^2\,\psi a\,\psi t-2\,e\,\alpha a\,\beta a\,\delta\,\epsilon\,\theta t\,\psi a\,\psi t-e\,\alpha a\,\beta a\,\delta\,\theta t^2\,\psi a\,\psi t+e\,\alpha a\,\beta a\,\delta\,\epsilon\,\theta t\,\mu t\,\psi a\,\psi t+e\,\alpha a\,\beta a\,\delta\,\theta t^2\,\mu t\,\psi a\,\psi t+\alpha a\,\beta a\,\delta\,\epsilon^2\,\rho\,\psi a\,\psi t+\alpha a\,\beta a\,\delta\,\epsilon\,\theta t\,\rho\,\psi a\,\psi t-$$
$$\psi a\sqrt{\left(4\,\alpha a\,\alpha t\,\delta\,(\epsilon+\theta t-\theta t\,\mu t)\,\tau a-\beta a\,\epsilon\,\rho\,\psi a+e\,(\epsilon+\theta t-\theta t\,\mu t)\,(la\,\beta a-\alpha a\,\eta a\,\tau a+\beta a\,\psi a)\right)\left(-e\,\left(lt\,\beta a^2\,\gamma\,\epsilon\,(\epsilon+\theta t)-\alpha t\,\left(\beta a^2\,\gamma\,\left(\epsilon\,(\lambda a+\lambda t)-\theta t\,\lambda a\,(-1+\mu t)\right)+\right.\right.\right.}$$
$$\left.\left.\left.\delta\,\eta a\,\theta a^2\,(\epsilon+\theta t-\theta t\,\mu t)\,\tau a-\beta a\,\theta a\,(\epsilon+\theta t-\theta t\,\mu t)\,(\delta\,\lambda a+\gamma\,\eta a\,\tau a)\right)+\beta a\,(\epsilon+\theta t)\,(\beta a\,\gamma\,\theta t\,(-1+\mu t)+\delta\,\theta a\,(\epsilon+\theta t-\theta t\,\mu t))\right)\psi t)+$$
$$\left.\left.\left.\theta a\,\mu a\,\left(lt\,\beta a\,\delta\,\epsilon\,(\epsilon+\theta t)\,\rho-\alpha t\,\left(\beta a\,\delta\,\epsilon\,\lambda t\,\rho-\beta a\,\gamma\,(\epsilon+\theta t-\theta t\,\mu t)\,\tau a+\delta\,\theta a\,(\epsilon+\theta t-\theta t\,\mu t)\,\tau a\right)+\beta a\,\delta\,\epsilon\,(\epsilon+\theta t)\,\rho\,\psi t\right)\right)+\right.\right.$$
$$\left.\left.\left.(lt\,\alpha a\,\beta a\,\delta\,\epsilon\,(\epsilon+\theta t)\,\rho-\alpha a\,\alpha t\,\beta a\,\delta\,\epsilon\,\lambda t\,\rho+\alpha a\,\alpha t\,\beta a\,\gamma\,\epsilon\,\tau a-\alpha a\,\alpha t\,\delta\,\epsilon\,\theta a\,\tau a+\alpha a\,\alpha t\,\beta a\,\gamma\,\theta t\,\tau a-\alpha a\,\alpha t\,\delta\,\theta a\,\theta t\,\tau a-\alpha a\,\alpha t\,\delta\,\epsilon\,\theta a\,\mu a\,\tau a-\alpha a\,\alpha t\,\delta\,\theta a\,\theta t\,\mu a\,\tau a-\alpha a\right.\right.\right.$$
$$\left.\left.\left.\alpha t\,\beta a\,\gamma\,\theta t\,\mu t\,\tau a+\alpha a\,\alpha t\,\delta\,\theta a\,\theta t\,\mu t\,\tau a+\alpha a\,\alpha t\,\delta\,\theta a\,\theta t\,\mu a\,\mu t\,\tau a+\alpha t\,\beta a\,\delta\,\epsilon\,\theta a\,\mu a\,\rho\,\psi a+\alpha a\,\beta a\,\delta\,\epsilon^2\,\rho\,\psi t+\alpha a\,\beta a\,\delta\,\epsilon\,\theta t\,\rho\,\psi t+e\,(la\,\alpha t\,\beta a\,(\beta a\,\gamma-\delta\,\theta a)\,(\epsilon+\theta t-\theta t\,\mu t)-\right.\right.\right.$$
$$\left.\left.\left.\left.\alpha t\,\beta a\,(\beta a\,\gamma\,\theta t\,(-1+\mu t)+\delta\,\theta a\,(\epsilon+\theta t-\theta t\,\mu t))\,\psi a-\alpha a\,(\epsilon+\theta t-\theta t\,\mu t)\,(\alpha t\,(\beta a\,\delta\,\lambda a+\beta a\,\gamma\,\eta a\,\tau a-2\,\delta\,\eta a\,\theta a\,\tau a)+\beta a\,\delta\,(\epsilon+\theta t)\,\psi t)\right)\right)^2\right)\right)\Big/$$
$$\left.\left.\left.(2\,\alpha a\,\alpha t\,\delta\,(\epsilon+\theta t-\theta t\,\mu t)\,(-\alpha a\,(\epsilon+\theta t-\theta t\,\mu t)\,\tau a+\beta a\,\epsilon\,\rho\,\psi a-e\,(\epsilon+\theta t-\theta t\,\mu t)\,(la\,\beta a-\alpha a\,\eta a\,\tau a+\beta a\,\psi a)))\right)\right\},\ Nt \to \frac{\epsilon+\theta t}{\alpha t},$$

$$
\begin{aligned}
Lt \to\ & \Big(e\,la\,\alpha t\,\beta a^2\,\gamma\,\epsilon - e\,la\,\alpha t\,\beta a\,\delta\,\epsilon\,\theta a + e\,la\,\alpha t\,\beta a^2\,\gamma\,\theta t - e\,la\,\alpha t\,\beta a\,\delta\,\theta a\,\theta t + e\,\alpha a\,\alpha t\,\beta a\,\delta\,\epsilon\,\lambda a + e\,\alpha a\,\alpha t\,\beta a\,\delta\,\theta t\,\lambda a - \\
& e\,la\,\alpha t\,\beta a^2\,\gamma\,\theta t\,\mu t + e\,la\,\alpha t\,\beta a\,\delta\,\theta a\,\theta t\,\mu t - e\,\alpha a\,\alpha t\,\beta a\,\delta\,\theta t\,\lambda a\,\mu t - \\
& lt\,\alpha a\,\beta a\,\delta\,\epsilon^2\,\rho - lt\,\alpha a\,\beta a\,\delta\,\epsilon\,\theta t\,\rho + \alpha a\,\alpha t\,\beta a\,\delta\,\epsilon\,\lambda t\,\rho + \\
& \alpha a\,\alpha t\,\beta a\,\gamma\,\epsilon\,\tau a - e\,\alpha a\,\alpha t\,\beta a\,\gamma\,\epsilon\,\eta a\,\tau a - \alpha a\,\alpha t\,\delta\,\epsilon\,\theta a\,\tau a + \alpha a\,\alpha t\,\beta a\,\gamma\,\theta t\,\tau a - \\
& e\,\alpha a\,\alpha t\,\beta a\,\gamma\,\eta a\,\theta t\,\tau a - \alpha a\,\alpha t\,\delta\,\theta a\,\theta t\,\tau a + \alpha a\,\alpha t\,\delta\,\epsilon\,\theta a\,\mu a\,\tau a + \\
& \alpha a\,\alpha t\,\delta\,\theta a\,\theta t\,\mu a\,\tau a - \alpha a\,\alpha t\,\beta a\,\gamma\,\theta t\,\mu t\,\tau a + e\,\alpha a\,\alpha t\,\beta a\,\gamma\,\eta a\,\theta t\,\mu t\,\tau a + \\
& \alpha a\,\alpha t\,\delta\,\theta a\,\theta t\,\mu t\,\tau a - \alpha a\,\alpha t\,\delta\,\theta a\,\theta t\,\mu a\,\mu t\,\tau a - e\,\alpha t\,\beta a\,\delta\,\epsilon\,\theta a\,\psi a + \\
& e\,\alpha t\,\beta a^2\,\gamma\,\theta t\,\psi a - e\,\alpha t\,\beta a\,\delta\,\theta a\,\theta t\,\psi a - e\,\alpha t\,\beta a^2\,\gamma\,\theta t\,\mu t\,\psi a + e\,\alpha t\,\beta a\,\delta\,\theta a\,\theta t\,\mu t\,\psi a + \\
& \alpha t\,\beta a\,\delta\,\epsilon\,\theta a\,\mu a\,\rho\,\psi a + e\,\alpha a\,\beta a\,\delta\,\epsilon^2\,\psi t + 2\,e\,\alpha a\,\beta a\,\delta\,\epsilon\,\theta t\,\psi t + e\,\alpha a\,\beta a\,\delta\,\theta t^2\,\psi t - \\
& e\,\alpha a\,\beta a\,\delta\,\epsilon\,\theta t\,\mu t\,\psi t - e\,\alpha a\,\beta a\,\delta\,\theta t^2\,\mu t\,\psi t - \alpha a\,\beta a\,\delta\,\epsilon^2\,\rho\,\psi t - \alpha a\,\beta a\,\delta\,\epsilon\,\theta t\,\rho\,\psi t + \\
& \sqrt{\big(4\,\alpha a\,\alpha t\,\delta\,\big(\alpha a\,\big(\epsilon + \theta t - \theta t\,\mu t\big)\,\tau a - \beta a\,\epsilon\,\rho\,\psi a + e\,\big(\epsilon + \theta t - \theta t\,\mu t\big)\,\big(la\,\beta a - \alpha a\,\eta a\,\tau a + \beta a\,\psi a\big)\big)} \\
& \quad \big(-e\,\big(lt\,\beta a^2\,\gamma\,\epsilon\,(\epsilon + \theta t) - \alpha t\,\big(\beta a^2\,\gamma\,\big(\epsilon\,(\lambda a + \lambda t) - \theta t\,\lambda a\,(-1 + \mu t)\big) + \delta\,\eta a\,\theta a^2\,\big(\epsilon + \theta t - \theta t\,\mu t\big)\,\tau a - \beta a\,\theta a\,\big(\epsilon + \theta t - \theta t\,\mu t\big)\,\big(\delta\,\lambda a + \gamma\,\eta a\,\tau a\big)\big) + \beta a\,(\epsilon + \theta t)\,\big(\beta a\,\gamma\,\theta t\,(-1 + \\
& \qquad \mu t) + \delta\,\theta a\,\big(\epsilon + \theta t - \theta t\,\mu t\big)\big)\,\psi t\big) + \theta a\,\mu a\,\big(lt\,\beta a\,\delta\,\epsilon\,(\epsilon + \theta t)\,\rho - \alpha t\,\big(\beta a\,\delta\,\epsilon\,\lambda t\,\rho - \beta a\,\gamma\,\big(\epsilon + \theta t - \theta t\,\mu t\big)\,\tau a + \delta\,\theta a\,\big(\epsilon + \theta t - \theta t\,\mu t\big)\,\tau a\big) + \beta a\,\delta\,\epsilon\,(\epsilon + \theta t)\,\rho\,\psi t\big)\big) + \\
& \quad \big(lt\,\alpha a\,\beta a\,\delta\,\epsilon\,(\epsilon + \theta t)\,\rho - \alpha a\,\alpha t\,\beta a\,\delta\,\epsilon\,\lambda t\,\rho + \alpha a\,\alpha t\,\beta a\,\gamma\,\epsilon\,\tau a - \alpha a\,\alpha t\,\delta\,\epsilon\,\theta a\,\tau a + \alpha a\,\alpha t\,\beta a\,\gamma\,\theta t\,\tau a - \alpha a\,\alpha t\,\delta\,\theta a\,\theta t\,\tau a - \alpha a\,\alpha t\,\delta\,\epsilon\,\theta a\,\mu a\,\tau a - \alpha a\,\alpha t\,\delta\,\theta a\,\theta t\,\mu a\,\tau a - \\
& \qquad \alpha a\,\alpha t\,\beta a\,\gamma\,\theta t\,\mu t\,\tau a + \alpha a\,\alpha t\,\delta\,\theta a\,\theta t\,\mu t\,\tau a + \alpha a\,\alpha t\,\delta\,\theta a\,\theta t\,\mu a\,\mu t\,\tau a + \alpha t\,\beta a\,\delta\,\epsilon\,\theta a\,\mu a\,\rho\,\psi a + \alpha a\,\beta a\,\delta\,\epsilon^2\,\rho\,\psi t + \alpha a\,\beta a\,\delta\,\epsilon\,\theta t\,\rho\,\psi t + e\,\big(la\,\alpha t\,\beta a\,\big(\beta a\,\gamma - \delta\,\theta a\big) \\
& \qquad \big(\epsilon + \theta t - \theta t\,\mu t\big) - \alpha t\,\beta a\,\big(\beta a\,\gamma\,\theta t\,(-1 + \mu t) + \delta\,\theta a\,\big(\epsilon + \theta t - \theta t\,\mu t\big)\big)\,\psi a - \alpha a\,\big(\epsilon + \theta t - \theta t\,\mu t\big)\,\big(\alpha t\,\big(\beta a\,\delta\,\lambda a + \beta a\,\gamma\,\eta a\,\tau a - 2\,\delta\,\eta a\,\theta a\,\tau a\big) + \beta a\,\delta\,(\epsilon + \theta t)\,\psi t\big)\big)^2\big)\big) \Big/ \\
& \big(2\,\alpha a\,\alpha t\,\delta\,\big(\epsilon + \theta t - \theta t\,\mu t\big)\,\big(-e\,\beta a\,\gamma + \beta a\,\gamma\,\rho + \delta\,\theta a\,(-1 + \mu a)\,\rho\big)\big),\ Ha \to -\Big(\big(e\,la\,\alpha t\,\beta a^2\,\gamma\,\epsilon + e\,la\,\alpha t\,\beta a\,\delta\,\epsilon\,\theta a + e\,la\,\alpha t\,\beta a^2\,\gamma\,\theta t + e\,la\,\alpha t\,\beta a\,\delta\,\theta a\,\theta t - \\
& e\,\alpha a\,\alpha t\,\beta a\,\delta\,\epsilon\,\lambda a - e\,\alpha a\,\alpha t\,\beta a\,\delta\,\theta t\,\lambda a - e\,la\,\alpha t\,\beta a^2\,\gamma\,\theta t\,\mu t - e\,la\,\alpha t\,\beta a\,\delta\,\theta a\,\theta t\,\mu t + e\,\alpha a\,\alpha t\,\beta a\,\delta\,\theta t\,\lambda a\,\mu t + lt\,\alpha a\,\beta a\,\delta\,\epsilon^2\,\rho + lt\,\alpha a\,\beta a\,\delta\,\epsilon\,\theta t\,\rho - \\
& \alpha a\,\alpha t\,\beta a\,\delta\,\epsilon\,\lambda t\,\rho + \alpha a\,\alpha t\,\beta a\,\gamma\,\epsilon\,\tau a - e\,\alpha a\,\alpha t\,\beta a\,\gamma\,\epsilon\,\eta a\,\tau a + \alpha a\,\alpha t\,\delta\,\epsilon\,\theta a\,\tau a + \alpha a\,\alpha t\,\beta a\,\gamma\,\theta t\,\tau a - e\,\alpha a\,\alpha t\,\beta a\,\gamma\,\eta a\,\theta t\,\tau a + \alpha a\,\alpha t\,\delta\,\theta a\,\theta t\,\tau a - \\
& \alpha a\,\alpha t\,\delta\,\epsilon\,\theta a\,\mu a\,\tau a - \alpha a\,\alpha t\,\delta\,\theta a\,\theta t\,\mu a\,\tau a - \alpha a\,\alpha t\,\beta a\,\gamma\,\theta t\,\mu t\,\tau a + e\,\alpha a\,\alpha t\,\beta a\,\gamma\,\eta a\,\theta t\,\mu t\,\tau a - \alpha a\,\alpha t\,\delta\,\theta a\,\theta t\,\mu t\,\tau a + \alpha a\,\alpha t\,\delta\,\theta a\,\theta t\,\mu a\,\mu t\,\tau a + \\
& e\,\alpha t\,\beta a\,\delta\,\epsilon\,\theta a\,\psi a + e\,\alpha t\,\beta a^2\,\gamma\,\theta t\,\psi a + e\,\alpha t\,\beta a\,\delta\,\theta a\,\theta t\,\psi a - e\,\alpha t\,\beta a^2\,\gamma\,\theta t\,\mu t\,\psi a - e\,\alpha t\,\beta a\,\delta\,\theta a\,\theta t\,\mu t\,\psi a - 2\,\alpha t\,\beta a\,\delta\,\epsilon\,\theta a\,\rho\,\psi a + \alpha t\,\beta a\,\delta\,\epsilon\,\theta a\,\mu a\,\rho\,\psi a - \\
& e\,\alpha a\,\beta a\,\delta\,\epsilon^2\,\psi t - 2\,e\,\alpha a\,\beta a\,\delta\,\epsilon\,\theta t\,\psi t - e\,\alpha a\,\beta a\,\delta\,\theta t^2\,\psi t + e\,\alpha a\,\beta a\,\delta\,\epsilon\,\theta t\,\mu t\,\psi t + e\,\alpha a\,\beta a\,\delta\,\theta t^2\,\mu t\,\psi t + \alpha a\,\beta a\,\delta\,\epsilon^2\,\rho\,\psi t + \alpha a\,\beta a\,\delta\,\epsilon\,\theta t\,\rho\,\psi t + \\
& \sqrt{\big(4\,\alpha a\,\alpha t\,\delta\,\big(\alpha a\,\big(\epsilon + \theta t - \theta t\,\mu t\big)\,\tau a - \beta a\,\epsilon\,\rho\,\psi a + e\,\big(\epsilon + \theta t - \theta t\,\mu t\big)\,\big(la\,\beta a - \alpha a\,\eta a\,\tau a + \beta a\,\psi a\big)\big)} \,\big(-e\,\big(lt\,\beta a^2\,\gamma\,\epsilon\,(\epsilon + \theta t) - \alpha t\,\big(\beta a^2\,\gamma\,\big(\epsilon\,(\lambda a + \lambda t) - \theta t\,\lambda a\,(-1 + \mu t)\big) + \\
& \qquad \delta\,\eta a\,\theta a^2\,\big(\epsilon + \theta t - \theta t\,\mu t\big)\,\tau a - \beta a\,\theta a\,\big(\epsilon + \theta t - \theta t\,\mu t\big)\,\big(\delta\,\lambda a + \gamma\,\eta a\,\tau a\big)\big) + \beta a\,(\epsilon + \theta t)\,\big(\beta a\,\gamma\,\theta t\,(-1 + \mu t) + \delta\,\theta a\,\big(\epsilon + \theta t - \theta t\,\mu t\big)\big)\,\psi t\big) + \\
& \quad \theta a\,\mu a\,\big(lt\,\beta a\,\delta\,\epsilon\,(\epsilon + \theta t)\,\rho - \alpha t\,\big(\beta a\,\delta\,\epsilon\,\lambda t\,\rho - \beta a\,\gamma\,\big(\epsilon + \theta t - \theta t\,\mu t\big)\,\tau a + \delta\,\theta a\,\big(\epsilon + \theta t - \theta t\,\mu t\big)\,\tau a\big) + \beta a\,\delta\,\epsilon\,(\epsilon + \theta t)\,\rho\,\psi t\big)\big) + \\
& \quad \big(lt\,\alpha a\,\beta a\,\delta\,\epsilon\,(\epsilon + \theta t)\,\rho - \alpha a\,\alpha t\,\beta a\,\delta\,\epsilon\,\lambda t\,\rho + \alpha a\,\alpha t\,\beta a\,\gamma\,\epsilon\,\tau a - \alpha a\,\alpha t\,\delta\,\epsilon\,\theta a\,\tau a + \alpha a\,\alpha t\,\beta a\,\gamma\,\theta t\,\tau a - \alpha a\,\alpha t\,\delta\,\theta a\,\theta t\,\tau a - \alpha a\,\alpha t\,\delta\,\epsilon\,\theta a\,\mu a\,\tau a - \alpha a\,\alpha t\,\delta\,\theta a\,\theta t\,\mu a\,\tau a - \\
& \qquad \alpha a\,\alpha t\,\beta a\,\gamma\,\theta t\,\mu t\,\tau a + \alpha a\,\alpha t\,\delta\,\theta a\,\theta t\,\mu t\,\tau a + \alpha a\,\alpha t\,\delta\,\theta a\,\theta t\,\mu a\,\mu t\,\tau a + \alpha t\,\beta a\,\delta\,\epsilon\,\theta a\,\mu a\,\rho\,\psi a + \alpha a\,\beta a\,\delta\,\epsilon^2\,\rho\,\psi t + \alpha a\,\beta a\,\delta\,\epsilon\,\theta t\,\rho\,\psi t + e\,\big(la\,\alpha t\,\beta a\,\big(\beta a\,\gamma - \delta\,\theta a\big)\,\big(\epsilon + \theta t - \theta t\,\mu t\big) - \\
& \qquad \alpha t\,\beta a\,\big(\beta a\,\gamma\,\theta t\,(-1 + \mu t) + \delta\,\theta a\,\big(\epsilon + \theta t - \theta t\,\mu t\big)\big)\,\psi a - \alpha a\,\big(\epsilon + \theta t - \theta t\,\mu t\big)\,\big(\alpha t\,\big(\beta a\,\delta\,\lambda a + \beta a\,\gamma\,\eta a\,\tau a - 2\,\delta\,\eta a\,\theta a\,\tau a\big) + \beta a\,\delta\,(\epsilon + \theta t)\,\psi t\big)\big)^2\big)\big) \Big/ \\
& \big(2\,\alpha t\,\beta a\,\delta\,\big(\alpha a\,\big(\epsilon + \theta t - \theta t\,\mu t\big)\,\tau a - \beta a\,\epsilon\,\rho\,\psi a + e\,\big(\epsilon + \theta t - \theta t\,\mu t\big)\,\big(la\,\beta a - \alpha a\,\eta a\,\tau a + \beta a\,\psi a\big)\big)\big)\big),\ Pa \to \\
& -\Big(\big(-e\,la\,\alpha t\,\beta a^2\,\gamma\,\epsilon\,\rho + e\,la\,\alpha t\,\beta a\,\delta\,\epsilon\,\theta a\,\rho - e\,la\,\alpha t\,\beta a^2\,\gamma\,\theta t\,\rho + e\,la\,\alpha t\,\beta a\,\delta\,\theta a\,\theta t\,\rho - e\,\alpha a\,\alpha t\,\beta a\,\delta\,\epsilon\,\lambda a\,\rho - e\,\alpha a\,\alpha t\,\beta a\,\delta\,\theta t\,\lambda a\,\rho + e\,la\,\alpha t\,\beta a^2\,\gamma\,\theta t\,\mu t\,\rho - \\
& e\,la\,\alpha t\,\beta a\,\delta\,\theta a\,\theta t\,\mu t\,\rho + e\,\alpha a\,\alpha t\,\beta a\,\delta\,\theta t\,\lambda a\,\mu t\,\rho + lt\,\alpha a\,\beta a\,\delta\,\epsilon^2\,\rho^2 + lt\,\alpha a\,\beta a\,\delta\,\epsilon\,\theta t\,\rho^2 - \alpha a\,\alpha t\,\beta a\,\delta\,\epsilon\,\lambda t\,\rho^2 - 2\,e\,\alpha a\,\alpha t\,\beta a\,\gamma\,\epsilon\,\tau a - 2\,e\,\alpha a\,\alpha t\,\beta a\,\gamma\,\theta t\,\tau a + \\
& 2\,e\,\alpha a\,\alpha t\,\beta a\,\gamma\,\theta t\,\mu t\,\tau a + \alpha a\,\alpha t\,\beta a\,\gamma\,\epsilon\,\rho\,\tau a + e\,\alpha a\,\alpha t\,\beta a\,\gamma\,\epsilon\,\eta a\,\rho\,\tau a - \alpha a\,\alpha t\,\delta\,\epsilon\,\theta a\,\rho\,\tau a + \alpha a\,\alpha t\,\beta a\,\gamma\,\theta t\,\rho\,\tau a + e\,\alpha a\,\alpha t\,\beta a\,\gamma\,\eta a\,\theta t\,\rho\,\tau a - \alpha a\,\alpha t\,\delta\,\theta a\,\theta t\,\rho\,\tau a + \\
& \alpha a\,\alpha t\,\delta\,\epsilon\,\theta a\,\mu a\,\rho\,\tau a + \alpha a\,\alpha t\,\delta\,\theta a\,\theta t\,\mu a\,\rho\,\tau a - \alpha a\,\alpha t\,\beta a\,\gamma\,\theta t\,\mu t\,\rho\,\tau a - e\,\alpha a\,\alpha t\,\beta a\,\gamma\,\eta a\,\theta t\,\mu t\,\rho\,\tau a + \alpha a\,\alpha t\,\delta\,\theta a\,\theta t\,\mu t\,\rho\,\tau a - \alpha a\,\alpha t\,\delta\,\theta a\,\theta t\,\mu a\,\mu t\,\rho\,\tau a + \\
& e\,\alpha t\,\beta a\,\delta\,\epsilon\,\theta a\,\rho\,\psi a - e\,\alpha t\,\beta a^2\,\gamma\,\theta t\,\rho\,\psi a + e\,\alpha t\,\beta a\,\delta\,\theta a\,\theta t\,\rho\,\psi a + e\,\alpha t\,\beta a^2\,\gamma\,\theta t\,\mu t\,\rho\,\psi a - e\,\alpha t\,\beta a\,\delta\,\theta a\,\theta t\,\mu t\,\rho\,\psi a - \alpha t\,\beta a\,\delta\,\epsilon\,\theta a\,\mu a\,\rho^2\,\psi a - \\
& e\,\alpha a\,\beta a\,\delta\,\epsilon^2\,\rho\,\psi t - 2\,e\,\alpha a\,\beta a\,\delta\,\epsilon\,\theta t\,\rho\,\psi t - e\,\alpha a\,\beta a\,\delta\,\theta t^2\,\rho\,\psi t + e\,\alpha a\,\beta a\,\delta\,\epsilon\,\theta t\,\mu t\,\rho\,\psi t + e\,\alpha a\,\beta a\,\delta\,\theta t^2\,\mu t\,\rho\,\psi t + \alpha a\,\beta a\,\delta\,\epsilon^2\,\rho^2\,\psi t + \alpha a\,\beta a\,\delta\,\epsilon\,\theta t\,\rho^2\,\psi t - \\
& \rho\,\sqrt{\big(4\,\alpha a\,\alpha t\,\delta\,\big(\alpha a\,\big(\epsilon + \theta t - \theta t\,\mu t\big)\,\tau a - \beta a\,\epsilon\,\rho\,\psi a + e\,\big(\epsilon + \theta t - \theta t\,\mu t\big)\,\big(la\,\beta a - \alpha a\,\eta a\,\tau a + \beta a\,\psi a\big)\big)} \,\big(-e\,\big(lt\,\beta a^2\,\gamma\,\epsilon\,(\epsilon + \theta t) - \alpha t\,\big(\beta a^2\,\gamma\,\big(\epsilon\,(\lambda a + \lambda t) - \theta t\,\lambda a\,(-1 + \mu t)\big) + \\
& \qquad \delta\,\eta a\,\theta a^2\,\big(\epsilon + \theta t - \theta t\,\mu t\big)\,\tau a - \beta a\,\theta a\,\big(\epsilon + \theta t - \theta t\,\mu t\big)\,\big(\delta\,\lambda a + \gamma\,\eta a\,\tau a\big)\big) + \beta a\,(\epsilon + \theta t)\,\big(\beta a\,\gamma\,\theta t\,(-1 + \mu t) + \delta\,\theta a\,\big(\epsilon + \theta t - \theta t\,\mu t\big)\big)\,\psi t\big) + \\
& \quad \theta a\,\mu a\,\big(lt\,\beta a\,\delta\,\epsilon\,(\epsilon + \theta t)\,\rho - \alpha t\,\big(\beta a\,\delta\,\epsilon\,\lambda t\,\rho - \beta a\,\gamma\,\big(\epsilon + \theta t - \theta t\,\mu t\big)\,\tau a + \delta\,\theta a\,\big(\epsilon + \theta t - \theta t\,\mu t\big)\,\tau a\big) + \beta a\,\delta\,\epsilon\,(\epsilon + \theta t)\,\rho\,\psi t\big)\big) +
\end{aligned}
$$

$$\Big(\mathrm{lt}\,\alpha\mathrm{a}\,\beta\mathrm{a}\,\delta\in\,(\epsilon+\theta\mathrm{t})\,\rho-\alpha\mathrm{a}\,\alpha\mathrm{t}\,\beta\mathrm{a}\,\delta\in\lambda\mathrm{t}\,\rho+\alpha\mathrm{a}\,\alpha\mathrm{t}\,\beta\mathrm{a}\,\gamma\in\tau\mathrm{a}-\alpha\mathrm{a}\,\alpha\mathrm{t}\,\delta\in\theta\mathrm{a}\,\tau\mathrm{a}+\alpha\mathrm{a}\,\alpha\mathrm{t}\,\beta\mathrm{a}\,\gamma\,\theta\mathrm{t}\,\tau\mathrm{a}-\alpha\mathrm{a}\,\alpha\mathrm{t}\,\delta\,\theta\mathrm{a}\,\theta\mathrm{t}\,\tau\mathrm{a}-\alpha\mathrm{a}\,\alpha\mathrm{t}\,\delta\in\theta\mathrm{a}\,\mu\mathrm{a}\,\tau\mathrm{a}-\alpha\mathrm{a}\,\alpha\mathrm{t}\,\delta\,\theta\mathrm{a}\,\theta\mathrm{t}\,\mu\mathrm{a}\,\tau\mathrm{a}-\alpha\mathrm{a}$$
$$\alpha\mathrm{t}\,\beta\mathrm{a}\,\gamma\,\theta\mathrm{t}\,\mu\mathrm{t}\,\tau\mathrm{a}+\alpha\mathrm{a}\,\alpha\mathrm{t}\,\delta\,\theta\mathrm{a}\,\theta\mathrm{t}\,\mu\mathrm{t}\,\tau\mathrm{a}+\alpha\mathrm{a}\,\alpha\mathrm{t}\,\delta\,\theta\mathrm{a}\,\theta\mathrm{t}\,\mu\mathrm{a}\,\mu\mathrm{t}\,\tau\mathrm{a}+\alpha\mathrm{t}\,\beta\mathrm{a}\,\delta\in\theta\mathrm{a}\,\mu\mathrm{a}\,\rho\,\psi\mathrm{a}+\alpha\mathrm{a}\,\beta\mathrm{a}\,\delta\,\epsilon^2\,\rho\,\psi\mathrm{t}+\alpha\mathrm{a}\,\beta\mathrm{a}\,\delta\in\theta\mathrm{t}\,\rho\,\psi\mathrm{t}+\mathrm{e}\,\big(\mathrm{la}\,\alpha\mathrm{t}\,\beta\mathrm{a}\,\big(\beta\mathrm{a}\,\gamma-\delta\,\theta\mathrm{a}\big)\,(\epsilon+\theta\mathrm{t}-\theta\mathrm{t}\,\mu\mathrm{t})-$$
$$\alpha\mathrm{t}\,\beta\mathrm{a}\,\big(\beta\mathrm{a}\,\gamma\,\theta\mathrm{t}\,(-1+\mu\mathrm{t})+\delta\,\theta\mathrm{a}\,(\epsilon+\theta\mathrm{t}-\theta\mathrm{t}\,\mu\mathrm{t})\big)\,\psi\mathrm{a}-\alpha\mathrm{a}\,(\epsilon+\theta\mathrm{t}-\theta\mathrm{t}\,\mu\mathrm{t})\,\big(\alpha\mathrm{t}\,\big(\beta\mathrm{a}\,\delta\,\lambda\mathrm{a}+\beta\mathrm{a}\,\gamma\,\eta\mathrm{a}\,\tau\mathrm{a}-2\,\delta\,\eta\mathrm{a}\,\theta\mathrm{a}\,\tau\mathrm{a}\big)+\beta\mathrm{a}\,\delta\,(\epsilon+\theta\mathrm{t})\,\psi\mathrm{t}\big)\big)^2\big)\Big)\Big/$$
$$\big(2\,\mathrm{e}\,\alpha\mathrm{a}\,\alpha\mathrm{t}\,\beta\mathrm{a}\,(\epsilon+\theta\mathrm{t}-\theta\mathrm{t}\,\mu\mathrm{t})\,\big(\mathrm{e}\,\beta\mathrm{a}\,\gamma-\big(\beta\mathrm{a}\,\gamma+\delta\,\theta\mathrm{a}\,(-1+\mu\mathrm{a})\big)\,\rho\big)\big)\Big],\ \mathrm{Na}\to\Big(\mathrm{e}\,\mathrm{la}\,\alpha\mathrm{t}\,\beta\mathrm{a}^2\,\gamma\,\epsilon-\mathrm{e}\,\mathrm{la}\,\alpha\mathrm{t}\,\beta\mathrm{a}\,\delta\in\theta\mathrm{a}+\mathrm{e}\,\mathrm{la}\,\alpha\mathrm{t}\,\beta\mathrm{a}^2\,\gamma\,\theta\mathrm{t}-$$
$$\mathrm{e}\,\mathrm{la}\,\alpha\mathrm{t}\,\beta\mathrm{a}\,\delta\,\theta\mathrm{a}\,\theta\mathrm{t}-$$
$$\mathrm{e}\,\alpha\mathrm{a}\,\alpha\mathrm{t}\,\beta\mathrm{a}\,\delta\in\lambda\mathrm{a}-$$
$$\mathrm{e}\,\alpha\mathrm{a}\,\alpha\mathrm{t}\,\beta\mathrm{a}\,\delta\,\theta\mathrm{t}\,\lambda\mathrm{a}-$$
$$\mathrm{e}\,\mathrm{la}\,\alpha\mathrm{t}\,\beta\mathrm{a}^2\,\gamma\,\theta\mathrm{t}\,\mu\mathrm{t}+$$
$$\mathrm{e}\,\mathrm{la}\,\alpha\mathrm{t}\,\beta\mathrm{a}\,\delta\,\theta\mathrm{a}\,\theta\mathrm{t}\,\mu\mathrm{t}+$$
$$\mathrm{e}\,\alpha\mathrm{a}\,\alpha\mathrm{t}\,\beta\mathrm{a}\,\delta\,\theta\mathrm{t}\,\lambda\mathrm{a}\,\mu\mathrm{t}+\mathrm{lt}\,\alpha\mathrm{a}\,\beta\mathrm{a}\,\delta\,\epsilon^2\,\rho+$$
$$\mathrm{lt}\,\alpha\mathrm{a}\,\beta\mathrm{a}\,\delta\in\theta\mathrm{t}\,\rho-\alpha\mathrm{a}\,\alpha\mathrm{t}\,\beta\mathrm{a}\,\delta\in\lambda\mathrm{t}\,\rho+$$
$$\alpha\mathrm{a}\,\alpha\mathrm{t}\,\beta\mathrm{a}\,\gamma\in\tau\mathrm{a}-\mathrm{e}\,\alpha\mathrm{a}\,\alpha\mathrm{t}\,\beta\mathrm{a}\,\gamma\in\eta\mathrm{a}\,\tau\mathrm{a}-$$
$$\alpha\mathrm{a}\,\alpha\mathrm{t}\,\delta\in\theta\mathrm{a}\,\tau\mathrm{a}+2\,\mathrm{e}\,\alpha\mathrm{a}\,\alpha\mathrm{t}\,\delta\in\eta\mathrm{a}\,\theta\mathrm{a}\,\tau\mathrm{a}+$$
$$\alpha\mathrm{a}\,\alpha\mathrm{t}\,\beta\mathrm{a}\,\gamma\,\theta\mathrm{t}\,\tau\mathrm{a}-\mathrm{e}\,\alpha\mathrm{a}\,\alpha\mathrm{t}\,\beta\mathrm{a}\,\gamma\,\eta\mathrm{a}\,\theta\mathrm{t}\,\tau\mathrm{a}-$$
$$\alpha\mathrm{a}\,\alpha\mathrm{t}\,\delta\,\theta\mathrm{a}\,\theta\mathrm{t}\,\tau\mathrm{a}+2\,\mathrm{e}\,\alpha\mathrm{a}\,\alpha\mathrm{t}\,\delta\,\eta\mathrm{a}\,\theta\mathrm{a}\,\theta\mathrm{t}\,\tau\mathrm{a}-$$
$$\alpha\mathrm{a}\,\alpha\mathrm{t}\,\delta\in\theta\mathrm{a}\,\mu\mathrm{a}\,\tau\mathrm{a}-\alpha\mathrm{a}\,\alpha\mathrm{t}\,\delta\,\theta\mathrm{a}\,\theta\mathrm{t}\,\mu\mathrm{a}\,\tau\mathrm{a}-$$
$$\alpha\mathrm{a}\,\alpha\mathrm{t}\,\beta\mathrm{a}\,\gamma\,\theta\mathrm{t}\,\mu\mathrm{t}\,\tau\mathrm{a}+\mathrm{e}\,\alpha\mathrm{a}\,\alpha\mathrm{t}\,\beta\mathrm{a}\,\gamma\,\eta\mathrm{a}\,\theta\mathrm{t}\,\mu\mathrm{t}\,\tau\mathrm{a}+$$
$$\alpha\mathrm{a}\,\alpha\mathrm{t}\,\delta\,\theta\mathrm{a}\,\theta\mathrm{t}\,\mu\mathrm{t}\,\tau\mathrm{a}-2\,\mathrm{e}\,\alpha\mathrm{a}\,\alpha\mathrm{t}\,\delta\,\eta\mathrm{a}\,\theta\mathrm{a}\,\theta\mathrm{t}\,\mu\mathrm{t}\,\tau\mathrm{a}+$$
$$\alpha\mathrm{a}\,\alpha\mathrm{t}\,\delta\,\theta\mathrm{a}\,\theta\mathrm{t}\,\mu\mathrm{a}\,\mu\mathrm{t}\,\tau\mathrm{a}-\mathrm{e}\,\alpha\mathrm{t}\,\beta\mathrm{a}\,\delta\in\theta\mathrm{a}\,\psi\mathrm{a}+$$
$$\mathrm{e}\,\alpha\mathrm{t}\,\beta\mathrm{a}^2\,\gamma\,\theta\mathrm{t}\,\psi\mathrm{a}-\mathrm{e}\,\alpha\mathrm{t}\,\beta\mathrm{a}\,\delta\,\theta\mathrm{a}\,\theta\mathrm{t}\,\psi\mathrm{a}-\mathrm{e}\,\alpha\mathrm{t}\,\beta\mathrm{a}^2\,\gamma\,\theta\mathrm{t}\,\mu\mathrm{t}\,\psi\mathrm{a}+$$
$$\mathrm{e}\,\alpha\mathrm{t}\,\beta\mathrm{a}\,\delta\,\theta\mathrm{a}\,\theta\mathrm{t}\,\mu\mathrm{t}\,\psi\mathrm{a}+\alpha\mathrm{t}\,\beta\mathrm{a}\,\delta\in\theta\mathrm{a}\,\mu\mathrm{a}\,\rho\,\psi\mathrm{a}-\mathrm{e}\,\alpha\mathrm{a}\,\beta\mathrm{a}\,\delta\,\epsilon^2\,\psi\mathrm{t}-$$
$$2\,\mathrm{e}\,\alpha\mathrm{a}\,\beta\mathrm{a}\,\delta\in\theta\mathrm{t}\,\psi\mathrm{t}-\mathrm{e}\,\alpha\mathrm{a}\,\beta\mathrm{a}\,\delta\,\theta\mathrm{t}^2\,\psi\mathrm{t}+\mathrm{e}\,\alpha\mathrm{a}\,\beta\mathrm{a}\,\delta\in\theta\mathrm{t}\,\mu\mathrm{t}\,\psi\mathrm{t}+$$
$$\mathrm{e}\,\alpha\mathrm{a}\,\beta\mathrm{a}\,\delta\,\theta\mathrm{t}^2\,\mu\mathrm{t}\,\psi\mathrm{t}+\alpha\mathrm{a}\,\beta\mathrm{a}\,\delta\,\epsilon^2\,\rho\,\psi\mathrm{t}+\alpha\mathrm{a}\,\beta\mathrm{a}\,\delta\in\theta\mathrm{t}\,\rho\,\psi\mathrm{t}+$$
$$\sqrt{\big(4\,\alpha\mathrm{a}\,\alpha\mathrm{t}\,\delta\,\big(\alpha\mathrm{a}\,\big(\epsilon+\theta\mathrm{t}-\theta\mathrm{t}\,\mu\mathrm{t}\big)\,\tau\mathrm{a}-\beta\mathrm{a}\,\epsilon\,\rho\,\psi\mathrm{a}+\mathrm{e}\,\big(\epsilon+\theta\mathrm{t}-\theta\mathrm{t}\,\mu\mathrm{t}\big)\,\big(\mathrm{la}\,\beta\mathrm{a}-\alpha\mathrm{a}\,\eta\mathrm{a}\,\tau\mathrm{a}+\beta\mathrm{a}\,\psi\mathrm{a}\big)\big)}$$
$$\big(-\mathrm{e}\,\big(\mathrm{lt}\,\beta\mathrm{a}^2\,\gamma\in(\epsilon+\theta\mathrm{t})-\alpha\mathrm{t}\,\big(\beta\mathrm{a}^2\,\gamma\,\big(\epsilon\,(\lambda\mathrm{a}+\lambda\mathrm{t})-\theta\mathrm{t}\,\lambda\mathrm{a}\,(-1+\mu\mathrm{t})\big)+\delta\,\eta\mathrm{a}\,\theta\mathrm{a}^2\,\big(\epsilon+\theta\mathrm{t}-\theta\mathrm{t}\,\mu\mathrm{t}\big)\,\tau\mathrm{a}-\beta\mathrm{a}\,\theta\mathrm{a}\,\big(\epsilon+\theta\mathrm{t}-\theta\mathrm{t}\,\mu\mathrm{t}\big)\,\big(\delta\,\lambda\mathrm{a}+\gamma\,\eta\mathrm{a}\,\tau\mathrm{a}\big)\big)+\beta\mathrm{a}\,(\epsilon+\theta\mathrm{t})\,\big(\beta\mathrm{a}\,\gamma\,\theta\mathrm{t}\,(-1+$$
$$\mu\mathrm{t})+\delta\,\theta\mathrm{a}\,\big(\epsilon+\theta\mathrm{t}-\theta\mathrm{t}\,\mu\mathrm{t}\big)\big)\,\psi\mathrm{t}\big)+\theta\mathrm{a}\,\mu\mathrm{a}\,\big(\mathrm{lt}\,\beta\mathrm{a}\,\delta\in(\epsilon+\theta\mathrm{t})\,\rho-\alpha\mathrm{t}\,\big(\beta\mathrm{a}\,\delta\in\lambda\mathrm{t}\,\rho-\beta\mathrm{a}\,\gamma\,\big(\epsilon+\theta\mathrm{t}-\theta\mathrm{t}\,\mu\mathrm{t}\big)\,\tau\mathrm{a}+\delta\,\theta\mathrm{a}\,\big(\epsilon+\theta\mathrm{t}-\theta\mathrm{t}\,\mu\mathrm{t}\big)\,\tau\mathrm{a}\big)+\beta\mathrm{a}\,\delta\in(\epsilon+\theta\mathrm{t})\,\rho\,\psi\mathrm{t}\big)\big)+$$
$$\big(\mathrm{lt}\,\alpha\mathrm{a}\,\beta\mathrm{a}\,\delta\in(\epsilon+\theta\mathrm{t})\,\rho-\alpha\mathrm{a}\,\alpha\mathrm{t}\,\beta\mathrm{a}\,\delta\in\lambda\mathrm{t}\,\rho+\alpha\mathrm{a}\,\alpha\mathrm{t}\,\beta\mathrm{a}\,\gamma\in\tau\mathrm{a}-\alpha\mathrm{a}\,\alpha\mathrm{t}\,\delta\in\theta\mathrm{a}\,\tau\mathrm{a}+\alpha\mathrm{a}\,\alpha\mathrm{t}\,\beta\mathrm{a}\,\gamma\,\theta\mathrm{t}\,\tau\mathrm{a}-\alpha\mathrm{a}\,\alpha\mathrm{t}\,\delta\,\theta\mathrm{a}\,\theta\mathrm{t}\,\tau\mathrm{a}-\alpha\mathrm{a}\,\alpha\mathrm{t}\,\delta\in\theta\mathrm{a}\,\mu\mathrm{a}\,\tau\mathrm{a}-\alpha\mathrm{a}\,\alpha\mathrm{t}\,\delta\,\theta\mathrm{a}\,\theta\mathrm{t}\,\mu\mathrm{a}\,\tau\mathrm{a}-$$
$$\alpha\mathrm{a}\,\alpha\mathrm{t}\,\beta\mathrm{a}\,\gamma\,\theta\mathrm{t}\,\mu\mathrm{t}\,\tau\mathrm{a}+\alpha\mathrm{a}\,\alpha\mathrm{t}\,\delta\,\theta\mathrm{a}\,\theta\mathrm{t}\,\mu\mathrm{t}\,\tau\mathrm{a}+\alpha\mathrm{a}\,\alpha\mathrm{t}\,\delta\,\theta\mathrm{a}\,\theta\mathrm{t}\,\mu\mathrm{a}\,\mu\mathrm{t}\,\tau\mathrm{a}+\alpha\mathrm{t}\,\beta\mathrm{a}\,\delta\in\theta\mathrm{a}\,\mu\mathrm{a}\,\rho\,\psi\mathrm{a}+\alpha\mathrm{a}\,\beta\mathrm{a}\,\delta\,\epsilon^2\,\rho\,\psi\mathrm{t}+\alpha\mathrm{a}\,\beta\mathrm{a}\,\delta\in\theta\mathrm{t}\,\rho\,\psi\mathrm{t}+\mathrm{e}\,\big(\mathrm{la}\,\alpha\mathrm{t}\,\beta\mathrm{a}\,\big(\beta\mathrm{a}\,\gamma-\delta\,\theta\mathrm{a}\big)$$
$$\big(\epsilon+\theta\mathrm{t}-\theta\mathrm{t}\,\mu\mathrm{t}\big)-\alpha\mathrm{t}\,\beta\mathrm{a}\,\big(\beta\mathrm{a}\,\gamma\,\theta\mathrm{t}\,(-1+\mu\mathrm{t})+\delta\,\theta\mathrm{a}\,\big(\epsilon+\theta\mathrm{t}-\theta\mathrm{t}\,\mu\mathrm{t}\big)\big)\,\psi\mathrm{a}-\alpha\mathrm{a}\,\big(\epsilon+\theta\mathrm{t}-\theta\mathrm{t}\,\mu\mathrm{t}\big)\,\big(\alpha\mathrm{t}\,\big(\beta\mathrm{a}\,\delta\,\lambda\mathrm{a}+\beta\mathrm{a}\,\gamma\,\eta\mathrm{a}\,\tau\mathrm{a}-2\,\delta\,\eta\mathrm{a}\,\theta\mathrm{a}\,\tau\mathrm{a}\big)+\beta\mathrm{a}\,\delta\,(\epsilon+\theta\mathrm{t})\,\psi\mathrm{t}\big)\big)^2\big)\Big)\Big/$$
$$\big(2\,\alpha\mathrm{a}\,\alpha\mathrm{t}\,\delta\,\big(-\alpha\mathrm{a}\,\big(\epsilon+\theta\mathrm{t}-\theta\mathrm{t}\,\mu\mathrm{t}\big)\,\tau\mathrm{a}+\beta\mathrm{a}\,\epsilon\,\rho\,\psi\mathrm{a}-\mathrm{e}\,\big(\epsilon+\theta\mathrm{t}-\theta\mathrm{t}\,\mu\mathrm{t}\big)\,\big(\mathrm{la}\,\beta\mathrm{a}-\alpha\mathrm{a}\,\eta\mathrm{a}\,\tau\mathrm{a}+\beta\mathrm{a}\,\psi\mathrm{a}\big)\big)\big)\Big\}$$

Equilibrium 10:

$$\left\{Pt \to -\left(\left(-2\,e\,la\,lt\,\alpha a\,\beta a\,\delta\,\epsilon^2 - 4\,e\,la\,lt\,\alpha a\,\beta a\,\delta\,\epsilon\,\theta t - 2\,e\,la\,lt\,\alpha a\,\beta a\,\delta\,\theta t^2 + 2\,e\,la\,\alpha a\,\alpha t\,\beta a\,\delta\,\epsilon\,\lambda t + 2\,e\,la\,\alpha a\,\alpha t\,\beta a\,\delta\,\theta t\,\lambda t + 2\,e\,la\,lt\,\alpha a\,\beta a\,\delta\,\epsilon\,\theta t\,\mu t + 2\,e\,la\,lt\,\alpha a\,\beta a\,\delta\,\theta t^2\,\mu t - 2\,e\,la\,\alpha a\,\alpha t\,\beta a\,\delta\,\theta t\,\lambda t\,\mu t - 2\,lt\,\alpha a^2\,\delta\,\epsilon^2\,\tau a + 2\,e\,lt\,\alpha a^2\,\delta\,\epsilon^2\,\eta a\,\tau a - 4\,lt\,\alpha a^2\,\delta\,\epsilon\,\theta t\,\tau a + 4\,e\,lt\,\alpha a^2\,\delta\,\epsilon\,\eta a\,\theta t\,\tau a - 2\,lt\,\alpha a^2\,\delta\,\theta t^2\,\tau a + 2\,e\,lt\,\alpha a^2\,\delta\,\eta a\,\theta t^2\,\tau a + 2\,\alpha a^2\,\alpha t\,\delta\,\epsilon\,\lambda t\,\tau a - 2\,e\,\alpha a^2\,\alpha t\,\delta\,\epsilon\,\eta a\,\lambda t\,\tau a + 2\,\alpha a^2\,\alpha t\,\delta\,\theta t\,\lambda t\,\tau a - 2\,e\,\alpha a^2\,\alpha t\,\delta\,\eta a\,\theta t\,\lambda t\,\tau a + 2\,lt\,\alpha a^2\,\delta\,\epsilon\,\theta t\,\mu t\,\tau a - 2\,e\,lt\,\alpha a^2\,\delta\,\epsilon\,\eta a\,\theta t\,\mu t\,\tau a + 2\,lt\,\alpha a^2\,\delta\,\theta t^2\,\mu t\,\tau a - 2\,e\,lt\,\alpha a^2\,\delta\,\eta a\,\theta t^2\,\mu t\,\tau a - 2\,\alpha a^2\,\alpha t\,\delta\,\theta t\,\lambda t\,\mu t\,\tau a + 2\,e\,\alpha a^2\,\alpha t\,\delta\,\eta a\,\theta t\,\lambda t\,\mu t\,\tau a - e\,la\,\alpha t\,\beta a^2\,\gamma\,\epsilon\,\psi a - 2\,e\,lt\,\alpha a\,\beta a\,\delta\,\epsilon^2\,\psi a + e\,la\,\alpha t\,\beta a\,\delta\,\epsilon\,\theta a\,\psi a - e\,la\,\alpha t\,\beta a^2\,\gamma\,\theta t\,\psi a - 4\,e\,lt\,\alpha a\,\beta a\,\delta\,\epsilon\,\theta t\,\psi a + e\,la\,\alpha t\,\beta a\,\delta\,\theta a\,\theta t\,\psi a - 2\,e\,lt\,\alpha a\,\beta a\,\delta\,\theta t^2\,\psi a + e\,\alpha a\,\alpha t\,\beta a\,\delta\,\epsilon\,\lambda a\,\psi a + e\,\alpha a\,\alpha t\,\beta a\,\delta\,\theta t\,\lambda a\,\psi a + 2\,e\,\alpha a\,\alpha t\,\beta a\,\delta\,\epsilon\,\lambda t\,\psi a + 2\,e\,\alpha a\,\alpha t\,\beta a\,\delta\,\theta t\,\lambda t\,\psi a + e\,la\,\alpha t\,\beta a^2\,\gamma\,\theta t\,\mu t\,\psi a + 2\,e\,lt\,\alpha a\,\beta a\,\delta\,\epsilon\,\theta t\,\mu t\,\psi a - e\,la\,\alpha t\,\beta a\,\delta\,\theta a\,\theta t\,\mu t\,\psi a + 2\,e\,lt\,\alpha a\,\beta a\,\delta\,\theta t^2\,\mu t\,\psi a - e\,\alpha a\,\alpha t\,\beta a\,\delta\,\theta t\,\lambda a\,\mu t\,\psi a - 2\,e\,\alpha a\,\alpha t\,\beta a\,\delta\,\theta t\,\lambda t\,\mu t\,\psi a + lt\,\alpha a\,\beta a\,\delta\,\epsilon^2\,\rho\,\psi a + lt\,\alpha a\,\beta a\,\delta\,\epsilon\,\theta t\,\rho\,\psi a - \alpha a\,\alpha t\,\beta a\,\delta\,\epsilon\,\lambda t\,\rho\,\psi a - \alpha a\,\alpha t\,\beta a\,\gamma\,\epsilon\,\tau a\,\psi a + e\,\alpha a\,\alpha t\,\beta a\,\gamma\,\epsilon\,\eta a\,\tau a\,\psi a + \alpha a\,\alpha t\,\delta\,\epsilon\,\theta a\,\tau a\,\psi a - 2\,e\,\alpha a\,\alpha t\,\delta\,\epsilon\,\eta a\,\theta a\,\tau a\,\psi a - \alpha a\,\alpha t\,\beta a\,\gamma\,\theta t\,\tau a\,\psi a + e\,\alpha a\,\alpha t\,\beta a\,\gamma\,\eta a\,\theta t\,\tau a\,\psi a + \alpha a\,\alpha t\,\delta\,\theta a\,\theta t\,\tau a\,\psi a - 2\,e\,\alpha a\,\alpha t\,\delta\,\eta a\,\theta a\,\theta t\,\tau a\,\psi a + \alpha a\,\alpha t\,\delta\,\epsilon\,\theta a\,\mu a\,\tau a\,\psi a + \alpha a\,\alpha t\,\delta\,\theta a\,\theta t\,\mu a\,\tau a\,\psi a + \alpha a\,\alpha t\,\beta a\,\gamma\,\theta t\,\mu t\,\tau a\,\psi a - e\,\alpha a\,\alpha t\,\beta a\,\gamma\,\eta a\,\theta t\,\mu t\,\tau a\,\psi a - \alpha a\,\alpha t\,\delta\,\theta a\,\theta t\,\mu t\,\tau a\,\psi a + 2\,e\,\alpha a\,\alpha t\,\delta\,\eta a\,\theta a\,\theta t\,\mu t\,\tau a\,\psi a - \alpha a\,\alpha t\,\delta\,\theta a\,\theta t\,\mu a\,\mu t\,\tau a\,\psi a + e\,\alpha t\,\beta a\,\delta\,\epsilon\,\theta a\,\psi a^2 - e\,\alpha t\,\beta a^2\,\gamma\,\theta t\,\psi a^2 + e\,\alpha t\,\beta a\,\delta\,\theta a\,\theta t\,\psi a^2 + e\,\alpha t\,\beta a^2\,\gamma\,\theta t\,\mu t\,\psi a^2 - e\,\alpha t\,\beta a\,\delta\,\theta a\,\theta t\,\mu t\,\psi a^2 - \alpha t\,\beta a\,\delta\,\epsilon\,\theta a\,\mu a\,\rho\,\psi a^2 - 2\,e\,la\,\alpha a\,\beta a\,\delta\,\epsilon^2\,\psi t - 4\,e\,la\,\alpha a\,\beta a\,\delta\,\epsilon\,\theta t\,\psi t - 2\,e\,la\,\alpha a\,\beta a\,\delta\,\theta t^2\,\psi t + 2\,e\,la\,\alpha a\,\beta a\,\delta\,\epsilon\,\theta t\,\mu t\,\psi t + 2\,e\,la\,\alpha a\,\beta a\,\delta\,\theta t^2\,\mu t\,\psi t - 2\,\alpha a^2\,\delta\,\epsilon^2\,\tau a\,\psi t + 2\,e\,\alpha a^2\,\delta\,\epsilon^2\,\eta a\,\tau a\,\psi t - 4\,\alpha a^2\,\delta\,\epsilon\,\theta t\,\tau a\,\psi t + 4\,e\,\alpha a^2\,\delta\,\epsilon\,\eta a\,\theta t\,\tau a\,\psi t - 2\,\alpha a^2\,\delta\,\theta t^2\,\tau a\,\psi t + 2\,e\,\alpha a^2\,\delta\,\eta a\,\theta t^2\,\tau a\,\psi t + 2\,\alpha a^2\,\delta\,\epsilon\,\theta t\,\mu t\,\tau a\,\psi t - 2\,e\,\alpha a^2\,\delta\,\epsilon\,\eta a\,\theta t\,\mu t\,\tau a\,\psi t + 2\,\alpha a^2\,\delta\,\theta t^2\,\mu t\,\tau a\,\psi t - 2\,e\,\alpha a^2\,\delta\,\eta a\,\theta t^2\,\mu t\,\tau a\,\psi t - e\,\alpha a\,\beta a\,\delta\,\epsilon^2\,\psi a\,\psi t - 2\,e\,\alpha a\,\beta a\,\delta\,\epsilon\,\theta t\,\psi a\,\psi t - e\,\alpha a\,\beta a\,\delta\,\theta t^2\,\psi a\,\psi t + e\,\alpha a\,\beta a\,\delta\,\epsilon\,\theta t\,\mu t\,\psi a\,\psi t + e\,\alpha a\,\beta a\,\delta\,\theta t^2\,\mu t\,\psi a\,\psi t + \alpha a\,\beta a\,\delta\,\epsilon^2\,\rho\,\psi a\,\psi t + \alpha a\,\beta a\,\delta\,\epsilon\,\theta t\,\rho\,\psi a\,\psi t + \psi a\sqrt{\left(4\,\alpha a\,\alpha t\,\delta\,(\alpha a\,(\epsilon + \theta t - \theta t\,\mu t)\,\tau a - \beta a\,\epsilon\,\rho\,\psi a + e\,(\epsilon + \theta t - \theta t\,\mu t)\,(la\,\beta a - \alpha a\,\eta a\,\tau a + \beta a\,\psi a))\,(-e\,(lt\,\beta a^2\,\gamma\,\epsilon\,(\epsilon + \theta t) - \alpha t\,(\beta a^2\,\gamma\,(\epsilon\,(\lambda a + \lambda t) - \theta t\,\lambda a\,(-1 + \mu t)) + \delta\,\eta a\,\theta a^2\,(\epsilon + \theta t - \theta t\,\mu t)\,\tau a - \beta a\,\theta a\,(\epsilon + \theta t - \theta t\,\mu t)\,(\delta\,\lambda a + \gamma\,\eta a\,\tau a)) + \beta a\,(\epsilon + \theta t)\,(\beta a\,\gamma\,\theta t\,(-1 + \mu t) + \delta\,\theta a\,(\epsilon + \theta t - \theta t\,\mu t))\,\psi t) + \theta a\,\mu a\,(lt\,\beta a\,\delta\,\epsilon\,(\epsilon + \theta t)\,\rho - \alpha t\,(\beta a\,\delta\,\epsilon\,\lambda t\,\rho - \beta a\,\gamma\,(\epsilon + \theta t - \theta t\,\mu t)\,\tau a + \delta\,\theta a\,(\epsilon + \theta t - \theta t\,\mu t)\,\tau a) + \beta a\,\delta\,\epsilon\,(\epsilon + \theta t)\,\rho\,\psi t)) + (lt\,\alpha a\,\beta a\,\delta\,\epsilon\,(\epsilon + \theta t)\,\rho - \alpha a\,\alpha t\,\beta a\,\delta\,\epsilon\,\lambda t\,\rho + \alpha a\,\alpha t\,\beta a\,\gamma\,\epsilon\,\tau a - \alpha a\,\alpha t\,\delta\,\epsilon\,\theta a\,\tau a + \alpha a\,\alpha t\,\beta a\,\gamma\,\theta t\,\tau a - \alpha a\,\alpha t\,\delta\,\theta a\,\theta t\,\tau a - \alpha a\,\alpha t\,\delta\,\epsilon\,\theta a\,\mu a\,\tau a - \alpha a\,\alpha t\,\delta\,\theta a\,\theta t\,\mu a\,\tau a - \alpha a\,\alpha t\,\beta a\,\gamma\,\theta t\,\mu t\,\tau a + \alpha a\,\alpha t\,\delta\,\theta a\,\theta t\,\mu t\,\tau a + \alpha a\,\alpha t\,\delta\,\theta a\,\theta t\,\mu a\,\mu t\,\tau a + \alpha t\,\beta a\,\delta\,\epsilon\,\theta a\,\mu a\,\rho\,\psi a + \alpha a\,\beta a\,\delta\,\epsilon^2\,\rho\,\psi t + \alpha a\,\beta a\,\delta\,\epsilon\,\theta t\,\rho\,\psi t + e\,(la\,\alpha t\,\beta a\,(\beta a\,\gamma - \delta\,\theta a)\,(\epsilon + \theta t - \theta t\,\mu t) - \alpha t\,\beta a\,(\beta a\,\gamma\,\theta t\,(-1 + \mu t) + \delta\,\theta a\,(\epsilon + \theta t - \theta t\,\mu t))\,\psi a - \alpha a\,(\epsilon + \theta t - \theta t\,\mu t)\,(\alpha t\,(\beta a\,\delta\,\lambda a + \beta a\,\gamma\,\eta a\,\tau a - 2\,\delta\,\eta a\,\theta a\,\tau a) + \beta a\,\delta\,(\epsilon + \theta t)\,\psi t)))^2)\Big)\Big/ (2\,\alpha a\,\alpha t\,\delta\,(\epsilon + \theta t - \theta t\,\mu t)\,(-\alpha a\,(\epsilon + \theta t - \theta t\,\mu t)\,\tau a + \beta a\,\epsilon\,\rho\,\psi a - e\,(\epsilon + \theta t - \theta t\,\mu t)\,(la\,\beta a - \alpha a\,\eta a\,\tau a + \beta a\,\psi a)))\Big),\ Nt \to \frac{\epsilon + \theta t}{\alpha t},$$

$$Lt \to -\left(\left(-e\,la\,\alpha t\,\beta a^2\,\gamma\,\epsilon + e\,la\,\alpha t\,\beta a\,\delta\,\epsilon\,\theta a - e\,la\,\alpha t\,\beta a^2\,\gamma\,\theta t + e\,la\,\alpha t\,\beta a\,\delta\,\theta a\,\theta t - e\,\alpha a\,\alpha t\,\beta a\,\delta\,\epsilon\,\lambda a - e\,\alpha a\,\alpha t\,\beta a\,\delta\,\theta t\,\lambda a + e\,la\,\alpha t\,\beta a^2\,\gamma\,\theta t\,\mu t - e\,la\,\alpha t\,\beta a\,\delta\,\theta a\,\theta t\,\mu t + e\,\alpha a\,\alpha t\,\beta a\,\delta\,\theta t\,\lambda a\,\mu t + lt\,\alpha a\,\beta a\,\delta\,\epsilon^2\,\rho + lt\,\alpha a\,\beta a\,\delta\,\epsilon\,\theta t\,\rho - \alpha a\,\alpha t\,\beta a\,\delta\,\epsilon\,\lambda t\,\rho - \alpha a\,\alpha t\,\beta a\,\gamma\,\epsilon\,\tau a + e\,\alpha a\,\alpha t\,\beta a\,\gamma\,\epsilon\,\eta a\,\tau a + \alpha a\,\alpha t\,\delta\,\epsilon\,\theta a\,\tau a - \alpha a\,\alpha t\,\beta a\,\gamma\,\theta t\,\tau a + e\,\alpha a\,\alpha t\,\beta a\,\gamma\,\eta a\,\theta t\,\tau a + \alpha a\,\alpha t\,\delta\,\theta a\,\theta t\,\tau a - \alpha a\,\alpha t\,\delta\,\epsilon\,\theta a\,\mu a\,\tau a - \alpha a\,\alpha t\,\delta\,\theta a\,\theta t\,\mu a\,\tau a + \alpha a\,\alpha t\,\beta a\,\gamma\,\theta t\,\mu t\,\tau a - e\,\alpha a\,\alpha t\,\beta a\,\gamma\,\eta a\,\theta t\,\mu t\,\tau a - \alpha a\,\alpha t\,\delta\,\theta a\,\theta t\,\mu t\,\tau a + \alpha a\,\alpha t\,\delta\,\theta a\,\theta t\,\mu a\,\mu t\,\tau a + e\,\alpha t\,\beta a\,\delta\,\epsilon\,\theta a\,\psi a - e\,\alpha t\,\beta a^2\,\gamma\,\theta t\,\psi a + e\,\alpha t\,\beta a\,\delta\,\theta a\,\theta t\,\psi a + e\,\alpha t\,\beta a^2\,\gamma\,\theta t\,\mu t\,\psi a - e\,\alpha t\,\beta a\,\delta\,\theta a\,\theta t\,\mu t\,\psi a - \alpha t\,\beta a\,\delta\,\epsilon\,\theta a\,\mu a\,\rho\,\psi a - e\,\alpha a\,\beta a\,\delta\,\epsilon^2\,\psi t - 2\,e\,\alpha a\,\beta a\,\delta\,\epsilon\,\theta t\,\psi t - e\,\alpha a\,\beta a\,\delta\,\theta t^2\,\psi t + e\,\alpha a\,\beta a\,\delta\,\epsilon\,\theta t\,\mu t\,\psi t + e\,\alpha a\,\beta a\,\delta\,\theta t^2\,\mu t\,\psi t + \alpha a\,\beta a\,\delta\,\epsilon^2\,\rho\,\psi t + \alpha a\,\beta a\,\delta\,\epsilon\,\theta t\,\rho\,\psi t + \sqrt{\left(4\,\alpha a\,\alpha t\,\delta\,(\alpha a\,(\epsilon + \theta t - \theta t\,\mu t)\,\tau a - \beta a\,\epsilon\,\rho\,\psi a + e\,(\epsilon + \theta t - \theta t\,\mu t)\,(la\,\beta a - \alpha a\,\eta a\,\tau a + \beta a\,\psi a))\,(-e\,(lt\,\beta a^2\,\gamma\,\epsilon\,(\epsilon + \theta t) - \alpha t\,(\beta a^2\,\gamma\,(\epsilon\,(\lambda a + \lambda t) - \theta t\,\lambda a\,(-1 + \mu t)) + \delta\,\eta a\,\theta a^2\,(\epsilon + \theta t - \theta t\,\mu t)\,\tau a - \beta a\,\theta a\,(\epsilon + \theta t - \theta t\,\mu t)\,(\delta\,\lambda a + \gamma\,\eta a\,\tau a)) + \beta a\,(\epsilon + \theta t)\,(\beta a\,\gamma\,\theta t\,(-1 + \mu t) + \delta\,\theta a\,(\epsilon + \theta t - \theta t\,\mu t))\,\psi t) + \theta a\,\mu a\,(lt\,\beta a\,\delta\,\epsilon\,(\epsilon + \theta t)\,\rho - \alpha t\,(\beta a\,\delta\,\epsilon\,\lambda t\,\rho - \beta a\,\gamma\,(\epsilon + \theta t - \theta t\,\mu t)\,\tau a + \delta\,\theta a\,(\epsilon + \theta t - \theta t\,\mu t)\,\tau a) + \beta a\,\delta\,\epsilon\,(\epsilon + \theta t)\,\rho\,\psi t)) + (lt\,\alpha a\,\beta a\,\delta\,\epsilon\,(\epsilon + \theta t)\,\rho - \alpha a\,\alpha t\,\beta a\,\delta\,\epsilon\,\lambda t\,\rho + \alpha a\,\alpha t\,\beta a\,\gamma\,\epsilon\,\tau a - \alpha a\,\alpha t\,\delta\,\epsilon\,\theta a\,\tau a + \alpha a\,\alpha t\,\beta a\,\gamma\,\theta t\,\tau a - \alpha a\,\alpha t\,\delta\,\theta a\,\theta t\,\tau a - \alpha a\,\alpha t\,\delta\,\epsilon\,\theta a\,\mu a\,\tau a - \alpha a\,\alpha t\,\delta\,\theta a\,\theta t\,\mu a\,\tau a - \alpha a\,\alpha t\,\beta a\,\gamma\,\theta t\,\mu t\,\tau a + \alpha a\,\alpha t\,\delta\,\theta a\,\theta t\,\mu t\,\tau a + \alpha a\,\alpha t\,\delta\,\theta a\,\theta t\,\mu a\,\mu t\,\tau a + \alpha t\,\beta a\,\delta\,\epsilon\,\theta a\,\mu a\,\rho\,\psi a + \alpha a\,\beta a\,\delta\,\epsilon^2\,\rho\,\psi t + \alpha a\,\beta a\,\delta\,\epsilon\,\theta t\,\rho\,\psi t + e\,(la\,\alpha t\,\beta a\,(\beta a\,\gamma - \delta\,\theta a)\,(\epsilon + \theta t - \theta t\,\mu t) - \alpha t\,\beta a\,(\beta a\,\gamma\,\theta t\,(-1 + \mu t) + \delta\,\theta a\,(\epsilon + \theta t - \theta t\,\mu t))\,\psi a - \alpha a\,(\epsilon + \theta t - \theta t\,\mu t)\,(\alpha t\,(\beta a\,\delta\,\lambda a + \beta a\,\gamma\,\eta a\,\tau a - 2\,\delta\,\eta a\,\theta a\,\tau a) + \beta a\,\delta\,(\epsilon + \theta t)\,\psi t)))^2)\Big)\Big/ (2\,\alpha a\,\alpha t\,\delta\,(\epsilon + \theta t - \theta t\,\mu t)\,(-e\,\beta a\,\gamma + \beta a\,\gamma\,\rho + \delta\,\theta a\,(-1 + \mu a)\,\rho))\Big),\ Ha \to -\Big(\Big(e\,la\,\alpha t\,\beta a^2\,\gamma\,\epsilon + e\,la\,\alpha t\,\beta a\,\delta\,\epsilon\,\theta a + e\,la\,\alpha t\,\beta a^2\,\gamma\,\theta t + e\,la\,\alpha t\,\beta a\,\delta\,\theta a\,\theta t - e\,\alpha a\,\alpha t\,\beta a\,\delta\,\epsilon\,\lambda a - e\,\alpha a\,\alpha t\,\beta a\,\delta\,\theta t\,\lambda a - e\,la\,\alpha t\,\beta a^2\,\gamma\,\theta t\,\mu t - e\,la\,\alpha t\,\beta a\,\delta\,\theta a\,\theta t\,\mu t + e\,\alpha a\,\alpha t\,\beta a\,\delta\,\theta t\,\lambda a\,\mu t + lt\,\alpha a\,\beta a\,\delta\,\epsilon^2\,\rho + lt\,\alpha a\,\beta a\,\delta\,\epsilon\,\theta t\,\rho - \alpha a\,\alpha t\,\beta a\,\delta\,\epsilon\,\lambda t\,\rho + \alpha a\,\alpha t\,\beta a\,\gamma\,\epsilon\,\tau a - e\,\alpha a\,\alpha t\,\beta a\,\gamma\,\epsilon\,\eta a\,\tau a + \alpha a\,\alpha t\,\delta\,\epsilon\,\theta a\,\tau a + \alpha a\,\alpha t\,\beta a\,\gamma\,\theta t\,\tau a - e\,\alpha a\,\alpha t\,\beta a\,\gamma\,\eta a\,\theta t\,\tau a + \alpha a\,\alpha t\,\delta\,\theta a\,\theta t\,\tau a - \alpha a\,\alpha t\,\delta\,\epsilon\,\theta a\,\mu a\,\tau a - \alpha a\,\alpha t\,\delta\,\theta a\,\theta t\,\mu a\,\tau a + \alpha a\,\alpha t\,\beta a\,\gamma\,\theta t\,\mu t\,\tau a - e\,\alpha a\,\alpha t\,\beta a\,\gamma\,\eta a\,\theta t\,\mu t\,\tau a - \alpha a\,\alpha t\,\delta\,\theta a\,\theta t\,\mu t\,\tau a + \alpha a\,\alpha t\,\delta\,\theta a\,\theta t\,\mu a\,\mu t\,\tau a +$$

```
e αt βa δ ϵ ϑa ψa + e αt βa² γ ϑt ψa + e αt βa δ ϑa ϑt ψa − e αt βa² γ ϑt μt ψa − e αt βa δ ϑa ϑt μt ψa − 2 αt βa δ ϵ ϑa ρ ψa + αt βa δ ϵ ϑa μa ρ ψa −
e αa βa δ ϵ² ψt − 2 e αa βa δ ϵ ϑt ψt − e αa βa δ ϑt² ψt + e αa βa δ ϵ ϑt μt ψt + e αa βa δ ϑt² μt ψt + αa βa δ ϵ² ρ ψt + αa βa δ ϵ ϑt ρ ψt −
√(4 αa αt δ (αa (ϵ + ϑt − ϑt μt) τa − βa ϵ ρ ψa + e (ϵ + ϑt − ϑt μt) (la βa − αa ηa τa + βa ψa)) (−e (lt βa² γ ϵ (ϵ + ϑt) − αt (βa² γ (ϵ (λa + λt) − ϑt λa (−1 + μt)) +
δ ηa ϑa² (ϵ + ϑt − ϑt μt) τa − βa ϑa (ϵ + ϑt − ϑt μt) (δ λa + γ ηa τa)) + βa (ϵ + ϑt) (βa γ ϑt (−1 + μt) + δ ϑa (ϵ + ϑt − ϑt μt)) ψt) +
ϑa μa (lt βa δ ϵ (ϵ + ϑt) ρ − αt (βa δ ϵ λt ρ − βa γ (ϵ + ϑt − ϑt μt) τa + δ ϑa (ϵ + ϑt − ϑt μt) τa) + βa δ ϵ (ϵ + ϑt) ρ ψt)) +
(lt αa βa δ ϵ (ϵ + ϑt) ρ − αa αt βa δ ϵ λt ρ + αa αt βa γ ϵ τa − αa αt δ ϵ ϑa τa + αa αt βa γ ϑt τa − αa αt δ ϑa ϑt τa − αa αt δ ϵ ϑa μa τa − αa αt δ ϑa ϑt μa τa −
αa αt βa γ ϑt μt τa + αa αt δ ϑa ϑt μt τa + αa αt δ ϑa ϑt μa μt τa + αt βa δ ϵ ϑa μa ρ ψa + αa βa δ ϵ² ρ ψt + αa βa δ ϵ ϑt ρ ψt + e (la αt βa (βa γ − δ ϑa) (ϵ + ϑt − ϑt μt) −
αt βa (βa γ ϑt (−1 + μt) + δ ϑa (ϵ + ϑt − ϑt μt)) ψa − αa (ϵ + ϑt − ϑt μt) (αt (βa δ λa + βa γ ηa τa − 2 δ ηa ϑa τa) + βa δ (ϵ + ϑt) ψt)))²)) /
(2 αt βa δ (αa (ϵ + ϑt − ϑt μt) τa − βa ϵ ρ ψa + e (ϵ + ϑt − ϑt μt) (la βa − αa ηa τa + βa ψa)))), Pa →
−((−e la αt βa² γ ϵ ρ + e la αt βa δ ϵ ϑa ρ − e la αt βa² γ ϑt ρ + e la αt βa δ ϑa ϑt ρ − e αa αt βa δ ϵ λa ρ − e αa αt βa δ ϑt λa ρ + e la αt βa² γ ϑt μt ρ −
e la αt βa δ ϑa ϑt μt ρ + e αa αt βa δ ϑt λa μt ρ + lt αa βa δ ϵ² ρ² + lt αa βa δ ϵ ϑt ρ² − αa αt βa δ ϵ λt ρ² − 2 e αa αt βa γ ϵ τa −
2 e αa αt βa γ ϑt τa + 2 e αa αt βa γ ϑt μt τa + αa αt βa γ ϵ ρ τa + e αa αt βa γ ϵ ηa ρ τa − αa αt δ ϵ ϑa ρ τa + αa αt βa γ ϑt ρ τa +
e αa αt βa γ ηa ϑt ρ τa − αa αt δ ϑa ϑt ρ τa + αa αt δ ϵ ϑa μa ρ τa + αa αt δ ϑa ϑt μa ρ τa − αa αt βa γ ϑt μt ρ τa −
e αa αt βa γ ηa ϑt μt ρ τa + αa αt δ ϑa ϑt μt ρ τa − αa αt δ ϑa ϑt μa μt ρ τa + e αt βa δ ϵ ϑa ρ ψa − e αt βa² γ ϑt ρ ψa +
e αt βa δ ϑa ϑt ρ ψa + e αt βa² γ ϑt μt ρ ψa − e αt βa δ ϑa ϑt μt ρ ψa − αt βa δ ϵ ϑa μa ρ² ψa − e αa βa δ ϵ² ρ ψt −
2 e αa βa δ ϵ ϑt ρ ψt − e αa βa δ ϑt² ρ ψt + e αa βa δ ϵ ϑt μt ρ ψt + e αa βa δ ϑt² μt ρ ψt + αa βa δ ϵ² ρ² ψt + αa βa δ ϵ ϑt ρ² ψt +
ρ √(4 αa αt δ (αa (ϵ + ϑt − ϑt μt) τa − βa ϵ ρ ψa + e (ϵ + ϑt − ϑt μt) (la βa − αa ηa τa + βa ψa)) (−e (lt βa² γ ϵ (ϵ + ϑt) − αt (βa² γ (ϵ (λa + λt) − ϑt λa (−1 + μt)) +
δ ηa ϑa² (ϵ + ϑt − ϑt μt) τa − βa ϑa (ϵ + ϑt − ϑt μt) (δ λa + γ ηa τa)) + βa (ϵ + ϑt) (βa γ ϑt (−1 + μt) + δ ϑa (ϵ + ϑt − ϑt μt)) ψt) +
ϑa μa (lt βa δ ϵ (ϵ + ϑt) ρ − αt (βa δ ϵ λt ρ − βa γ (ϵ + ϑt − ϑt μt) τa + δ ϑa (ϵ + ϑt − ϑt μt) τa) + βa δ ϵ (ϵ + ϑt) ρ ψt)) +
(lt αa βa δ ϵ (ϵ + ϑt) ρ − αa αt βa δ ϵ λt ρ + αa αt βa γ ϵ τa − αa αt δ ϵ ϑa τa + αa αt βa γ ϑt τa − αa αt δ ϑa ϑt τa − αa αt δ ϵ ϑa μa τa − αa αt δ ϑa ϑt μa τa − αa
αt βa γ ϑt μt τa + αa αt δ ϑa ϑt μt τa + αa αt δ ϑa ϑt μa μt τa + αt βa δ ϵ ϑa μa ρ ψa + αa βa δ ϵ² ρ ψt + αa βa δ ϵ ϑt ρ ψt + e (la αt βa (βa γ − δ ϑa) (ϵ + ϑt − ϑt μt) −
αt βa (βa γ ϑt (−1 + μt) + δ ϑa (ϵ + ϑt − ϑt μt)) ψa − αa (ϵ + ϑt − ϑt μt) (αt (βa δ λa + βa γ ηa τa − 2 δ ηa ϑa τa) + βa δ (ϵ + ϑt) ψt)))²)) /
(2 e αa αt βa (ϵ + ϑt − ϑt μt) (e βa γ − (βa γ + δ ϑa (−1 + μa)) ρ))), Na → −((−e la αt βa² γ ϵ + e la αt βa δ ϵ ϑa − e la αt βa² γ ϑt + e la αt βa δ ϑa ϑt +
e αa αt βa δ ϵ λa + e αa αt βa δ ϑt λa + e la αt βa² γ ϑt μt − e la αt βa δ ϑa ϑt μt − e αa αt βa δ ϑt λa μt − lt αa βa δ ϵ² ρ −
lt αa βa δ ϵ ϑt ρ + αa αt βa δ ϵ λt ρ − αa αt βa γ ϵ τa + e αa αt βa γ ϵ ηa τa + αa αt δ ϵ ϑa τa − 2 e αa αt δ ϵ ηa ϑa τa −
αa αt βa γ ϑt τa + e αa αt βa γ ηa ϑt τa + αa αt δ ϑa ϑt τa − 2 e αa αt δ ηa ϑa ϑt τa + αa αt δ ϵ ϑa μa τa + αa αt δ ϑa ϑt μa τa +
αa αt βa γ ϑt μt τa − e αa αt βa γ ηa ϑt μt τa − αa αt δ ϑa ϑt μt τa + 2 e αa αt δ ηa ϑa ϑt μt τa − αa αt δ ϑa ϑt μa μt τa +
e αt βa δ ϵ ϑa ψa − e αt βa² γ ϑt ψa + e αt βa δ ϑa ϑt ψa + e αt βa² γ ϑt μt ψa − e αt βa δ ϑa ϑt μt ψa − αt βa δ ϵ ϑa μa ρ ψa +
e αa βa δ ϵ² ψt + 2 e αa βa δ ϵ ϑt ψt + e αa βa δ ϑt² ψt − e αa βa δ ϵ ϑt μt ψt − e αa βa δ ϑt² μt ψt − αa βa δ ϵ² ρ ψt − αa βa δ ϵ ϑt ρ ψt +
√(4 αa αt δ (αa (ϵ + ϑt − ϑt μt) τa − βa ϵ ρ ψa + e (ϵ + ϑt − ϑt μt) (la βa − αa ηa τa + βa ψa)) (−e (lt βa² γ ϵ (ϵ + ϑt) − αt (βa² γ (ϵ (λa + λt) − ϑt λa (−1 + μt)) +
δ ηa ϑa² (ϵ + ϑt − ϑt μt) τa − βa ϑa (ϵ + ϑt − ϑt μt) (δ λa + γ ηa τa)) + βa (ϵ + ϑt) (βa γ ϑt (−1 + μt) + δ ϑa (ϵ + ϑt − ϑt μt)) ψt) +
ϑa μa (lt βa δ ϵ (ϵ + ϑt) ρ − αt (βa δ ϵ λt ρ − βa γ (ϵ + ϑt − ϑt μt) τa + δ ϑa (ϵ + ϑt − ϑt μt) τa) + βa δ ϵ (ϵ + ϑt) ρ ψt)) +
(lt αa βa δ ϵ (ϵ + ϑt) ρ − αa αt βa δ ϵ λt ρ + αa αt βa γ ϵ τa − αa αt δ ϵ ϑa τa + αa αt βa γ ϑt τa − αa αt δ ϑa ϑt τa − αa αt δ ϵ ϑa μa τa − αa αt δ ϑa ϑt μa τa −
αa αt βa γ ϑt μt τa + αa αt δ ϑa ϑt μt τa + αa αt δ ϑa ϑt μa μt τa + αt βa δ ϵ ϑa μa ρ ψa + αa βa δ ϵ² ρ ψt + αa βa δ ϵ ϑt ρ ψt + e (la αt βa (βa γ − δ ϑa) (ϵ + ϑt − ϑt μt) −
αt βa (βa γ ϑt (−1 + μt) + δ ϑa (ϵ + ϑt − ϑt μt)) ψa − αa (ϵ + ϑt − ϑt μt) (αt (βa δ λa + βa γ ηa τa − 2 δ ηa ϑa τa) + βa δ (ϵ + ϑt) ψt)))²)) /
(2 αa αt δ (−αa (ϵ + ϑt − ϑt μt) τa + βa ϵ ρ ψa − e (ϵ + ϑt − ϑt μt) (la βa − αa ηa τa + βa ψa)))))}
```

Figures

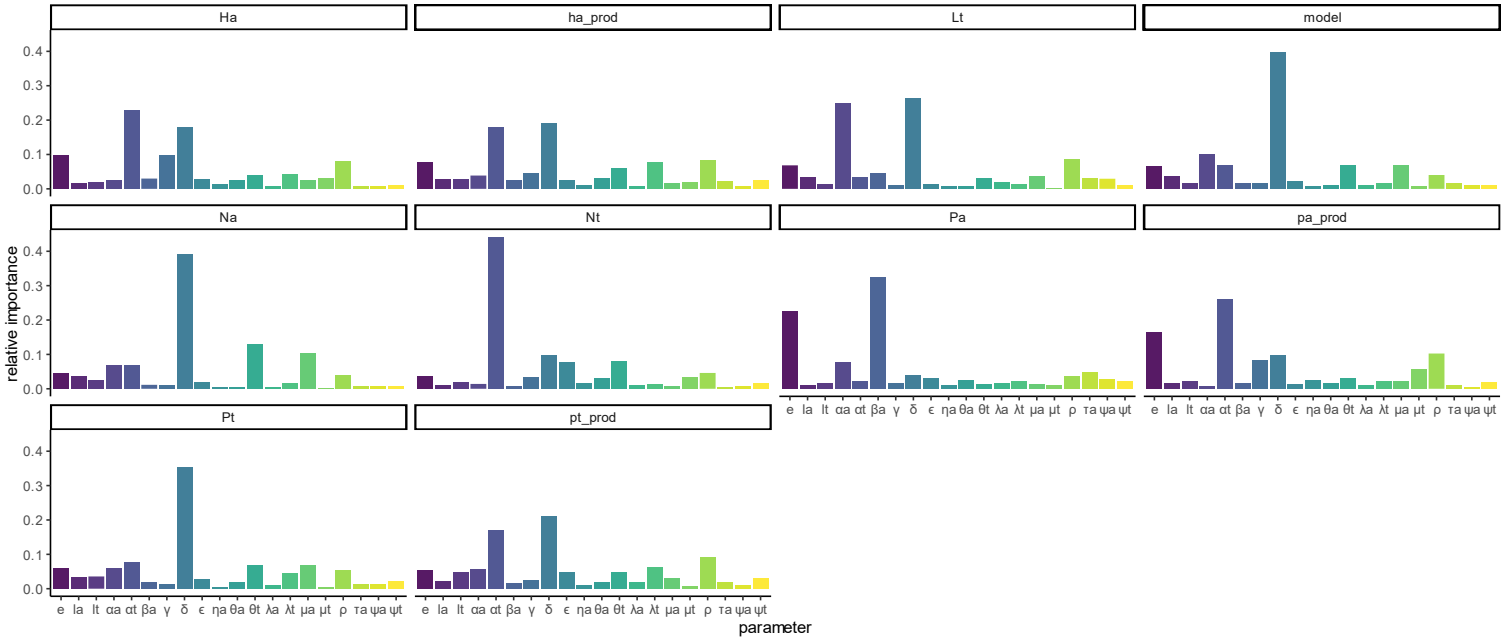

Figure B14: results from the global sensitivity analysis on the meta-ecosystem model. Subplots show the relative importance of each parameter in the model for each of the main components of the meta-ecosystem: benthic invertebrate biomass (H_a), benthic invertebrate productivity, leaf litter (L_t), inorganic aquatic nutrients (N_a), inorganic terrestrial nutrients (N_t), periphyton biomass (P_a), periphyton productivity, tree biomass (P_t), tree productivity, and the model as a whole. These results were used to validate the functioning of the model and inform the parameters that were altered in future disturbance simulations.

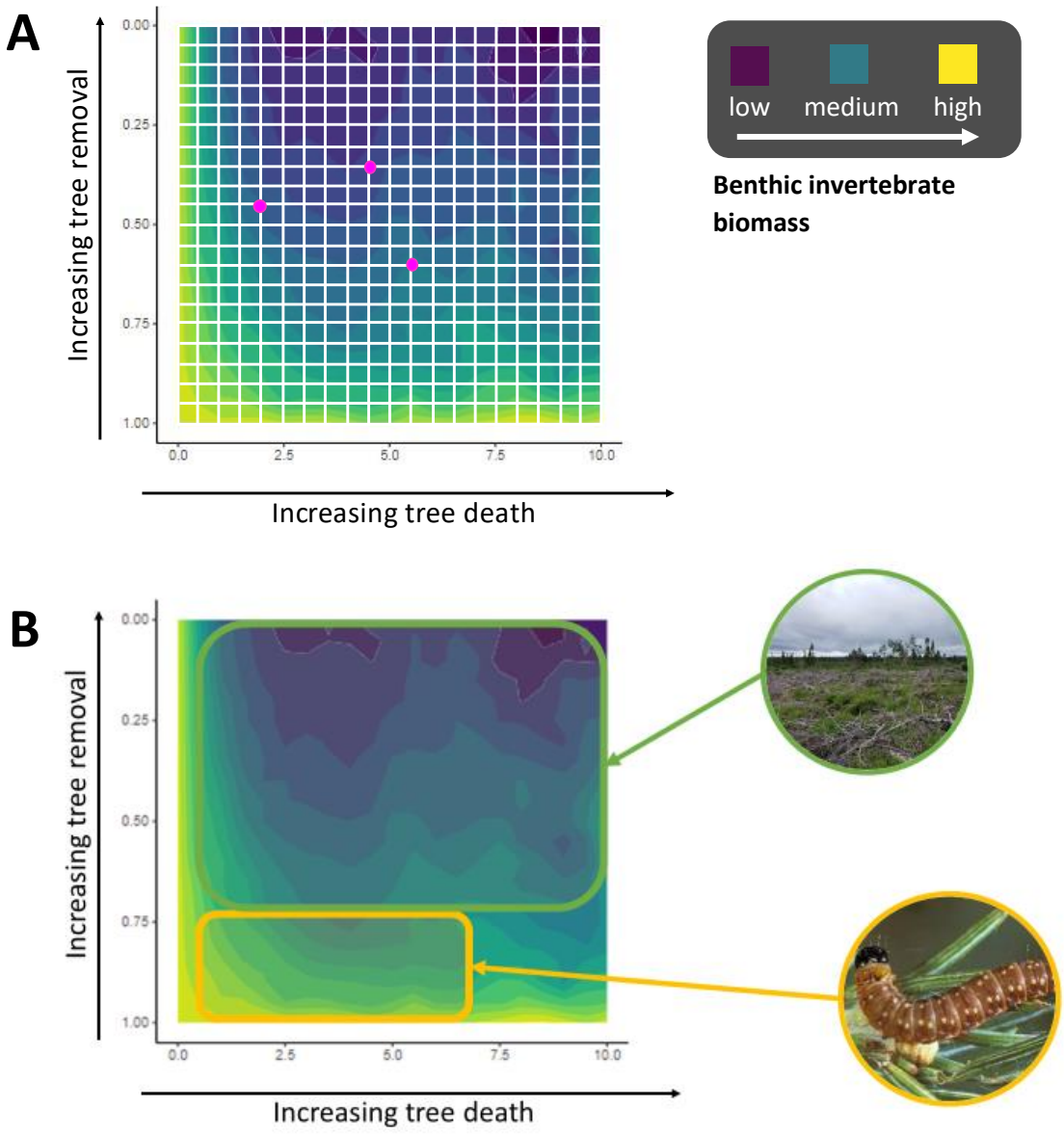

Figure B15: Visualization of the disturbance simulation method on a sample surface plot showing benthic invertebrate biomass across a range of parameter values. Tree death (θ_t) increases along the x axis and tree removal (reduced recycling; 1-μ_t) increases along the y axis, Overall disturbance intensity increases diagonally from bottom left to top right of the plot. (A) each node in the grid (marked in pink) represents 1000 simulations with that value of θ_t and μ_t. These simulations are selected for feasibility and stability, and the mean value from the selected simulations are plotted at each node, creating the surface plot. (B) Each plot can be separated into compartments for disturbance type based on the intensity of each parameter. In these forest disturbance plots the bottom left section of the plot represents a spruce budworm outbreak as tree removal remains low. The top right section of the plot represents a logging disturbance since tree removal ranges from moderate to high.

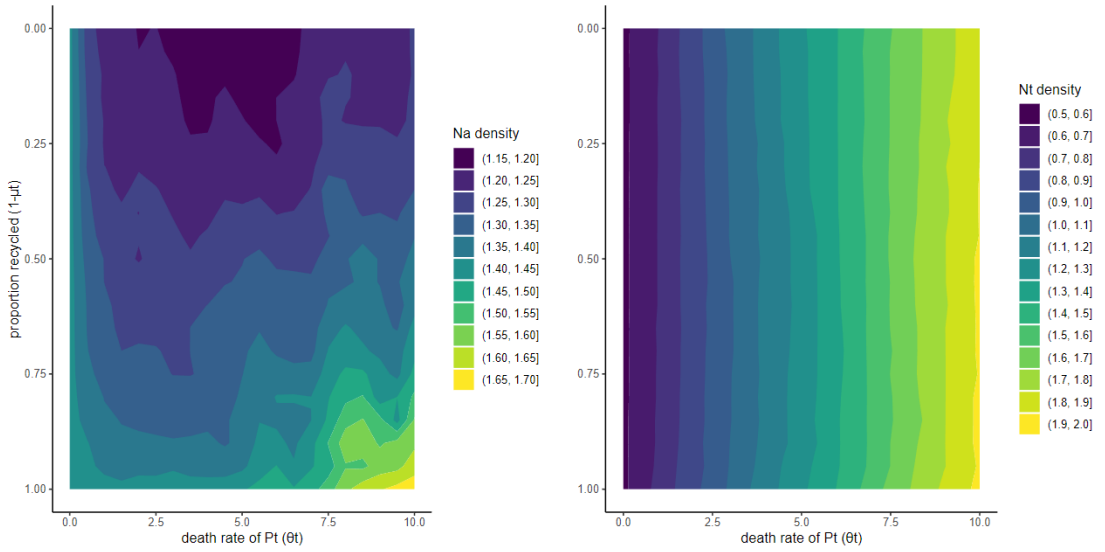

Figure B16: Surface plots of (a) aquatic and (b) terrestrial inorganic nutrient density across a range of mortality rates (θ_t) and tree recycling (μ_t), simulating tree mortality and/or removal from insect outbreaks and logging in the meta-ecosystem model. An insect outbreak is represented by the moderate mortality rate and recycling rate found in the top quadrant of each subplot, and logging is represented by the high mortality rate and low recycling rate found in the bottom quadrant.

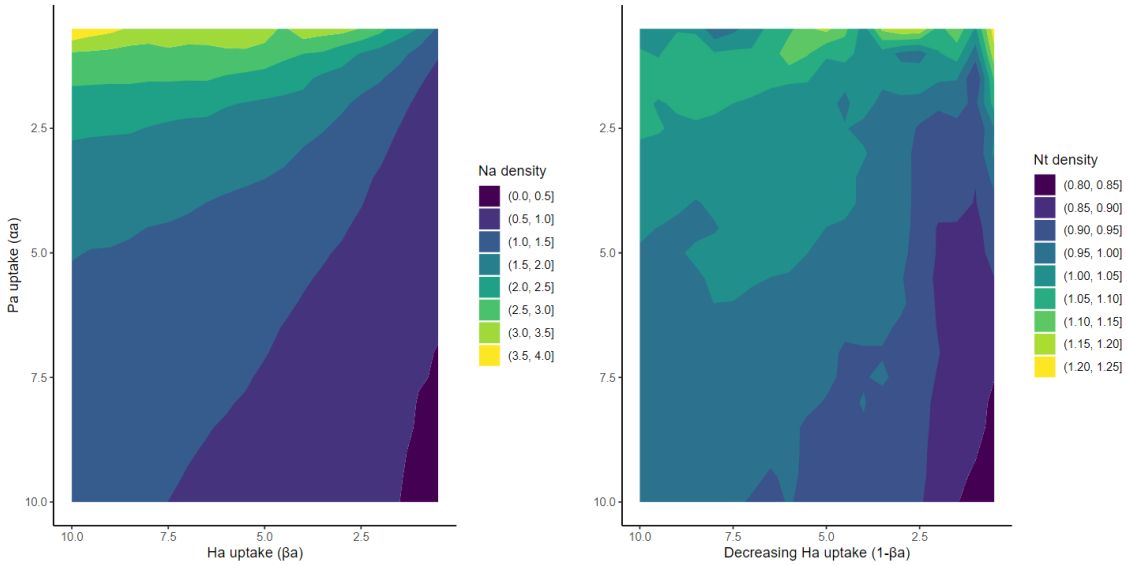

Figure B17: Surface plots of (a) aquatic and (b) terrestrial inorganic nutrient density across a range of periphyton (α_t) and benthic invertebrate (β_t) uptake rates, simulating disturbance from ATV trail presence in the meta-ecosystem model. High ATV trail and logging road density is represented by the low periphyton and benthic invertebrate uptake rates found in the bottom left quadrant of each subplot.

Tables

Table B18: median values and standard deviations for model parameters and variables in the 1000 feasible and stable "undisturbed" meta-ecosystems.

Parameter/variable	**Value**
θ_t	2.90(2.77)
μ_t	0.55(0.29)
α_a	5.67(2.74)
β_a	6.31(2.60)
H_a	0.54(23.61)
H_a productivity	1.89(136.77)
P_a	0.77(6.44)
P_a productivity	4.83(1347.79)
L_t	0.78(48.88)

Table B19: Total data points represented at each disturbance increment in the forest disturbance simulation, corresponding with figure 5 in the main text. These data points are retained after selecting feasible and stable meta-ecosystem equilibria from 1000 original parameter combinations. Colour gradient is used to visualize the magnitude of data points retained across the range of disturbance.

μ_t/θ_a	0	0.5	1	1.5	2	2.5	3	3.5	4	4.5	5	5.5	6	6.5	7	7.5	8	8.5	9	9.5	10
0	767	807	807	773	730	691	656	626	595	558	527	500	471	456	422	383	358	328	305	279	256
0.05	767	808	805	774	736	691	666	632	600	563	531	503	477	458	429	385	361	333	311	283	260
0.1	767	810	811	776	738	696	670	634	604	572	535	506	483	460	432	389	363	335	317	289	266
0.15	767	810	813	778	746	699	674	640	606	575	537	512	481	461	435	390	364	337	321	299	270
0.2	767	811	813	781	743	706	688	645	612	584	540	518	487	465	436	394	367	339	324	305	279
0.25	767	811	812	783	752	713	694	651	620	591	551	519	495	471	436	399	370	343	329	308	286
0.3	767	812	812	792	753	711	697	663	632	595	562	526	500	477	443	407	370	344	331	308	287
0.35	767	811	812	795	761	717	699	668	641	598	567	536	506	483	450	413	375	346	335	307	289
0.4	767	813	804	794	763	719	704	674	645	608	568	537	517	489	458	418	382	350	333	310	291
0.45	767	813	805	800	766	729	707	676	652	617	574	543	517	498	470	430	385	359	335	311	290
0.5	767	813	805	797	768	733	710	681	651	620	582	549	521	500	473	432	398	360	340	313	292
0.55	767	811	803	794	769	734	715	680	656	627	580	549	526	499	476	435	405	374	349	324	299
0.6	767	812	809	792	770	743	715	681	658	628	587	546	524	507	475	438	407	380	354	332	311
0.65	767	811	808	794	770	743	727	691	661	629	595	553	527	507	481	441	415	382	358	337	318
0.7	767	806	810	789	773	740	730	701	671	642	597	558	528	508	482	449	420	389	368	340	319
0.75	767	805	808	788	771	745	730	698	678	645	597	560	524	505	480	449	420	395	373	356	331
0.8	767	799	801	791	765	738	728	700	671	642	600	557	524	506	483	446	429	403	376	362	333
0.85	767	795	795	792	773	735	722	693	664	637	599	557	528	503	486	452	431	410	389	364	338
0.9	767	792	791	787	756	736	726	703	666	633	597	562	537	512	495	459	438	416	392	364	341
0.95	767	785	776	774	755	726	710	681	658	627	594	565	540	517	484	443	422	408	390	369	349
1	767	779	765	756	741	713	689	661	633	604	580	543	507	484	461	430	405	388	370	349	334

Table B20: Total data points represented at each disturbance increment in the unpaved road disturbance simulation, corresponding with figure 6 in the main text. These data points are retained after selecting feasible and stable meta-ecosystem equilibria from 1000 original parameter combinations. Colour gradient is used to visualize the magnitude of data points retained across the range of disturbance.

α_a/β_a	0.5	1	1.5	2	2.5	3	3.5	4	4.5	5	5.5	6	6.5	7	7.5	8	8.5	9	9.5	10
0.5	73	108	120	128	135	141	138	137	126	122	116	116	114	111	106	114	110	107	105	107
1	92	156	206	219	243	252	269	261	262	257	256	256	251	241	238	233	230	221	215	211
1.5	106	161	224	291	295	316	333	326	333	332	335	338	333	327	333	328	322	324	318	308
2	120	183	246	315	346	376	401	408	412	402	395	398	402	395	398	388	388	396	399	386
2.5	127	197	253	318	371	416	455	460	476	466	462	464	466	457	458	442	437	434	441	438
3	130	204	258	322	380	420	476	507	521	518	524	512	503	510	496	492	486	487	480	476
3.5	135	206	258	331	394	438	483	530	550	559	556	562	556	547	544	546	538	539	528	522
4	137	204	261	325	385	441	494	535	567	583	587	596	603	597	594	587	579	576	575	565
4.5	139	206	258	324	383	451	490	549	570	597	612	624	627	632	621	623	620	607	605	596
5	138	206	261	323	384	442	495	544	589	607	634	637	649	658	646	646	646	648	642	626
5.5	137	203	257	318	377	442	488	542	591	619	641	660	661	665	674	670	661	659	654	655
6	137	202	251	321	371	438	490	548	583	621	649	664	674	681	676	678	675	672	673	664
6.5	133	201	251	317	370	433	479	538	579	616	647	670	678	681	681	682	685	683	685	677
7	135	199	248	315	374	424	476	533	576	610	640	665	677	686	689	692	687	694	696	691
7.5	139	197	250	315	372	423	473	529	566	610	633	658	675	688	689	695	693	691	697	698
8	136	199	244	309	373	425	466	526	560	605	633	659	669	687	690	697	700	697	697	696
8.5	136	198	240	305	366	421	458	521	556	600	626	655	665	677	689	692	700	702	703	702
9	137	197	239	307	364	415	457	503	547	590	622	644	665	670	688	694	699	702	700	704
9.5	135	193	238	303	363	410	454	496	539	581	617	638	658	664	676	695	697	698	700	696
10	133	189	239	301	359	402	448	491	530	573	613	632	652	660	670	681	699	696	694	696

References

Bellmore, J.R. *et al.* (2014) 'The response of stream periphyton to Pacific salmon: Using a model to understand the role of environmental context', *Freshwater Biology*, 59(7), pp. 1437–1451. Available at: https://doi.org/10.1111/fwb.12356.

Carnell, R. (2022) 'lhs: Latin Hypercube Samples'.

Harper, E.B., Stella, J.C. and Fremier, A.K. (2011) *Global sensitivity analysis for complex ecological models: a case study of riparian cottonwood population dynamics*, *Ecological Applications*.

Jacquet, Claire *et al.* (2022) 'Meta-ecosystem dynamics drive the spatial distribution of functional groups in river networks', *Oikos* [Preprint]. Available at: https://doi.org/10.1111/oik.09372.

Liaw, A. and Wiener, M. (2001) 'Classification and Regression by RandomForest', *Forest*, 23.

Wolfram Research, I. (2022) 'Mathematica'. Champaign, Illinois: Wolfram Research, Inc. Available at: https://www.wolfram.com/mathematica.